Menoufyia University
Faculty of Electronic Engineering
Dept. of Computer Science & Engineering

MULTIMEDIA APPLICATIONS OVER ASYNCHRONOUS TRANSFER MODE (ATM) NETWORK

A thesis submitted for
The degree of M. Sc.
By

Eng. Ayman El-Sayed Ahmed El-Sayed

Supervisors

Prof. Dr. Ibrahem Z. Morsi
Dept. of Electrical Engineering,
Faculty of Engineering
Menoufyia University
[ ]

Ass. Prof. Dr. Nabil A. Ismail
Dept. of Computer Science & Eng.
Faculty of Electronic Engineering
Menoufyia University
[ ]

Dr. Ehab A. Khalil
Dept. of Computer Science & Eng.
Faculty of Electronic Engineering
Menoufyia University
[ ]

Menoufyia University
Faculty of Electronic Engineering
Dept. of Computer Science & Engineering

MULTIMEDIA APPLICATIONS OVER ASYNCHRONOUS TRANSFER MODE (ATM) NETWORK

A thesis submitted for
The degree of M. Sc.
By

Eng. Ayman El-Sayed Ahmed El-Sayed

Examiners Committee

Prof. Dr. Mohamed Gamal El-Den Darwish
Faculty of Computer & Information
Cairo University
[ ]

Prof. Dr. Abdel Hameed M. Ragab
Head of Computer Science & Eng. Dept.
Faculty of Electronic Engineering
Menoufyia University
[ ]

Prof. Dr. Ibrahem Z. Morsi
Dept. of Electrical Engineering,
Faculty of Engineering
Menoufyia University
[ ]

Ass. Prof. Dr. Nabil A. Ismail
Dept. of Computer Science & Eng.
Faculty of Electronic Engineering
Menoufyia University
[ ]

Acknowledgment

I would like to express my sincere thanks to my supervisor Dr. E. A. Khalil for his invaluable help, advice, guidance and encouragement throughout the development of this work. I gratefully acknowledge his assistance in submitting recent references to me.

I'm very grateful to my supervisor Prof. N. A. Ismail for his valuable suggestions. I have constantly benefited from his discussion and encouragement to development of this work.

It is with great pleasure that I take the opportunity to thank my supervisor Prof. Ibrahem Z. Morsi for his enthusiastic supervision, help, and guidance throughout the work in this thesis. I'm indebted to him for his constructive discussions.

I would like also to thank all those they have helped, advised, and give fruitful discussions during this work. Many thanks also are to the staff of Computer Science and Engineering Department, Faculty of Electronic Engineering.

Finally, my sincere appreciation and gratitude is to my parents, my brothers, and especially to my wife and my daughter.

ABSTRACT

Asynchronous Transfer Mode or ATM is a network transfer technique capable of supporting a wide variety of multimedia applications with diverse service and performance requirements. It supports traffic bandwidths ranging from a few kilobits per second (e.g., text terminal) to several hundred megabits per second (e.g., high definition video) and traffic types ranging from continuous, fixed-rate traffic (e.g., file transfer) to highly bursty traffic (e.g. interactive data and video).

The bandwidth, delay, and loss requirements of real-time multimedia traffics are different from that of traditional non-real time traffic. The non-real time traffic requires reliable service, but it can tolerate delay. In contrast, the real-time traffics are stream-oriented, in the sense that they can tolerate some loss, but they should be delivered within a bounded delay to obtain the desired quality of service (QoS). To support multimedia communications, it is desirable to use a network that meets these contradictory requirements. The ATM network is applicable of the Broadband Integrated Service Digital Network (B-ISDN) that can be used to satisfy this ambition, owing to its simplicity and efficiency.

This thesis investigates the performance of the VP-Based Ring ATM Network for supporting multimedia applications using extensive simulation methodology. For the given traffic characteristics and a single ATM ring Add and Drop Multiplexing (ADM) architecture, many parameters such as mean waiting time, mean buffer size, maximum number of sources can be supported, and offered load are discussed. Also, the thesis proposes a control mechanism method in order to guarantee the fairness among the applicable traffics to the network, and cross all the requirements of each traffic.

A check point analysis to the proposed simulator, confirms that the simulator is working properly and in an efficient manner. The performance study confirms that, the VP-Based Ring ATM networks with the proposed control mechanism method can effectively handle both real-time synchronous traffic such as video and voice and non-real time traffic such as data traffic.

Abbreviations

AAL	:	ATM Adaptation Layer
ADM	:	Add-Drop Multiplexer.
ATM	:	Asynchronous Transfer Mode.
AUU	:	ATM-user-to-ATM-user.
BCC	:	Bellcore Client Campanies.
BD	:	Band Division method.
B-ICI	:	Broadband InterCarrier Interface.
BIP	:	Bit Interleaved Parity
B-ISDN	:	Broadband Integrated Services Digital Network.
B-NT	:	Brodband Network Terminator.
CBR	:	Constant Bit Rate.
CCITT	:	Consultative Committee on International Telegraph and Telephone.
CLP	:	Cell Loss Priority.
CLR	:	Cell Loss Ratio.
CN	:	Custemer Network.
CS	:	Convergence Sublayer.
DS-x	:	Digital Signal, level x (x = 0,1,2,3).
EIA-232	:	Electronics Industry Association - 232.
FCS	:	Frame Check Sequence.
FIFO	:	First In First Out.
GFC	:	Generic Flow Control.
GOB	:	Group Of Block.
HEC	:	Header Error Check.
ISD	:	Integrated Services Digital.
ISO	:	International Organization for Standardization.
ITU	:	International Telecommunications Union. CCITT's parent standards body and replacement name.
JPEG	:	Joint Photographic Experts Group.
Kbps	:	Kilobits per second (10^3).
LAN	:	Local Area Network.
LANE	:	LAN Emulation.
LOH	:	Line Overhead.
MAC	:	Medium Access Control.
MAN	:	Metropolitan Area Network.
Mbps	:	Megabits per second (10^6).
MBR	:	Mean Bit Rate.
MBS	:	Maximum Buffer Size in cells.
MPEG	:	Motion Picture Experts Group.
MSB	:	Most Significant Bit.

MWT	:	Mean Waiting Time in cell time.
NT	:	Network Termination.
NNI	:	Network-Network Interface.
OAM	:	Operations Administration and Maintenance.
OC	:	Optical Carrier.
OSI	:	Open System Interface.
PBR	:	Peak Bit Rate.
PBX	:	Private Branch eXchange.
PCM	:	Pulse Code Modulation
PDU	:	Packet Data Unit.
PHY	:	PHYsical layer.
PM	:	Physical Medium.
POH	:	Path OverHead.
PQC	:	Priority Queue Control method.
PRM	:	Protocol Reference Model.
PT	:	Payload Type.
PTI	:	Payload Type Identifier.
PVC	:	Permanent Virtual Circuit. Similar to a leased line.
PVCC	:	Permanent Virtual Channel Connection.
PVPC	:	Permanent Virtual Path Connection.
QoS	:	Quality of Service.
SAP	:	Service Access Point.
SAR	:	Segmentation And Reassembly.
SARPVP	:	SONET/ATM Ring architecture using Point-to-point VP's.
SDH	:	Synchronous Digital Hierarchy.
SDU	:	Service Data Unit.
SMDS	:	Switched Multimegabit Data Service.
SOH	:	Section Overhead.
SONET	:	Synchronous Optical NETwork.
SPE	:	Synchronous Payload Environment.
STM	:	Synchronous Transport Mode.
STS-3c	:	Synchronous Transport System-level 3.
TA	:	Terminal Adapter.
TC	:	Transmission Control.
TCP	:	Transmission Control Protocol.
TCS	:	Transmission Convergence Sublayer.
TDM	:	Time Division Multiplexing.
TEn	:	Terminal Equipment type n (n = 1,2).
TSA	:	Time Slot Assignment.
TSI	:	Time Slot Interchange.
UBR	:	Unspecified Bit Rate.

UNI	**:**	User-Network Interfaces.
VBR	**:**	Variable Bit Rate.
VC	**:**	Virtual Channel.
VCC	**:**	Virtual Channel Connection
VCI	**:**	Virtual Channel Identifier.
VP	**:**	Virtual Path.
VPC	**:**	Virtual Path Connection.
VPI	**:**	Virtual Path Identifier.
WAN	**:**	Wide Area Network

List of Symbols

D	:	*Number of cells of data traffic per cycle.*
F_s	:	*Transmission Frame size in cells = 44 cells.*
GR_{da}	:	*Data generated rate in cell/ms.*
GR_t	:	*Average transit rate in cell/ms*
GR_{vi}	:	*Video generated rate of each source in cell/ms.*
GR_{vo}	:	*Voice generated rate of each source in cell/ms.*
M	:	*Ratio of video cells per cycle.*
M_{siz}	:	*Message Size in cells*
m	:	*Mean arrival time of data traffic.*
N	:	*Ratio of voice cells per cycle.*
N_{vi}	:	*Number of Video sources.*
N_{vo}	:	*Number of Voice sources.*
OL	:	*Total Offered Load*
OL_{da}	:	*Data offered load.*
OL_{tr}	:	*Transit offered load.*
OL_{vi}	:	*Video offered load.*
OL_{vo}	:	*Voice offered load.*
R_T	:	*Transmission rate in cell/ms.*
R_{vi}	:	*Video encoding rate for each source, in Mbps.*
R_{vo}	:	*Voice PCM encoding rate for each source in Kbps.*
t_f	:	*Transmission frame time = 0.125 ms.*
TP	:	*Total Throughput per Node.*
TP_{da}	:	*Data Throughput per Node.*
TP_{vi}	:	*Video Throughput per Node.*
TP_{vo}	:	*Voice Throughput per Node.*
U_{da}	:	*Data Utilization*
U_{vi}	:	*Video Utilization*
U_{vo}	:	*Voice Utilization*

Chapter 1

Introduction

Emerging multimedia, high-speed data, and imaging applications are generating a demand for public networks to be able to multiplex and switch simultaneously a wide spectrum of data rates. These networks must be able to transport a large number of services such as low speed telemetry, telefax, low speed data, medium speed (Hi- Fi sound, video telephony), and very high speed (high quality video distribution, video library, video education).

These services are the target of B-ISDN. B-ISDN schemes are now being developed to provide various services, such as video, voice, and data to support these services effectively, various types of path connection, such as point-to-point, multipoint-to-point, and point-to-multipoint, need to be established in broadband networks. ATM is a key technique to realize B-ISDN because ATM can transfer broadband services at high speed, and various types of path connection can be established easily by using Virtual Paths (VP's)

The truth seems to be that ATM should be thought of as both big bits and small packets, and which description is more accurate depends on the context. For instance, at high bandwidth (a few 100 Mbps or faster), ATM cells look very much like bits. Each cell takes a negligible amount of time to send, and is too small for a sending or receiving computer to handle efficiently. But at low bandwidths (64 Kbps or slower), cells start to look big. A cell takes over 6 ms to transmit, a long time in a world where processors perform an instruction every few nanoseconds. The ATM concept results from the merging of two concepts: packet switching and Time Division Multiplexing (TDM). Each of these techniques has been modified in the following manner.

Related to packet switching, neither error control (on the data field) nor flow controls on the links inside the ATM network. Connection-oriented at the lowest level, all information is transferred in a virtual circuit assigned for the

complete duration of the connection. Packets have a fixed and small length. Instead of allowing variable-length packets to be switched, only small fixed-length packets (called cells) are accepted by the network. This choice allows the use of very high speed switching nodes and puts no constraints on services, since large information entities will be segmented into cells. Limited functionality in the header of the cells. The primary functionality supported by the header of the ATM cells is the identification and characterization of the virtual circuit. In addition, some error detection and correction on the virtual circuit identifier are provided.

Related to TDM, the time-slotted operation is kept, but the time transparency is shifted to the network's edges. This means that no time relation is maintained inside the network. Time slots are no longer characterized by their relative position in a frame as in TDM. To identify a certain time, an additional field called a header is needed to contain a virtual circuit identifier. To keep overhead to a minimum, the header is 5-bytes and the cell information field is 48-bytes, giving a total cell size of 53-bytes.

It is also important to note that ATM is going to use the Synchronous Optical Network (SONET), which in Europe is called Synchronous Digital Hierarchy (SDH), which has defined speed in the multigigabit range. In such range bandwidth is not the limiting factor but latency due to the speed of light becomes the limiting factor. This has impact on congestion and flow control issues. In this case closed feedback control methods of flow control is too sluggish. Other methods should be sought like rate-based flow control in which the user is permitted to transmit at a maximum allowable rate. We have an ATM-based ring network as a subscriber network, because the ring architecture allows network resource sharing, it can realize a cost-effective network.

1.1 Objective of the Thesis

The first objective of this research is to evaluate the performance of the VP-Based ATM Ring network for supporting multimedia applications; in particular voice and video traffics. First we have studied the network performance carrying individual traffic. Then, we have dropped the previously mentioned premise of individual traffic and consider the case when two traffics are handled. Finally, the effect of including another traffic with the previous integrated two traffics. Our primary performance measure is the maximum number of sources that can be carried by the proposed network. The major performance measures are including:

I) The mean waiting time (MWT) for video, voice, and data cells;

II) The maximum buffer size (MBS) (queue length) for video, voice, and data cells;

III) The maximum number of video/voice sources that can be supported with the network while satisfying the real-time constraints of both video and voice; and

IV) The achievable throughput and utilization of each traffic.

Our study has confirmed that the VP-Based ATM Ring Network can effectively handle real-time synchronous transmission of video and voice. The control allowed method in [1] caused data traffic to suffer from very large latency and very low throughput. This is because, the control mechanism method gives high priority to video and voice traffics, however data traffic is only serve when there is no video and voice cells or the load of video and voice traffics is light.

Consequently, we have proposed a control mechanism method to guarantee fairness among traffics. Though the video and voice traffics remain having higher priority than data traffic. In the proposed control mechanism method, the number of cells to be picked up from each queue depending upon its offered loads for completing the transmission frame

In order to achieve the objectives of evaluating of the network's performance, we have implemented a computer simulation and used a check point analysis to check the proposed simulator, which has proved that the simulator is working properly. Although the real performance of a communication system is only clear in practical use, theoretical performance evaluations can be used to investigate its basic stability under different load conditions. Also, simulators are valuable tools in helping us understand how complex systems could operate and perform without need to build an actual physical model to test. We have built up our simulation model using the C programming language. The simulator itself is designed to be flexible, it can be easily changed to accommodate different experiments. Most of the changes can be made in the constants of the program header.

1.2 Literature Overview

The increasing number of customers requires network to access with high bandwidth and low delay over long distances. To satisfy these needs, several high-speed network techniques have been developed recently. ATM is superior compared to other networking technologies as it offers high bandwidth and is scalable in the sense that the bandwidth capacity of an ATM system is not fundamentally limited to the technology itself [2].

The history behind ATM including the ATM standards, the different parts of the ATM set of specifications, the network topologies, and the network management aspects of ATM are explained in [3, 4].

In 1987, ATM was selected by CCITT (now ITU-T) as the bearer service to support B-ISDN. In 1990, CCITT agreed on a set of 13 recommendations that specify the most important characteristics of ATM. In 1991, the ATM forum was established by Adaptive Corp, Cisco, Northern Telecom., and Sprint. This forum defines and develops ATM standards. ATM forum released the first ATM specification in 1992. In 1996, the forum approved the Anchorage Accord,

which led to the convergence and interoperability of about 60 ATM specifications. Most ATM specification is now complete, said George Dobrowski, Chair of the ATM forum's Worldwide Technical Committee [5].

While it may be foreseen that ATM will drive the development of new networking interfaces, it will still be required to support the existing networking interfaces. It is necessary to define an ATM service, which emulates services of existing LANs on an ATM network without the need of any change in the ATM terminal equipment interface to the MAC layer. LAN Emulation is exactly designed to meet this requirement, more details in [6].

Since ATM doesn't provide media access control, it has been a concern that the throughput will be low if an ATM network experience congestion; in fact there is already practical evidence to this effect. Remanow and Floyed [7], investigated the throughput behavior of TCP over ATM for best-effort traffic when there is network congestion.

Originally, two feedback mechanisms were under consideration in the ATM forum: a rate-based scheme [8,9], and credit-based scheme [10,11]. An integrated approach to ATM flow control is described in [12].

The term Self-healing refers to the capability of the network to reconfigure itself around failures quickly and gracefully with the goal of approaching 100 % service availability an end-to-end basis. For more detail, see [13,14,15]. Shenghong and Zemin [16] present a new simple traffic model that can be realized arbitrary marginal distribution and its correlation may be not only long range dependence but also short-range dependence. As a result, compared with any existing traffic model, their proposed model is a more general traffic model.

P.S. Eom and etc. [17] investigate a Connection Admission Control (CAC) problem in a multimedia wireless ATM network that supports various multimedia applications based on micro/pico cellular architectures. They have presented a method that can decide the optimal CAC threshold values of their CAC scheme.

S.S. Petrovic [18], presented an adaptive closed loop congestion Control Scheme. He assumed two types of traffic share the ATM network resources. The first type consists of Variable Bit Rate (VBR) traffic, which is delay sensitive i.e. which has stringent delay requirements and is not subjected to any control, hence it is uncontrollable. The second type of traffic requires good loss performance, but agrees to have its bit rate controlled when necessary, thus accepting the possibility of longer mean delays during periods of high demand, i.e. cell loss is avoided at the expense of delay and hence is controllable. All delay insensitive, or best effort, or Available Bit Rate (ABR) traffic can join this group.

Gan and Mckenzie [19] investigated the traffic policing and bandwidth management strategies at the User Network Interface (UNI) of an ATM network. They assumed policing function, called the super leaky bucket (S-LB), it is based on the leaky bucket (LB), but handles three types of traffic differently according to their quality of service (QoS) requirement. Their simulations clearly demonstrate the advantages of the proposed strategy in providing improved levels of service for all types of traffic.

E. Yaprak and et al [20], proposed a shared buffer architecture associated with threshold based virtual partition among output ports. They investigated the system behavior under varying traffic patterns via simulation. Their study shows that the threshold based dynamic buffer allocation scheme ensures a fair share of the buffer space even under bursty loading conditions.

The few literatures mentioned, and many are not mentioned here have studied different cases of applications on ATM networks. Our goal is the integration of multimedia traffic such as video, voice, and data over a proposed VP-Based ATM Ring network. In our study we have considered that each station on the network can generate different types of traffic.

1.3 Organization of the Thesis

The thesis is organized into eight Chapters. The introduction and the outline of the thesis are presented in chapter one. In Chapter two, an overview of B-ISDN (Broadband-Integrated Services Digital Network) protocol reference model and its layers briefly explores what is the ATM network, the description of both the reference points and function groupings of ATM networks and the SONET/SDH specifications are included.

The multimedia traffic over ATM Network in more details, the traffic parameters, the ATM forum traffic categories, and the details of video, voice and data traffic assumptions are discussed and described in Chapter three. Chapter four outlines the characteristics of the system under consideration. The description of the VP-Based Ring architecture using VP concepts and ATM Ring Routing, the network operation and topology, the ADM node of VP-Based Ring network, the queue models and the previous control methods are included. Also, the proposed control mechanism method and the B-ISDN performance are explained. The simulation results when the proposed network is exclusive only one type of traffic are presented in Chapter five. Chapter six presents the simulation results for the proposed ADM/ATM network exclusive two different traffics such as video/data traffics and video/voice traffics. The performance measurements and characteristics for the service of multimedia traffic such as video, voice, and data over the ADM/ATM network is completely studied in Chapter seven. Finally, conclusion of the thesis and proposed future work are presented in Chapter eight.

Chapter 2

An Overview of ATM Network

ATM is a form of packet switching technology. That is, ATM networks transmit their information in small, fixed length packets called “cell” each of which contains 48-octets (or bytes) of data and 5-octets of header information. The small, fixed cell size was chosen to facilitate the rapid processing of packet in hardware and to minimize the amount of time required to fill a single packet. This is particularly important for real-time applications such as voice and video that require short packetization delays. ATM is the transfer mode for implementing Broadband Integrated Service Digital Networks (B-ISDN) [21].

The term transfer comprises both transmission and switching aspects, so a transfer mode is a specific way of transmitting and switching information in a network. The term asynchronous, in new transfer mode name refers to the fact that, in the context of multiplexed transmission, cells allocated to the same connection may exhibit an irregular recurrence pattern as they are filled according to the actual demand, this is shown in Figure 2-1(a).

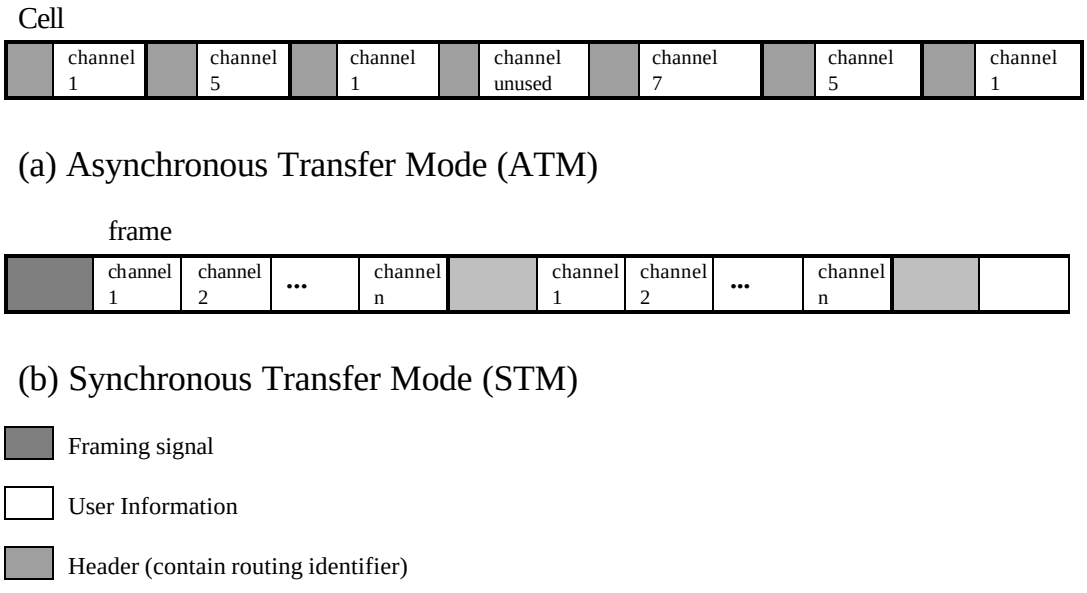

Figure 2-1 Synchronous and Asynchronous Transfer Modes.

Figure 2-1 describes the difference between the Synchronous Transfer Mode (STM), and the Asynchronous Transfer Mode (ATM). As we have mentioned above that ATM is the data transfer interface for B-ISDN, let's give short notes about B-ISDN standards.

2-1 B-ISDN Standards

In 1988, the telecommunication standardization sector of the ITU, the international standards agency commissioned by the United Nations for the global standardization of telecommunications, has developed a number of standards for ATM networks. Other standards bodies and consortia (e.g., the ATM Forum, ANSI) have also contributed to the development of ATM standards. The following subsection presents an overview of the standards, with particular emphasis on the protocol reference model used by ATM [22].

2-1-1 Protocol Reference Model

The B-ISDN protocol reference model, defined in ITU-T recommendation I-321, is shown in Figure 2-2 [23]. The purpose of the protocol reference model is to clarify the functions that ATM networks perform by grouping them into a set of interrelated, function-specific layers and planes. The reference model consists of a user plane, a control plane and a management plane (more details about these planes are in [24, 25, 26]. Within the user and control planes is a hierarchical set of layers. The user plane defines a set of functions for the transfer of user information between communication end-points; the control plane defines control functions such as call establishment, call maintenance, and call release, and the management plane defines the operations necessary to control information flow between planes and layers, and maintain accurate and fault-tolerant network operation.

Within the user and control planes, there are three layers; the physical layer, the ATM layer, and the ATM adaptation layer (AAL).

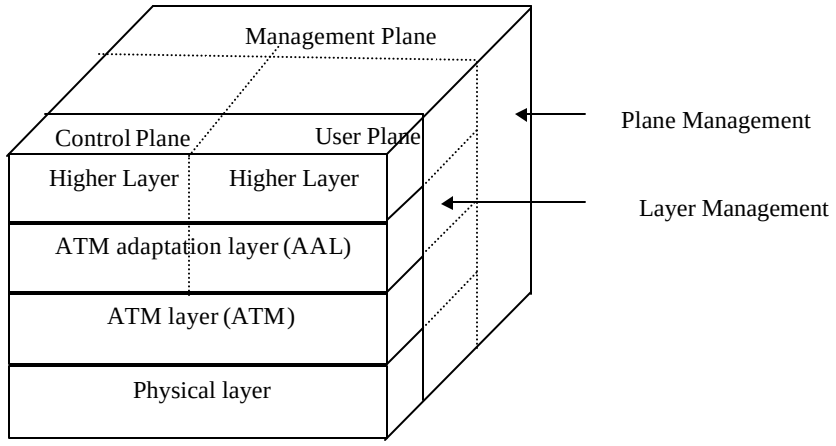

Figure 2-2 Protocol Reference Model for ATM

Table 2-1 summarizes the functions of each layer [23]. The physical layer performs primarily bit level functions, the ATM layer is primarily responsible for the switching of ATM cells, and the ATM adaptation layer is responsible for the conversion of higher layer protocol forms into ATM cells. The function that the physical, ATM, and adaptation layers perform are described in more detail in the following:

	Higher Layer Functions	Higher Layers		
Layer management	.convergence	CS	AAL	
	.segmentation and reassembly	SAR		
	.generic flow control .cell-header generation/extraction .cell VPI/VCI translation .cell multiplex and demultiplex	ATM layer		
	.cell-rate decoupling .HEC, header-sequence generation/verification .cell delineation .transmission-frame adaptation .transmission-frame generation/recovery	TC	physical layer	PHY independent
	bit timing physical medium	PM		PHY dependent

AAL : ATM Adaptation layer.
CS : Convergence Sublayer.
SAR : Segmentation And Reassembly.
VPI : Virtual Path Identifier.
VCI : Virtual Channel Identifier.
HEC : Header Error Control.
TC : Transmission Control.
PM : Physical Medium

Table 2-1 the Functions of B-ISDN in Relation to the B-ISDN PRM.

2-1-2 Physical Layer

The physical layer is divided into two sublayers: the physical medium sublayer, and the transmission convergence sublayer [23].

2-1-2-1 Physical Medium (PM) sublayer

The physical medium sublayer performs medium-dependent functions. For example, it provides bit transmission capabilities including bit alignment, line coding and electrical/optical conversion. The PM sublayer is also responsible for bit timing, i.e., the insertion and extraction of bit timing information. The PM sublayer currently supports two types of interface: optical and electrical.

2-1-2-2 Transmission Convergence (TC) sublayer

Above the physical medium sublayer is the transmission convergence sublayer, which is primarily responsible for framing of data transported over the physical medium. The ITU-T recommendation specifies two options for TC sublayer transmission frame structure: cell-based and Synchronous Digital Hierarchy (SDH). In the cell-based case, cells are transported continuously without any regular frame structure. Under SDH, cells are carried in a special frame structure based on the North American SONET (Synchronous Optical Network) protocol [27]. Regardless of which transmission frame structure is used, the TC sublayer is responsible for the following four functions: cell rate decoupling, header error control, cell delineation, and transmission frame adaptation. Cell rate decoupling is the insertion of idle cells at the sending side to adapt the ATM cell stream's rate to the rate of the transmission path. Header error control is the insertion of an 8-bit CRC polynomial in the ATM cell header to protocol the contents of the ATM cell header. Cell delineation is the detection of cell boundaries. Transmission frame adaptation is the encapsulation of

departing cells into an appropriate framing structure (either cell-based or SDH-based).

2-1-3 ATM Layer

The ATM layer lies a top the physical layer and specifies the functions required for the switching and flow control of ATM cells [23].

There are two interfaces in an ATM network; the user-network-interface (UNI) between the ATM end-point and the ATM switch, and the network-network interface (NNI) between two ATM switches. Although a 48-octets cell payload is used at both interfaces, the 5-octets cell header differs slightly at these interfaces. Figure 2-3 shows the cell header structures used at the UNI and NNI [23]. At the UNI, the header contains a 4-bits Generic Flow Control (GFC) field, a 24-bits label field containing VPI and VCI subfields (8-bits for the VPI and 16-bits for the VCI), a 2-bits payload type (PT) field, a 1-bit priority (PR) field, and an 8-bit header error check (HEC) field. The cell header for an NNI cell is identical to that for the UNI cell, except that it lacks the GFC field; these four bits are used for an additional 4 VPI bits in the NNI cell header.

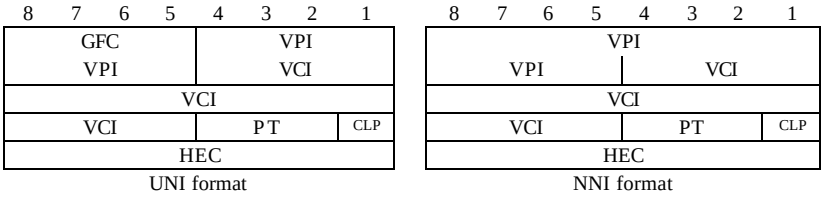

Figure 2-3 ATM Cell Header Format

The VCI and VPI fields are identifier values for VC and VP respectively. A virtual channel connects two ATM communication end-points. A virtual path connects two ATM devices, which can be switches or end-points, and several

virtual channels may be multiplexed onto the same virtual path. The 2-bit PT field identifiers whether the cell payload contains data or control infomation. The CLP bit is used by the user for explicit indication of cell loss priority. If the value of the CLP is 1, then the cell is subject to discarding in case of congestion. The HEC field is an 8-bit CRC polynomial that protects the contents of the cell header. The GFC field, which appears only at the UNI, is used to assist the customer premises network in controlling the traffic flow for different qualities of service. At the time of writing, the exact procedures for use of this field have not been agreed upon.

2-1-3-1 ATM Layer Functions

The primary function of the ATM layer is VPI/VCI translation. As ATM cells arrive at ATM switches, the VPI and VCI values contained in their headers are examined by the switch to determine which output port should be used to forward the cell. The process, the switch translates the cell's original VPI and VCI values into new outgoing VPI and VCI values, which are used in turn by the next ATM switch to send the cell toward its intended destination. The table used to perform this translation is initialized during the establishment of the call.

An ATM switch may either be a VP switch, in which case it only translates the VPI values contained in cell headers, or it may be a VP/VC switch, in which case it translates the incoming VCI value into an outgoing VPI/VCI pair. Since VPI and VCI values do not represent a unique end-to-end virtual connection, they can be reused at different switches through the network. This is important, because the VPI and VCI fields are limited in length and would be quickly exhausted if they were used simply as destination addresses.

The ATM layer supports two types of virtual connections; switched virtual connection (SVC) and permanent, or semi-permanent, virtual connections (PVC). Switched virtual connections are established and torn down dynamically

by an ATM signaling procedure. That is, they only exist for the duration of a single call. Permanent virtual connections, on the other hand, are established by network administrators and continue to exist as long as the administrator leaves them up, even if they are not used to transmit data.

Other important functions of the ATM layer include cell multiplexing and demultiplexing, cell header creation and extraction, and generic flow control. Cell multiplexing is the merging of cells from several calls onto a single transmission path. Cell header creation is the attachment of a 5-octets cell header to each 48-octets block of user payload, and generic flow control is used at the UNI to prevent short-term overload condition from occurring within the network.

2-1-3-2 The AAL Functions

AAL functions are organized in two sublayers. The essential functions of the Segmentation And Reassembly (SAR) sublayer are, at the transmitting side, segmentation of higher layer Packet Data Units (PDUs) into a suitable size for the information field of the ATM cell and, at receiving side, Reassembly of the particular information fields into higher layer PDUs. The Convergence Sublayer (CS) is service dependent and provides the AAL service at the AAL-SAP. No Service Access Point (SAP) has yet been defined between these two sublayers.

Figure 2-4 depicts the AAL classes. Not all-possible combinations make sense and therefore only four classes are distinguished [25].

	Class A	Class B	Class C	Class D
Timing relation between source and destination	Required		Not required	
Bit rate	Constant	Variable		
Connection mode	Connection oriented			Connectionless

Figure 2- 4 Service Classification of AAL

AAL Type 1: This service is used by the applications that require a Constant Bit Rate (CBR), such as uncompressed voice and video, and usually referred to as isochronous. This type of application is extremely time-sensitive and therefore end-to-end timing is paramount and must be supported. Isochronous traffic is assigned service class A.

AAL Type 2: again this service is used for compressed voice and video (packetized isochronous traffic), however, it is primarily developed for multimedia applications. The compression allows for a Variable Bit Rate (VBR) service without losing voice and video quality. The compression of voice and video (class B) however, does not negate the need for end-to-end timing. However, timing is still important and is assigned a service class just below that of AAL Type 1.

AAL Type ¾: This adaptation layer supports both connection-oriented and compatibility with IEEE 802.6 that is used by Switched Multimegabit Data Service (SMDS). Connection-oriented AAL Type 3 and AAL Type 4 payloads are provided with a service class C while connectionless-oriented AAL Type 3 and AAL Type 4 payloads are assigned the service class D. The support for IEEE 802.6 significantly increases cell overhead for data transfer when compared with AAL Type 5.

AAL Type 5: For data transport, AAL Type 5 is the preferred AAL to be used by applications. Its connection-oriented mode guarantees delivery of data by the servicing applications and doesn't add any cell overhead.

2-2 The B-ISDN Layers

In ATM, all information to be transferred is packed into fixed-size length called cell, the structure is shown in Figure 2-5, in which the information field (48 octets) is available for the user. The header field carries information that pertains

to the ATM layer functionality itself, mainly the identification of cell by means of a label.

Header (5 octets)	**Information field** (48 octets)

Figure 2-5 Cell Structure

Octets are sent in increasing order starting with octet 1. Bits within an octet are sent in decreasing order starting with bit 8. For all fields, the first bit sent is the most significant bit (MSB). The header consists of primarily of virtual path/ channel identifiers (VPI/VCI). The layers in the ATM contain the physical layer, and ATM layer as shown in Figure 2-6.

Higher layer	
ATM Layer	Virtual channel level
	Virtual path level
	Transmission path level
Physical layer	Digital section level
	Regenerator section level

Figure 2-6 ATM Layer Hierarchy

Figure 2-7 demonstrates the relationship between virtual channel, virtual path and transmission path. A transmission path may comprise several virtual paths and each virtual path may carry several virtual channels. Concerning the levels of the ATM layer (virtual channel and virtual path), it is helpful to distinguish between links and connections.

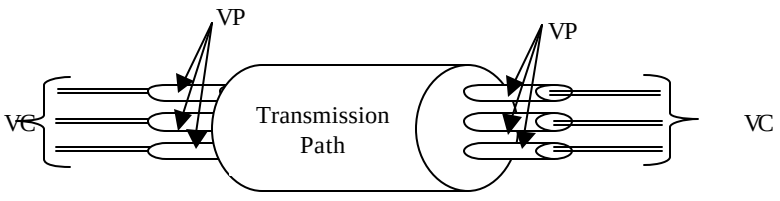

Figure 2-7 Relationships between Virtual Channel, Virtual Path, and Transmission Path

A Virtual Channel Link: means unidirectional transport of ATM cells between a point where a VCI value is assigned and the point where that value is translated or removed. Similarly, the points where VPI value is assigned and translated or removed terminate a Virtual Path link. A concatenation of VC links is called a Virtual Channel Connection (VCC) and likewise, a concatenation of VP links is called a Virtual Path Connection (VPC). The relationship between different levels of the ATM transport network is shown in Figure 2-8. A VCC may consist of several concatenations VC links, each of which is embedded, in a VPC. The VPC's usually consists of several concatenations VP links. Each VP link is implemented on a transmission path, which hierarchically comprises digital section and regenerator sections.

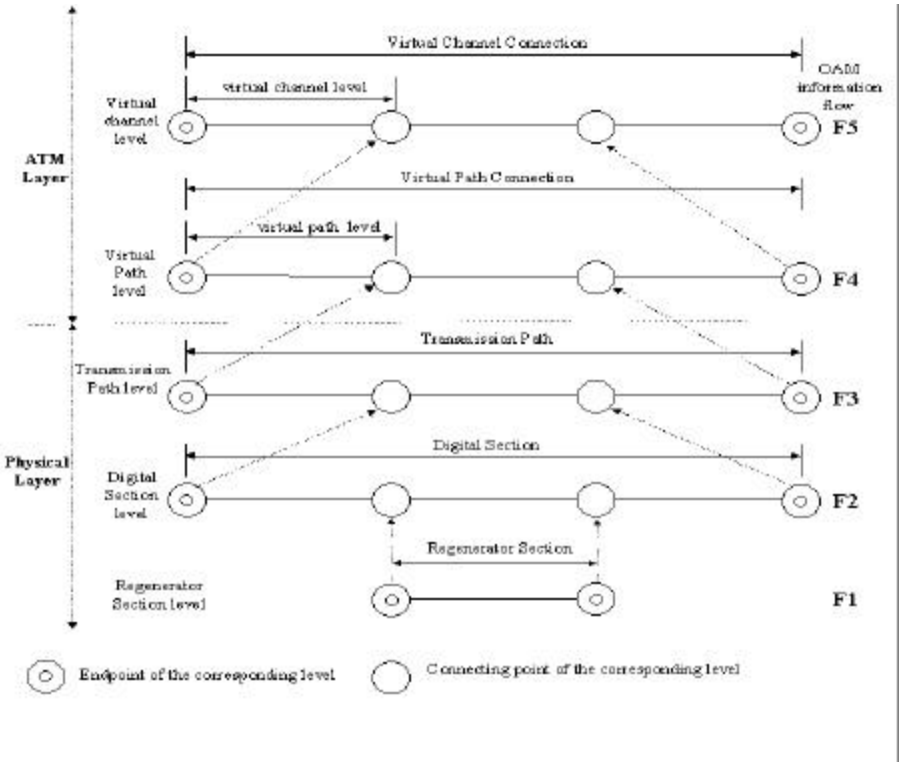

Figure 2-8 Hierarchical Layer-to-Layer Relationship.

2-2-1 The Physical Layer

1- Transmission path level extends between network elements that assemble and disassemble the payload of a transmission system. For end to end communication, the payload is end-user information. For user-to-network communication, the payload may be signaling information. Cell delineation and HEC functions are required at the end-points of each transmission path.

2- Digital section level extends between network elements that assemble and disassemble a continuous bit or byte stream. This refers to the exchange or signal-transfer points in a network that are involved in switching data streams.

3- Regenerator section level, a portion of a digital section. An example of this level is a repeater that is used to simply regenerate the digital signal a long a transmission path that is too long to be used without such regeneration no switching is involved.

2-2-2 The ATM Layer

The logical connection in ATM is referred to as virtual channel connection (VCC). VCC is analogous to a virtual circuit in frame relay logical connection. It is the basic unit of switching in B-ISDN, a VCC is setup between two end users through the network, and a variable rate, and full-duplex flow of fixed-size cells is exchanged over the connection. VCCs are also used for user-network exchange (control signaling) and network-network exchange (management and routing).

The second sublayer of processing has been introduced that deals with the concepts of virtual path. A virtual path connection (VPC) is a bundle of VCCs that has the same end points. Thus, all the cells flowing over all the VCCs in a single VPC are switched together.

2-3 Signaling: Making ATM Connections

Signaling is responsible for setting up the desired connection or virtual circuit and tearing it down when the transmission is completed.

2-3-1 Connection Types

There are two types of connection depending on how the virtual channel established. One is Permanent Virtual Circuit (PVC) and the other is Switched Virtual Circuit (SVC).

2-3-1-1 Permanent Virtual Circuits (PVCs)

PVCs are those data connections that require the circuit to be manually setup. Typically, a VPI/VCI combination is stored into look-up tables on ATM hardware on the network. To set up the connection, the network administrator will specify a set of VPI/VCI source and destination option. The ATM end-station can then be connected to another end-station over the network via a switched path.

2-3-1-2 Switched Virtual Circuits (SVCs)

Switched signaling mechanisms facilitate dynamic links between end-stations. The setup and tear down of a virtual circuit can be accomplished without manual intervention.

2-3-2 Call Types

Now that the mechanisms for signaling have been established, data may be transferred between the calling and the called party. This section covers the various types of desired connections and how they are established.

1. Point-to-Point

Connections made between two end-stations compose a point-to-point link. Point-to-point links may be bidirectional or full duplex. In these cases the sender and receiver both make a data transfer request. Each issues the appropriate connection setup messages. They can then send data on their separately established virtual circuit connections. If the service connections are identical for each end-station (e.g., same bandwidth and other quality of service parameters), then the connection is said to be symmetric. Should the bandwidth requests be different for each end-station, then the connection is said to be asymmetric.

2. Point-to-Multipoint

Point-to-Multipoint works much the same as point-to-point. Here however, one virtual circuit connection established from one end-station specifies many recipients. The initiating end-station is dassified as the root station. All called end-stations are classified as leaves. A point-to-point link is established from the root to each leaf, one at a time, until all leaves are connected via the root virtual circuit or connection. While a point-to-point link may be established in a two-way (full-duplex) mode, leaves are not able to initiate a call back to the root.

3. Multipoint-to-Multipoint

The signaling mechanism established so far for ATM VCCs supports the exchange of addresses between end-station only. This precludes the ability of the current signaling mechanism to set up many-to-many users or Multipoint-to-Multipoint connections. The Signaling Working Group (SWG) of the ATM Forum addresses this area.

2-3-3 Call Setup and Tear down

Messages are exchanged between the calling end-station and its nearest neighbor. These messages are passed along the network until the called party is reached and can acknowledge the call. This is illustrated in Figure 2-9.

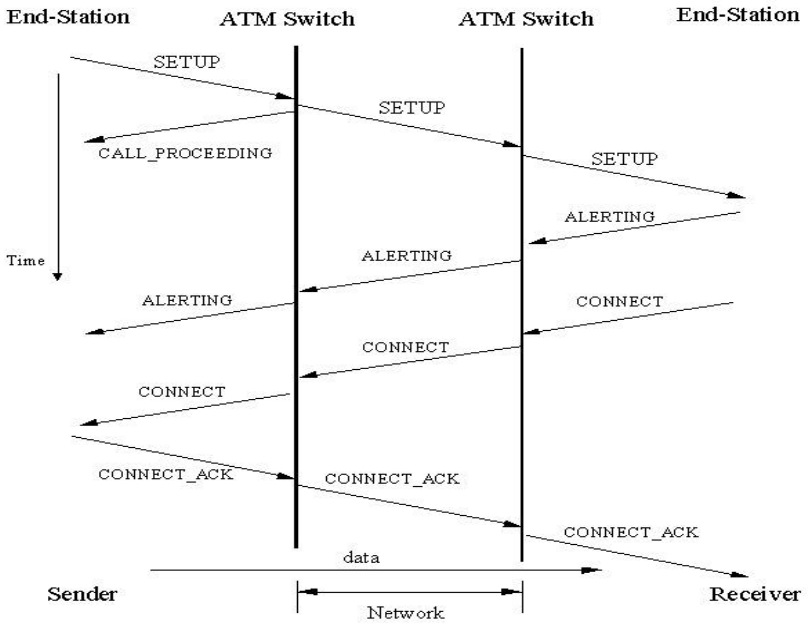

Figure 2-9 Call Setup

Call Completed

Here, we look at an end-station successfully completing a call to another end-station across an ATM network. Initially a call SETUP message is transmitted from the sending end-station. The nearest neighbor, here a switch, return a CALL_PROCEEDING message to the end-station. Meanwhile, the SETUP message is being forwarded to the receiving end-station via the network of switches. Once it reviews the SETUP request message and can accommodate the call, the receiver forwards an ALERTING message through the network that presages a CONNECT message. At this time, or at the time a CALL_PROCEEDING message is received by the sender, a VPI/VCI number is determined and allocated to the sender.

Once the sender receives the CONNECT message, it returns a CONNECT_ACK, or acknowledge message, to the receiver. When the data transmission is completed, a RELEASE_COMPLETE message is transmitted,

causing the circuit to tear down. This allows other end-stations access to the network.

Call Refused

If a call cannot be completed, the situation is such that a ELEASE_COMPLETE is transmitted back to the sender instead of an ALERT, followed by a CONNECT message.

2-4 SONET/SDH Specifications

Signal Hierarchy:

The SONET (Synchronous Optical Network) specification defines a hierarchy of standardized digital data rates, as shown in Table 2-2 [28].

SONET Designation	CCITT Designation	Data Rate (Mbps)	Payload Rate
STS-1/OC-1	-	51.84	50.112
STS-3/OC-3	STM-1	155.52	150.336
STS-9/OC-9	STM-3	466.56	451.008
STS-12/OC-12	STM-4	622.08	601.344
STS-18/OC-18	STM-6	933.12	902.016
STS-24/OC-24	STM-8	1,244.16	1202.688
STS-36/OC-36	STM-12	1,866.24	1804.032
STS-48/OC-48	STM-16	2,488.32	2405.376

STS : Synchronous Transport Signal OC : Optical Carrier STM: Synchronous Transport Module.

Table 2-2 SONET/ SDH Signal Hierarchy.

System Hierarchy

SONET capabilities have been mapped into a four-layer hierarchy Figure 2-10, more details in [24]. Figure 2-11 shows the physical realization of the logical layers.

1. **Photonic**: This is the physical layer, it includes a specification of the type of optical fiber that may be used and details such as the required minimum powers and dispersion characteristics of the transmitting lasers and the required sensitivity of the receivers. This layer is also

responsible for converting STS (electrical) signals to OC (optical) signals.

2. **Section**: This layer creates the basic SONET frames. Transmission functions include framing scrambling, and error monitoring.
3. **Line**: This layer is responsible for synchronization, multiplexing of data onto the SONET frames, and protection switching.
4. **Path**: This layer is responsible for end-to-end transport of data at the appropriate signaling speed.

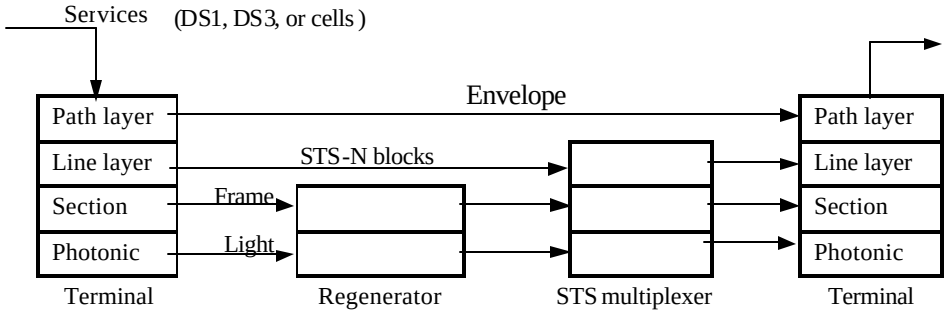

Figure 2-10 Logical Hierarchy of SONET System.

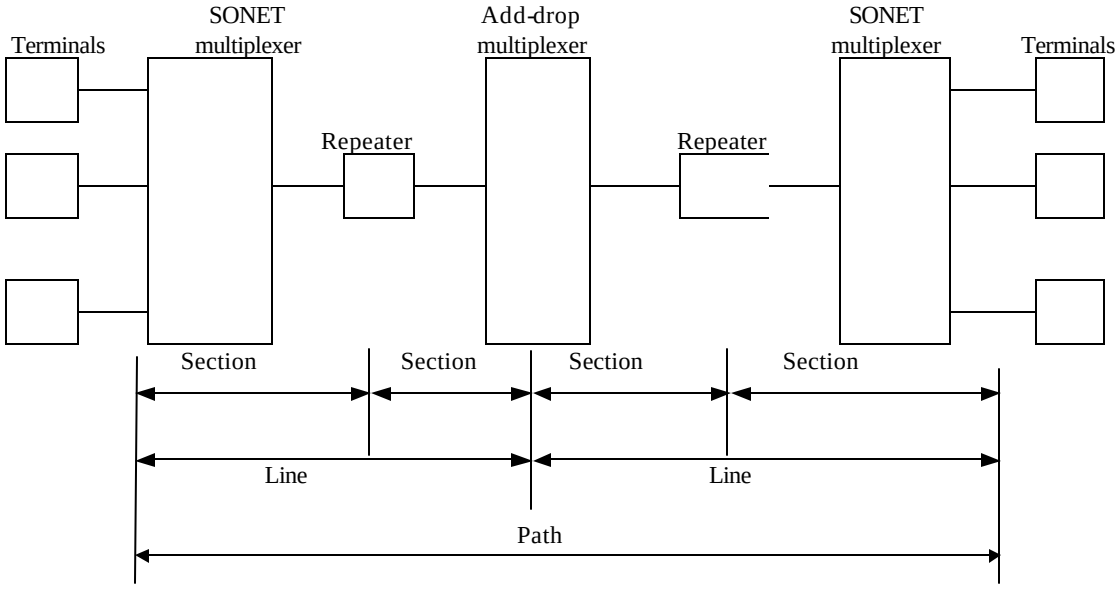

Figure 2-11 Physical Hierarchy of SONET System

The SONET Frame Format:

The basic SONET building block is the STS-1 frame, which consists of 810-octets and is transmitted once every 125 μs (micro-second). For an overall data rate of 51.84 Mbps is shown in Figure 2-12 (a). The frame can logically be viewed as a matrix of nine rows of 90 octets each, with transmission being one row at a time, from left to right and top to bottom. Figure 2-12 (b), illustrates the size of the matrix of STM-N frame format.

2-4-1 SDH-Based Interface at 51.84 Mbps (STS-1)

The first three elements (9 x 3 = 27 octets) of the frame are devoted to overhead octets with 9 octets being devoted to section-related overhead and 18 octets to line overhead. Figure 2-13, shows the arrangement of overhead octets, and Table 2-3 defines the various fields. The remainder of the frame is payload, which is provided by the path layer. The payload includes a column of path overhead, which is not necessarily in the first available column position, the line overhead contains a pointer that indicates where the path overhead starts.

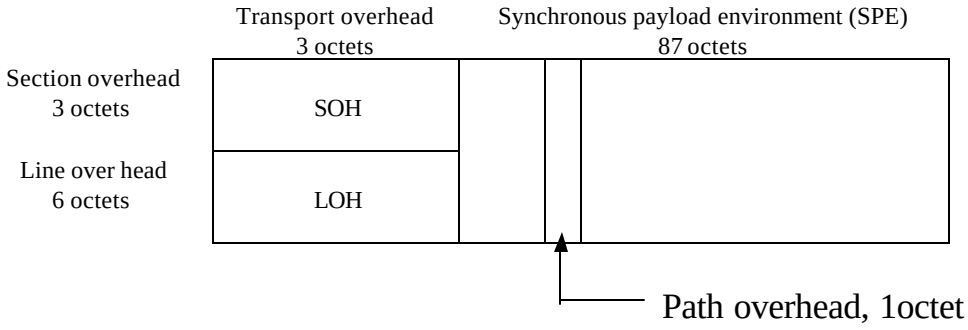

(a) STS-1 frame format

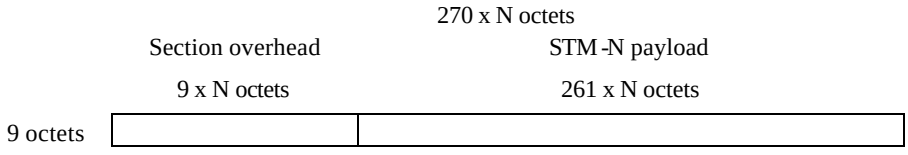

(b) STM-N frame format

Figure 2-12 SONET/SDH Frame Format

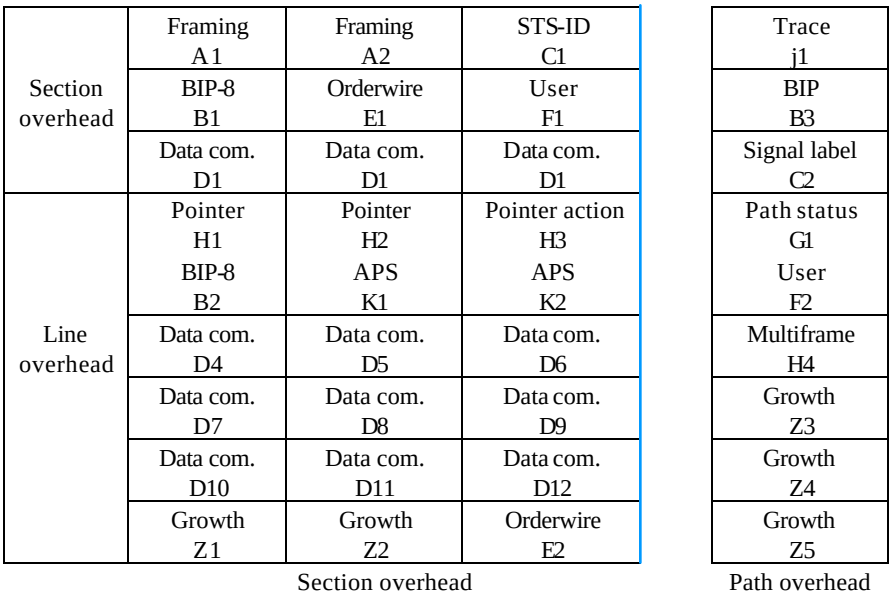

Figure 2-13 SONET STS-1 Overhead octets.

Section overhead	
A1,A2	Framing bytes =F6, 28hex; used to synchronize the beginning of the frame.
C1	STS-1 ID identifies the STS-1 number (1 to N) for each STS-1 within an STS-n multiplex.
B1	Bit-interleaved Parity byte providing even parity over previous STS-N frame after scrambling; the i^{th} bit of this octet contains the even parity value calculated from the i^{th} bit position of all octets in the previous frame.
E1 F1	Section-level 64-Kbps PCM Orderwire; optional 64-Kbps voice channel to be used between section-terminating equipment, hubs, and remote terminals. 64-Kbps channel set aside for user purposes.
D1-D3	192-Kbps data communications channel for alarms, maintenance, control, and administration between sections.
Line Overhead	
H1-H3	pointer bytes used in frame alignment and frequency adjustment of payload data
B2	Bit-interleaved parity byte for line-level error monitoring.
K1,K2	Two bytes allocated for signaling between line-level automatic-protection switching equipment; uses a bit- oriented protocol that provides for error protection and management of the SONET optical link.
D4-D12	576-Kbps data communication channel for alarms, maintenance, control, monitoring and administration at the line level.
Z1,Z2	Reserved for future use.
E2	64-Kbps PCM voice channel for line-level Orderwire.

Table 2-3 STS-1 Overhead Bits

Path Overhead	
j1	64-Kbps channel used to repetitively send a 64-octet fixed-length string so a receiving terminal can continuously verify the integrity of a path; the contents of the message are user-programmable.
B3	Bit-interleaved parity byte at the path level, calculated over all bits of the previous SPE.
C2	STS path signal label to designate equipped versus unequipped STS signals. Unequipped means that the line connection is complete but there are no path data to send. For equipped signals, the label can indicate the specific STS payload mapping that might be needed in receiving terminals to interpret the payloads.
G1	Status byte sent from path-terminating equipment back to path-originating equipment to convey the status of terminating equipment and path error performance.
F2	64-Kbps channel for path user.
H4	Multiframe indicator for payloads needing frames that are longer than a single STS frame; Multiframe indicators are used when packing lower-rate channels (virtual tributaries) into the SPE.
Z3-Z5	Reserved for future use.

Table 2-3 STS-1 Overhead Bits (continue).

2-4-2 SDH-Based interface at 155.52 Mbps (STS-3)

At the physical bit level the B-ISDN UNI has a bit rate of 155.520 Mbps or 622.080 Mbps. The interface transfer capability is defined as the bit rate available for user information cells, signaling cells and ATM and higher layer operation and maintenance (OAM) information cells, excluding physical layer frame structure bytes or physical layer cells. Its value of 149.760 Mbps for the 155.52 Mbps interface complies with SDH. The transfer capacity of the 622.08 Mbps interface is 599.04 Mbps (four times 149.76 Mbps). The transmission frame structure for an SDH-based interface at 155.52 Mbps is shown in Figure 2-14.

This frame is byte-structured and consists of 9 rows and 270 columns. The frame repetition frequency is 8 kHz (9 x 270 byte x 8 bit x 8 kHz) = 155.520 Mbps. The first 9 columns comprise section overhead (SOH) and administrative pointer-4 (AU-4). Another 9-byte column is dedicated to the path overhead

(POH). Generation of the SDH-based UNI signal is as follows. First, the ATM cell stream is mapped into Container-4 (C-4) which is a 9 rows x 260 columns container corresponding to the transfer capability of 149.76 Mbps. Next C-4 is packet in Virtual Container-4 (VC-4) along with the VC-4 POH. The ATM cell boundaries are aligned with the byte boundaries of the frame. It should be noted that an ATM cell may cross a C-4 boundary as the C-4 capacity (2340 bytes) is not an integer multiple of the cell length (53 bytes). VC-4 is then mapped into the 9 x 270 byte frame (known as the synchronous transport module 1 (STM-1). The AU-4 pointer is used to find the first byte of VC-4. POH bytes J1, B3, C2, G1 are then activated.

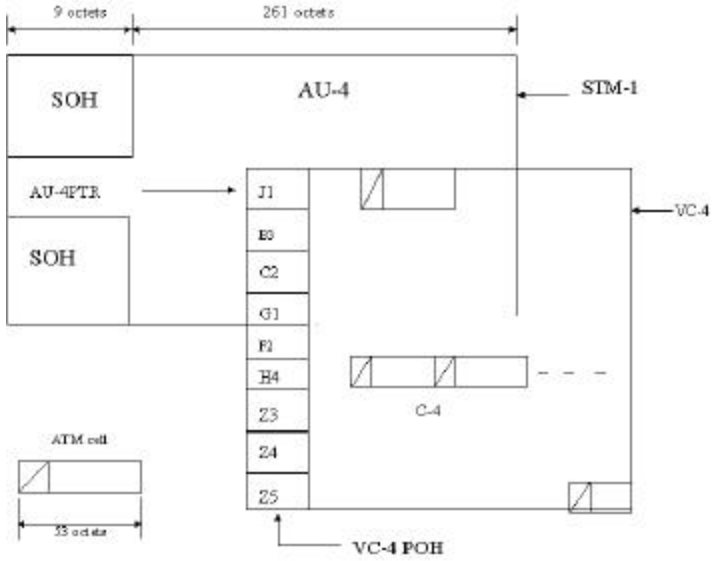

PTR : Pointer
c : Container
VC-4: Virtual Container 4

POH : Path OverHead
AU :Administrative unit

SOH : Section OverHead
STM-1:Synchronous Transport Module 1

Figure 2-14 Frame Structure of the 155.52 Mb/s SDH-Based Interface.

Chapter 3

ATM and Multimedia Traffic

In the middle of the 1980, the telecommunications world started the design of a network technology that could act as a great unifier to support all digital services, including low-speed telephony and very high–speed data communication. The concept of a network capable of integrating all ranges of digital service emerged. The name given to this network was broadband integrated services digital network (B-ISDN).

Several groups and telecommunication companies worked in parallel on alternative proposals for the technical implementation of the network. At the end of a long process, ATM technology was selected to support the B-ISDN network. ATM as a technology designed to support various classes of service, is the solution of choice for supporting long-haul digital multimedia applications.

The possibility of setting up the virtual connections at speed of several dozen megabits per second with a variety of guaranteed levels for the bit rate and the jitter, should satisfy most applications. The typical transit delay of a couple to a tenth of millisecond propagation delay excluded is compatible with most of the applications of multimedia. For applications requiring a constant bit rate, the circuit emulation service can be used.

The residual cell loss rate of 10^{-8} to 10^{-10} is suitable for all types of real time transmission of voice and video streams.

The issues regarding the risks of congestion should not in practice affect users in the long term, because the manufacturers are expected to take the necessary measures to limit the statistical nature of the multiplexing if the quality of service cannot be satisfactorily guaranteed. Some early services may, however, suffer from serious teething problem [29].

3-1 ATM and Traffic

As mentioned the ATM Network can support variety of services, such as video, voice and data on a single infrastructure, to do so ATM networks must provide traffic management [30]. We can describe the traffics as time-based and non-time-based information [31], time-based information is sensitive to time varying as video, and voice, non-time-based is insensitive to time varying as image, and data.

Its traffic characteristics and the corresponding communication requirements can characterize an application. Its traffic generation process can formally specify the traffic characteristics of an application. Since the traffic generation process (or traffic pattern) is basically a sequence of packets generated at arbitrary instants, two stochastic processes can characterize the traffic pattern:

a) The packet generation process (or packet arrival process).

b) Packet length distribution function.

The communications requirements of an application include bandwidth, delay, and error guarantees. The bandwidth requirements of an application (in each direction) are typically specified in terms of peak and average bandwidth. For CBR applications, the peak and average bandwidth are the same. For image browsing applications, a full screen photo image of 3 Mbytes (1000 x 1000 x 24 byte), after compression 300 Kbytes by Joint Photographic Experts Group (JPEG) compression [32]. This requires about 24 Mbps link (peak) bandwidth to satisfy the response time requirements.

An application can be classified according to its information delivery requirements as a real-time or non-real time application. A real time application is one that requires information delivery for immediate consumption, for example, a telephone conversation. Non-real time application information is stored (perhaps

temporarily) at the receiving points for later consumption, for example, sending electronic mail. Figure 3-1 shows one new view [33,34].

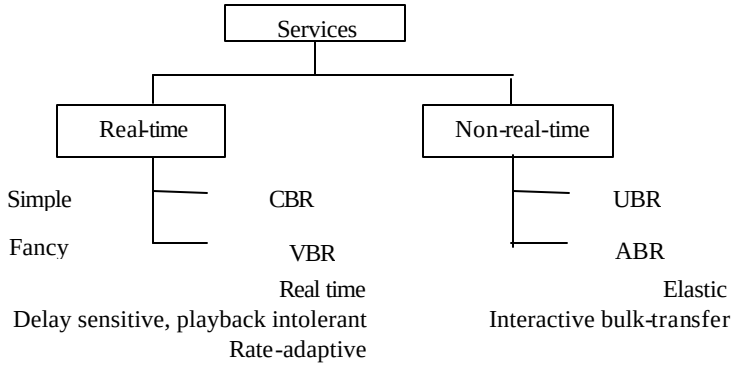

Figure 3-1 ATM Model "*Hierarchy*".

3-1-1 ATM Forum Traffic Categories

The ATM forum has defined the following traffic categories based on the different requirements Constant Bit Rate (CBR), real time and non-real time Variable Bit Rate (VBR), Unspecified Bit Rate (UBR), and more recently Available Bit Rate (ABR). These categories are discussed below.

Constant Bit Rate (CBR):

The CBR category is intended for applications requiring tightly constrained delay and delay variation. Such as voice and video applications which are expected to transmit at a continuos rate. CBR services use ATM Adaptation Layer Type-1 [21], because it receives/delivers SDU (Service Data Unit) with a constant bit rate from/to the layer above. The CBR class of service is the preferred choice for many video dial tone service providers [35].

Variable Bit Rate (VBR):

The VBR category is intended for applications that share the requirements for tightly constrained delay and delay variation of CBR traffic, but which transmit at a variable rate. Compressed voice with silence suppression, and

variable rate video codecs are examples of this category of traffic. ATM Adaptation Layer Type-2 is proposed for VBR services with a timing relation between source and destination [21], for example VBR Voice or video.

Undefined (or Unspecified) Bit Rate (UBR):

The UBR was originally intended for data application, which do not require tightly constrained delay or delay variation. The sources are not required to specify the bandwidth they will require.

Available Bit Rate (ABR):

The ABR mechanisms provide flow control back to the source to change the rate at which the source is submitting traffic to the network, ABR is intended for application that need a more reliable service than provided by UBR, such as critical data transfers and computer server applications.

3-1-2 Traffic Parameters

The performance of any application using an ATM network can be defined in terms of the following parameter [30]:

Throughput : Called **goodput,** bits per second delivered to the application.

Latency : The sum of the transmission delay (reduced by higher transmission speed), propagation delay (determined by physics), and queuing delay through each network element (switch).

Jitter : The variation in delay, or the variation in the inter cell arrival of consecutive cells. Certain applications, such as voice, are very sensitive to jitter.

Cell Loss : The amount of cell or packet loss the application can tolerate. Continuous services are relatively intolerant of cell loss.

3-2 Multimedia of Traffic Models

Multimedia application includes the voice, video, and data traffics, these traffics are different in nature and can applied at the terminal (TE) as shown in Figure 3-2.

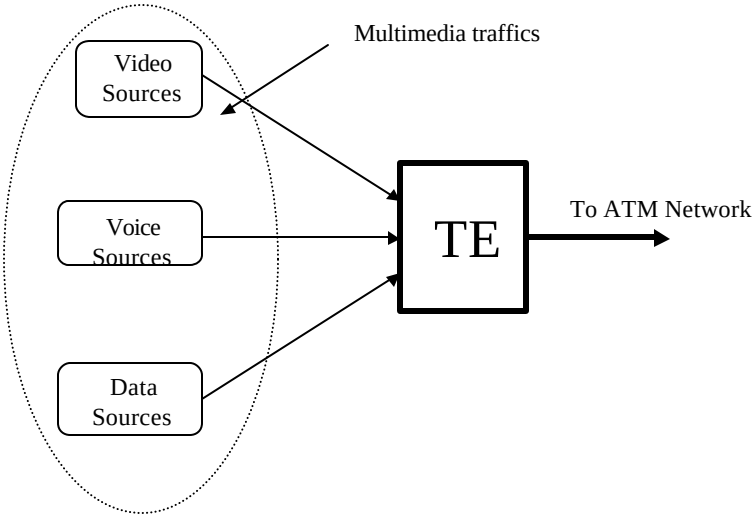

Figure 3-2 TE Trafics Configuration.

3-2-1 Voice Traffic

Figure 3-3 illustrates the block diagram of a station that encodes and sends a voice stream. Each voice source has a continuous time, analog signal is digitized by a coder as in [36]. The generated samples are accumulated in a packetizer, when the number of samples in the packetizer reaches the pre-determined cell length, header is attached then a voice cell is generated. The voice cell generation process may be synchronized to an external timing. The generated cells are stored in the transmit buffer in the order of their generation waiting for transmission.

Note that, in some LAN, the voice samples are transmitted directly using an assigned TDM channel on the network. In most other LAN protocols, the voice is transmitted in the form of cells where each cell consists of a number of voice samples within a packetization interval [37].

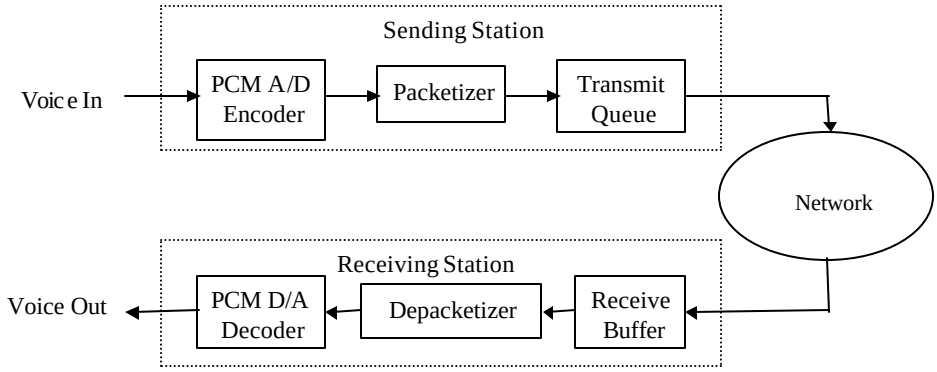

Figure 3-3 Block Diagram of a Station that encodes and sends a Voice Stream.

The voice cell delay time of end-to-end have to be in range of 250-600 ms. For voice communication (telephone), the information must be transmitted to the destination terminal in a transparent way also in ATM, as in the conventional line switching. Even if a little information is lost, the communication quality is not deteriorated. Consequently, the cell loss due to the buffer overflow (10^{-4}-10^{-3}) can be tolerated [1]. The information can be transmitted at a constant rate without fluctuation by the CBR service; a serve requirement is imposed that the end-to-end delay must be several milliseconds or less, excluding the transmission delay.

The voice is classified as voiced and unvoiced periods. In the voiced period, a cell is generated, in contrast, there is no cell generated in the unvoiced period. We can also call that the voiced period as a talkspurt and unvoiced period as a silent period. The voice source is represented by mean bit rate (MBR), and peak bit rate (PBR). Several models were introduced to model the burstiness and correlation characteristics of the cell arrival process from a voice source. The basic model is a periodic process alternating between a talkspurt and a silent period, as shown in Figure 3-4.

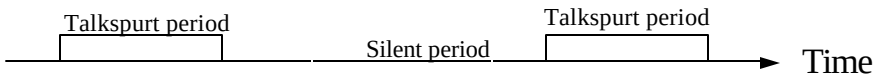

Figure 3-4 Single Voice Source Model.

Each period can be represented by an exponential distribution of means $1/a$ and $1/b$ respectively. The number of cells generated within the talkspurt period is then a geometric multiple of the cell length. Each voice source is sampled at 16 kHz and encoded using embedded PCM (Pulse Code Modulation). Hence, at a coding rate of 4 bits/sample, the source peak-rate is 64 Kbps. Let T represents the cell interarrival time, then the average arrival rate per source S (cells/sec) is given by equation (3-1).

$$S = \frac{(1/\alpha)}{T(1/\alpha + 1/\beta)} \qquad \text{---------- (3-1)}$$

It is to be noted that the randomness introduced by the deterministic time is replaced by an exponential one. The first burstiness parameter set has $1/\alpha$ = 352 ms and $1/\beta$ = 650 ms which corresponds to a 35 % activity factor [38]. The source rate is 64 Kbps, then the cell's time is 6 ms. Table 3-1 shows the scheme used in North America (also used in Japan) plus the International (CCITT) standard [39].

(a) North American			(b) International (CCITT)		
Digital signal Number	Number of voice channels	Data Rate (Mbps)	Level Number	Number of voice channels	Data Rate (Mbps)
DS-1	24	1.544	1	30	2.048
DS-1C	48	3.152	2	120	8.448
DS-2	96	6.312	3	480	34.368
DS-3	672	44.736	4	1920	139.264
DS-4	4032	274.176	5	7680	565.148

Table 3-1 North American and International TDM Carrier Standards.

The talkspurt and silent periods can also represented by the following:

$$y = 1 - e^{-\lambda t}$$

$(1- y) = e^{-\lambda t}$, take the logarithmic for both sides, we obtain

$t = - (1 / \lambda) Ln (1 - y)$

Where

(1-y): from 0.0 to 1.0

$(1 / \lambda)$: mean value of period.

3-2-2 Video Traffic

The video stream is encoded according to the standard coding such as H.261 [40] or MPEG [41,42]. In both MPEG and H.261, the frame is divided into number of 16x16 “macroblocks”, and macroblock can be coded differentially with respect to the previous frame. Moreover, in MPEG, the coded differentially with respect to both the preceding and the following frame. Figure 3-5 shows the block diagram of a station that encodes and sends a video stream over a communication network [36,41,43]. A frame is taken in the video camera, and sent as an analog signal into the frame grabber, where it is digitized. Then, the encoder compresses it. A rate buffer its purpose is to smooth out the variations in the encoder’s output rate, and follows the encoder which producing a constant bit rate stream.

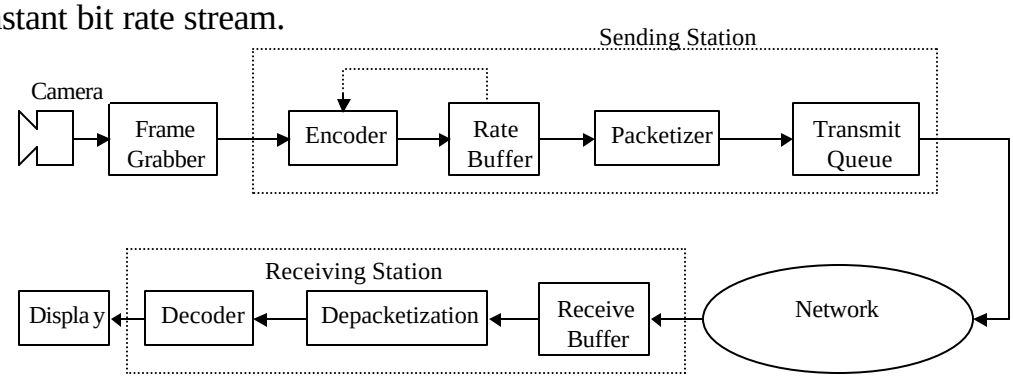

Figure 3-5 Block Diagram of a Station that encodes and Sends a Video Stream.

The buffer occupancy is used by the encoder as feedback to control the encoder output rate (and hence quality) so that the rate buffer doesn’t overflow or underflow. The constant bit rate stream is passed from the rate buffer onto the

main memory through the system bus. In order to send streams over the network, the sending station packetizes streams (as cells). The cells are sent over the network to destination station. The destination station buffers the received cells to compensate for the delay variation due to the network. The contents of the buffer are passed to the decoder, which decompresses the stream and delivers it to the display. According to a coding standard such as H.261 or MPEG, a frame is composed of a number of Groups of Blocks (GOBs). Depending on the number of pixels in a frame, it is divided into either 3 or 12 GOBs. Each GOB is in turn divided into 33 macroblocks. A macroblock contains information for an area of 16 x 16 pixels and consists of three 'blocks', two for each color component and one for the luminance. A macroblock is the smallest unit that can be encoded/decoded without any future information. Also, in both H.261 and MPEG, a macroblock can be coded differentially with respect to the previous frame [41].

A delay constraint comes from the need to support interactive communications; it is well known fact that human beings can tolerate up to 200-250 ms of delay in two-way conversation. In the communications system using compressed video, there are two delays the first in the encoder and in the decoder that can be as high as 100 ms, as well as delays in the local networks to which the video stations are attached [44]. Therefore, a reasonable constraint for the wide-area component of the delay would be 40 ms. We applied two low quality compressed video stream such as 192 Kbps, and 384 Kbps (H.261), we have also applied high-quality compressed video stream such as 1.5 Mbps and 2 Mbps.

3-2-3 Data Traffic

The data traffic is a message arrived in specific distribution. The message comes in instant of time to be sent through the network. It is insensitive to the delay time, in other word, the data arrives to the destination at any time. The buffer size must be small as possible to reduce the cost.

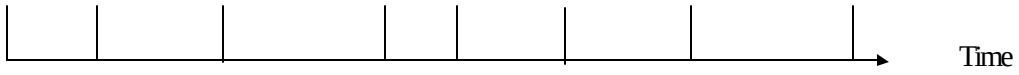

Figure 3-6 Data Traffic Generation. At every Vertical Line, the Fixed Size Message Arrives

The data traffics arrival process is defined by two parameters. First parameter is message size, and the second parameter is the interarrival period time. Figure 3-6, depicts the data traffic generation. We suppose that the message size is fixed and the interarrival period time has exponential distribution with mean value such as 5 ms, or 10 ms.

Chapter 4

ATM VP-Based Ring Network

ATM VP-based network architecture is essentially a compromise of the SONET/STM and ATM network architectures: it takes a system simplicity concept from the SONET/STM network and keeps the flexibility of ATM technology. The requirement of flexible bandwidth allocation can be achieved by the inherent characteristic of ATM technology, and the requirement of less expensive ADM's can be achieved by the simplicity of the virtual path concept and its associated nonhierarchical path multiplexing structure.

The SONET ring architecture has been widely accepted by Bellcore Client Companies (BCC's) as a cost-effective, survivable SONET network architecture due to its standard signal interface, economical high-speed signal and drop capability, fast self-healing capability, and simple network operations [4, 13].

Figure 4-1 presents SONET ring only use either the centralized ring grooming or non-demand grooming system, since the distributed ring grooming system at the DS1 (1.554 Mbps) level is too expensive to be implemented.

The centralized ring grooming system, as illustrated in Figure 4-1(a), includes a SONET ring with an ADM in each node. The ADM used in this centralized ring grooming system can be a simple add-drop multiplexer since it doesn't need the grooming capability. The signal add-drop in this case can be implemented by using a time slot assignment (TSA) method that assigns dedicated timeslots for each node and those dedicated timeslots can be dynamically assigned to DS1 ports.

Figure 4-1(b) illustrates the distribution ring grooming system, which demand grooming capability into each ring node by using a Time Slot Interchange (TSI) switching fabric within each ADM. The TSI function in this distribution ring grooming architecture is performed at the VT (DS1) level rather

than the STS-1 (51.84Mbps) (DS3) level, as commonly used for self-healing architecture [45]. Compared to the centralized ring grooming system, the distributed ring grooming system generally requires less ring capacity for the same DS1 demand requirement, but at the expensive of more complex and expensive ADM's.

To reduce SONET ring cost, an enhanced grooming system must combine the best features of centralized and distributed ring-grooming systems. In other words, the new more cost effective SONET ring grooming system should have bandwidth allocation flexibility to reduce the ring capacity requirement, as does the distributed ring grooming system using ADM/TSI's and should use simpler and less expensive ADM's like the ADM/TSA. The conceptual diagram for this enhanced SONET ring grooming is depicted in figure 4-1(c).

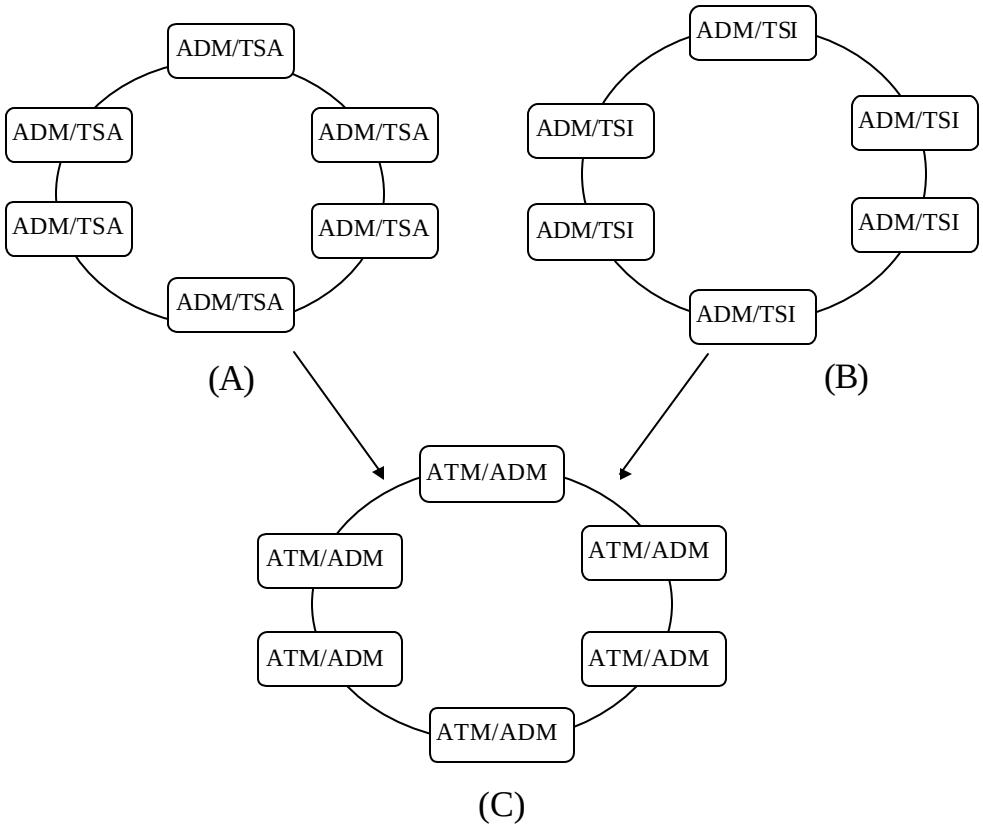

Figure 4-1 SONET Bandwidth Management System (a) Centralized. (b) Distributed. (c) Enhanced ATM system.

4-1 An ATM Ring Architecture Using VP Concepts

The VP concept is primarily used for nodal addressing for supporting different traffics routing. Figure 4-2 depicts a SONET/ATM Ring architecture using Point-to-point VP's (denoted by SARPVP with one direction only). The VP used in the point-to-point VP add-drop multiplexing scheme carries VC connections between the same two ring nodes.

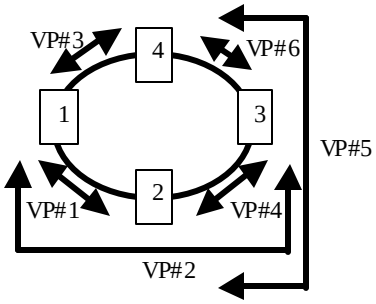

Figure 4-2 An ATM VP Ring Architecture (SARPVP)

In this SARPVP architecture, each ring node pair is preassigned a duplex VP, as shown from Figure 4-2, the VP#2 and VP# $\overline{2}$ (not shown in the Figure) are carrying all VC connections from nodes 1 to 3 and from node 3 to node 1, respectively. The physical route assignment for the VP depends upon the type unidirectional or bidirectional of the considered SONET ring. If the considered ring is a unidirectional ring two diverse routes which form a circle are assigned to each VP. From Figure 4-2, the two physical routes 1-2-3 and 3-4-1 are assigned to VP#2 and VP#2' (not shown in the Figure) that is if the considered ring is unidirectional. If the considered ring is bidirectional, only one route is assigned to each duplex VP (e.g., route 1-2-3 is assigned to both the VP#2 and VP# $\overline{2}$), and demands between nodes 1 and 3 are routed through route 1-2-3 bidirectionally. More details on SONET unidirectional and bidirectional ring architecture can be found in [45, 46].

In order to avoid the VP translation at intermediate ring nodes of VP connection, the VPI value is assigned on a global basis. The ATM cell add-drop or pass-through at each ring node is performed by checking the cell's VPI value. Since the VPI value has global significance and only one route is available for all outgoing cells, it needed not be translated at each intermediate ring node. Thus, no VP cross-connect capability is needed for the ATM/ADM of this SARPVP ring architecture. The ATM ADM for the SARPVP architecture can be implemented in different ways depending on physical SONET STS-Nc terminations.

The global VPI value assignment presents no problem here, since only one route exists for all outgoing ATM cells and the number of nodes supported by a ring is usually limited. For example, the 12-bit VPI field in the Network-to-Network Interface (NNI) ATM cell represents up to 4096 VPI values available for use. Thus, the maximum number of ring nodes is 91; let N be the number of ring nodes. The maximum number of ring nodes is the number satisfying the equation 4-1.

$$[N (N - 1)] / 2 <= 4096 \quad \text{----------} \quad (4\text{-}1)$$

Then the maximum number of nodes is 91; which is enough to practically support BCCs interoffice and loop rings. If the point-to-point VP ring is used to support present DS1 (1.544 Mbps) services (via circuit emulation), each DS1 comprises a VC connection and is assigned a VPI/VCI based on its addressing information and the relative position of the DS1 within all the DS1's terminating at the same source and destination on the ring. For example, VPI= 2 and VCI = 3 represents a DS1 that is the third DS1 of the DS1 group terminating at Node 1 and Node 3.

4-2 ATM Ring Routing

The physical route assignment for the VP depends upon the type of the considered SONET ring. There are two types, the first one is called unidirectional SONET ring and the second one is called bidirectional SONET ring. In the unidirectional SONET ring, the routing in ATM/ADM node is point-to-point as shown in Figure 4-3.

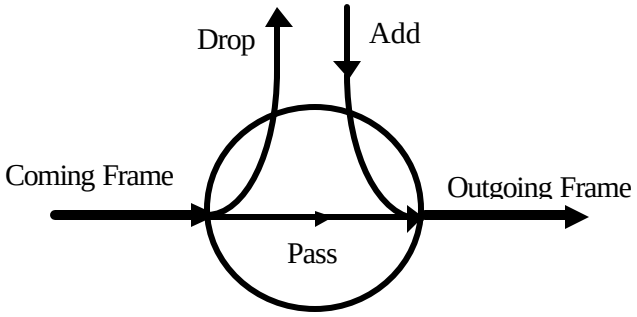

Figure 4-3 ATM/ADM Node in Unidirectional SONET Ring Network

The maximum number of physical hops in the unidirectional SONET ring is (N-1) hops, depending upon the number of nodes (N). By using VPIs, it can define that node as either transit node or terminator node. For example, the node #1 transmits cells to node #2 via the route 1→2. Node #2 transmits cells to node #1 via route 2→3→4→1, obviously that the number of physical hops in a direction is more than in opposite direction, so the time needed to the pair conversation is not equal.

In the bi-directional SONET ring, the routing is point-to-point, as can be noted in an ATM/ADM node shown in Figure 4-4. The maximum number of physical hops is | N/2 | hops, and it is also dependent on the number of nodes (N). Each node has VPIs values counting (N-1) values.

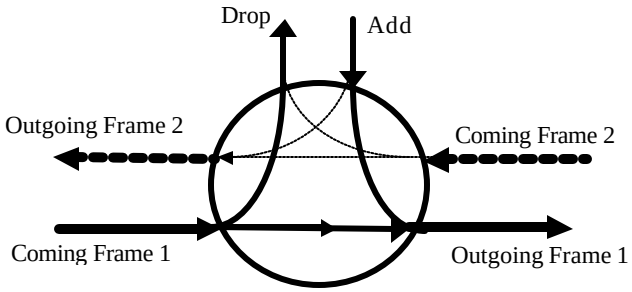

Figure 4-4 ATM/ADM Node in Bidirectional SONET Ring Network

That is lead us to say the direction is forward if it takes the path of (1 → 2→3→…→N), other wise, the direction is reverse if it takes the path (N→ (N-1) →...→3→2→1). If (N-1) is even, the number of VPIs for both forward and reverse directions are equal, but with different values of VPIs, however, there is no VPI has the same value in the ring network. If (N -1) is odd, the number of VPIs in forward direction is more than the number of VPIs in reverse direction by one. The direction that the send cells can follow depends upon the location of source and destination and the number of hops between them the following algorithms are used for these purposes: -

Algorithm 1:

Hop_count algorithm (S: source , D : destination)

Min = MINMUM (S, D)

Max = MAXIMUM (S, D)

if (|N/2| >= (Max - Min) hop_count = Max - Min

Else Hop_count = N - (Max - Min)

Algorithm 2:

```
Dir_flag algorithm (S: source, D: destination)
    Min = MINMUM (S, D)
    Max = MAXIMUM (S, D)
    Hop = Hop_count (S, D)
    If (hop = Max - Min)
        If (S < D)      Dir_flag = forward
        Else            Dir_flag = reverse
    If (hop = N - (Max - Min))
        If (S < D)      Dir_flag = reverse
        Else            Dir_flag = forward.
```

Each node can determine its cell direction and the number of hops to other node by using the above algorithm. Finally, we assume that there is a queue for each direction that makes the bidirectional SONET ring works as two separated unidirectional SONET ring. In other word, the bidirectional SONET ring can service number of sources equals to double of the number of sources in the case of unidirectional SONET ring.

In case of the number of nodes is odd, if there are two routing paths available which have the same number of physical hops, it choose the forward direction because that direction is the original direction and it has the highest priority. It is to be noted that, the forward direction is the routing of (1→2→3→...→N), and the reverse direction is the routing of (N → (N-1) →... →3→ 2→1).

4- 3 ATM Add-Drop Multiplexer (ADM) for VP Rings

The ATM/ADM for the SARPVP architecture can be implemented in different ways depending on physical SONET STS-Nc terminations. The most

common architectures are in [4]. The ATM STS-Nc terminations are STS-3c, STS-12c, and STS-48c, although only the STS-3c ATM termination has been specified in current CCITT Recommendations.

4-3-1 The Cost Model for SARPVP Ring.

Figure 4-5 depicts a functional diagram for an ATM/ADM STS-3c termination for SARPVP ring. In this Figure, each STS-3c needs a chip to implement a full-duplex ATM and SONET interface function, and a chip for the ATM header processor (checking VPI values and idle cells).

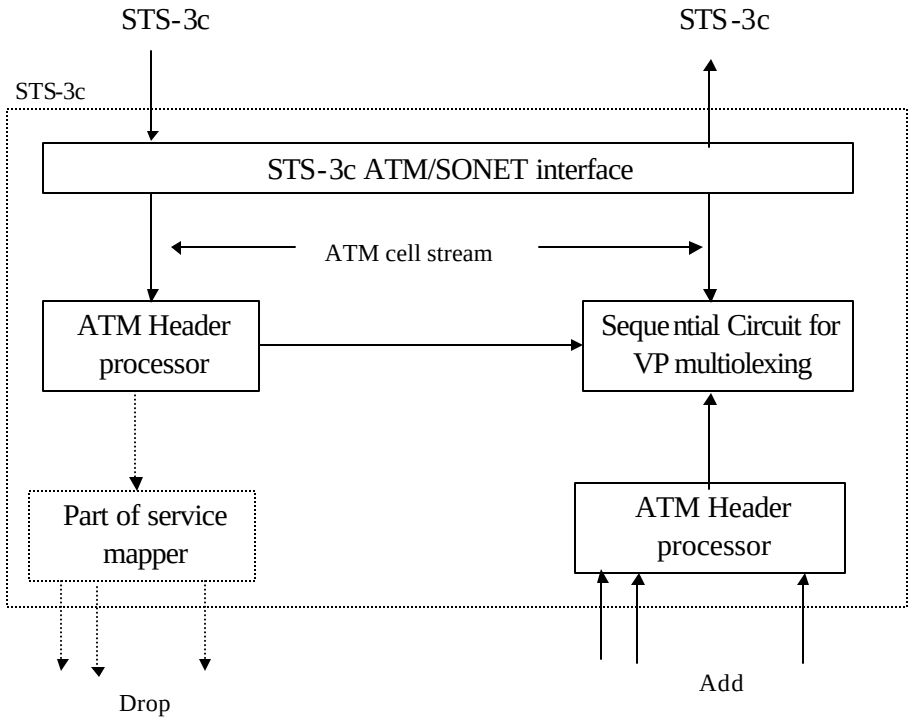

Figure 4-5 STS-3c Chip Count Model for the SARPVP Ring.

A chip performing ATM cell processing for added cells is also needed. A chip is needed for the sequential access protocol for VP multiplexing. Thus, each STS-3c termination requires four chips to the necessary VP add-drop functions. Each STS-3c payload may carry up to 86 DS1 for circuit emulation as computed below. The cell format for DS1 circuit emulation (i.e., Class I in the AAL layer) is

depicted in Figure 4-6. In this Figure, each ATM cell has a fixed length of 53 bytes. There are five bytes for the ATM layer overhead and one additional byte is needed for cell sequencing and its protection. Thus, only 47 bytes are available for carrying DS1 service demands.

SN : Sequence Number.
SNP : Sequence Number Protection.
SAR : Segmentation and Reassembly.
SDU : Service Data Unit.

Figure 4-6, ATM Cell Format for DS1 Circuit Emulation.

Thus, the maximum number of DS1's that can be carried by each STS-3c payload is calculated by equation 4-2 [4].

$$\text{Max. number of DS1's} = \left| \frac{(T\_Rate) \, x \, (R\_Frame) \, x \, (R\_Cell)}{DS\,1} \right| =$$

$$= \left| \frac{155.52 \, x \, \frac{260}{270} \, x \, \frac{47}{53}}{1.544} \right| = 86 \qquad \text{----------} \quad (4\text{-}2)$$

T_Rate : Transmission data rate in Mbps
R_Frame : Ratio of transmission frame payload to transmission frame
R_Cell : Ratio of cell payload to cell.

Note that, 260/270 is the ratio of non-SONET overhead bytes to the SONET frame size for a STS-3c, and 47/53 is the ratio of payload information field to the ATM cell size. Finally, the ratio of payload to the frame size equals to (260/270) x (47/53), thus the payload is equal to 155.52 times the fraction of payload. Thus, the maximum number of DS1 in STS-3c is equal to the fraction of data rate line (payload) over data rate of each DS1 (1.544 Mbps). We can also

define the maximum number of sources by the previous equation, the 1.544 Mbps is replaced by the source rate.

4-3-2 ATM/ADM for SARPVP Ring

Figure 4-7 depicts a possible ADM configuration with STS-3c termination for a SARPVP ring implementation that supports many services via circuit emulation. The ATM VP add-drop function, which is performed at the STS-3c level, requires three major modules.

The **first module** is the ATM/SONET interface, which converts the STS-3c payload to an ATM cells stream and vice versa. The functions performed in this module include all delineation, self-synchronization, and scrambling. The scramble process here is to increase the security and robustness of the cell delineation process against malicious users or unintended simulations of a cell header followed by a correct Header Error Control (HEC) in the information field. This mechanism is required for ATM cell delineation.

The **second module** is to perform header processing, which includes cell addressing (VPI in this case) and HEC. In order to perform cell add-drop/pass-through, this module checks VPI value of each cell to determine if it should be dropped or passed through. This module also identifies idle cells which can be used to insert cells from the considered office (i.e. signal adding) via a simple sequential access protocol. This sequential access protocol can be implemented by the third module that passes through each nonidle cell and inserts the added cells from each queue into outgoing idle cells in a sequential order.

The **third module** is the sequential access protocol that passes through each nonidle cell and insert the added cells into outgoing idle cells in a sequential order. The third functional module also includes a service-mapping module that maps ATM cells to their corresponding destination cards based on VPI/VCI values of ATM cells. This service distributes ATM cells to corresponding

groups according to their VPI values. For each group, the ATM cells are further divided and distributed to the corresponding cards by checking their VCI values. This service-mapping module essentially just performs a simple VPI/VCI comparison function.

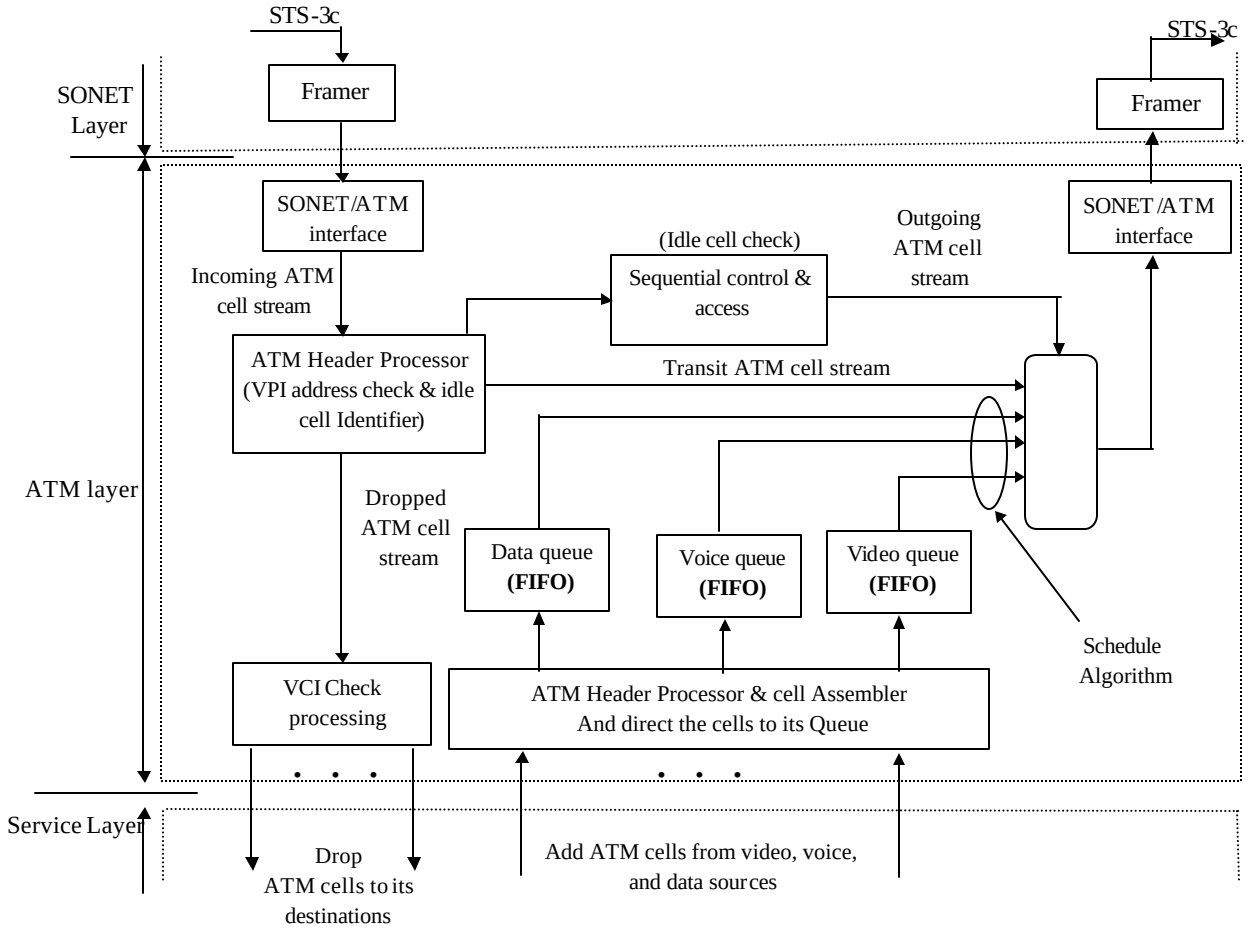

Figure 4-7 An STS-3c Add-Drop Hardware Configuration for the SARPVP Ring

4-4 The Queue Model in ATM ADM *Node.*

4-4-1 Queue Model for One Traffic.

This subsection describes the queue model for one queue to each source within the node and a single queue for the node as shown in Figure 4-8. The coming cell to the input of the queue has longer waiting time from all the sources. Clearly that all the cells entered to the input queue of the node are mixed from different sources and service as FIFO.

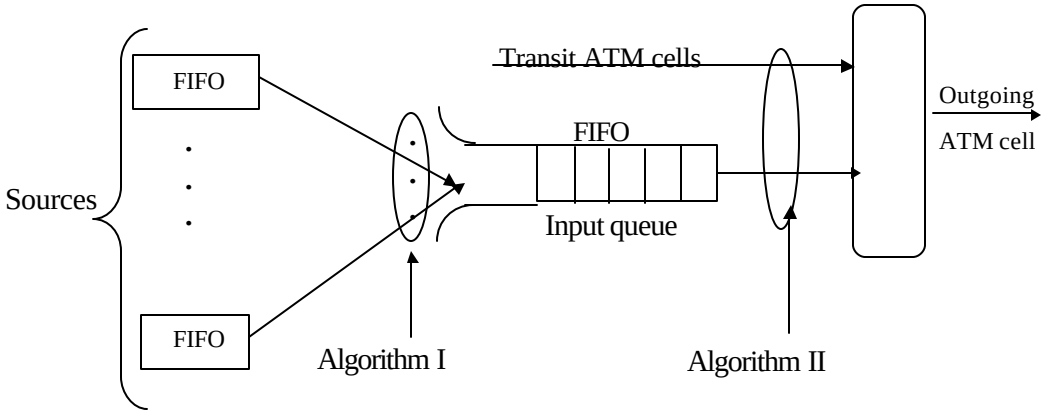

Figure 4-8 Queue Model of ATM/ADM Node.

Two algorithms are used with that queue model as shown in Figure 4-8. Algorithm I, determines which cell has longest waiting time to enter into the input queue of the node. Algorithm II, determines the number of transit ATM cells, and completes the stream flow from the input queue, the following steps describe the two algorithms:

Algorithm I:

1- Determine the longest waiting time cell from the whole sources within the node.

2- Push these cell in the input queue of the node.

3- Go top step 1.

Algorithm II:

1- Get transit ATM *cell.*

2- Determine the number of transit ATM *cells.*

3- If (the number of transit cells < the frame size in cells)

Then, Add cells from input queue to complete the frame.

Else, No addition.

4- Transmit stream of cells as Frame size cells.

5- Go to step 1.

4-4-2 Queue Model for More Than Traffic

This subsection describes the queue model for more than traffic with a single input queue of a particular node. There are three kinds of control methods, described in details in [1].

First method: Single Queue method (SQ). The cells are arriving from various sources in a mixed way and entered to the input queue and processed by FIFO rule.

Second method: Band Division method (BD). Here the band is divided and allocated before hand to various kinds of medium and the cells from a single kind of medium utilize the allocated semi-fixed bandwidth (corresponding to the virtual path).

In this method, the model contains the dedicated queue and server for each medium, as shown in Figure 4-9, FIFO processing is applied to each medium. In Figure 4-7, the sum of the processing powers of the servers is kept constant since it corresponds to the total bandwidth of the transmission channel.

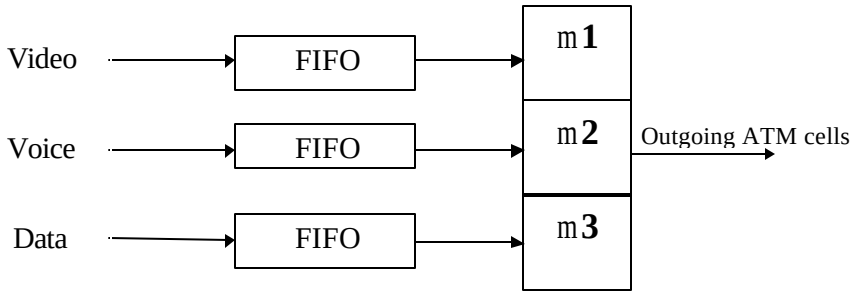

Figure 4-9 Queuing Model of BD Method.

Third method: Priority Queue Control method (PQC). The queue in this method, is provided for each medium and the number of cells to be picked up from the queue is specified with their the priority. This method can be modeled as the multiple queues, as shown in Figure 4-10.

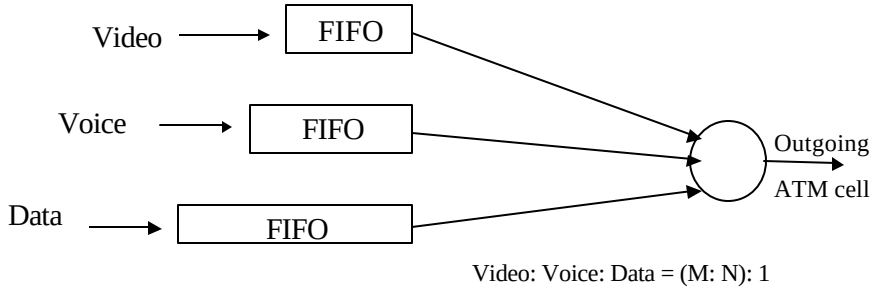

Figure 4-10 Queuing Model of PQC Method

The processing rule in each queue is FIFO. The method is divided into the following two:

1- video cell exhaustive method: As shown in the Figure 4-11, the video cell is processed as long as a cell exists in the video queue. If the video queue becomes empty, the voice and data cells are processed alternately.

2- processing ratio control method: In this method, the number of cells to be picked up from the queue corresponding to each medium is determined as following.

- *For the voice and the video cells with severe requirements for the delay, the ratio of cells picked up from the queues is set as N : M when either of the queues becomes empty, the cells are only picked up from the other queue for service.*
- *Only, if both of the aforementioned queues are empty, a cell picked up from the data queue.*

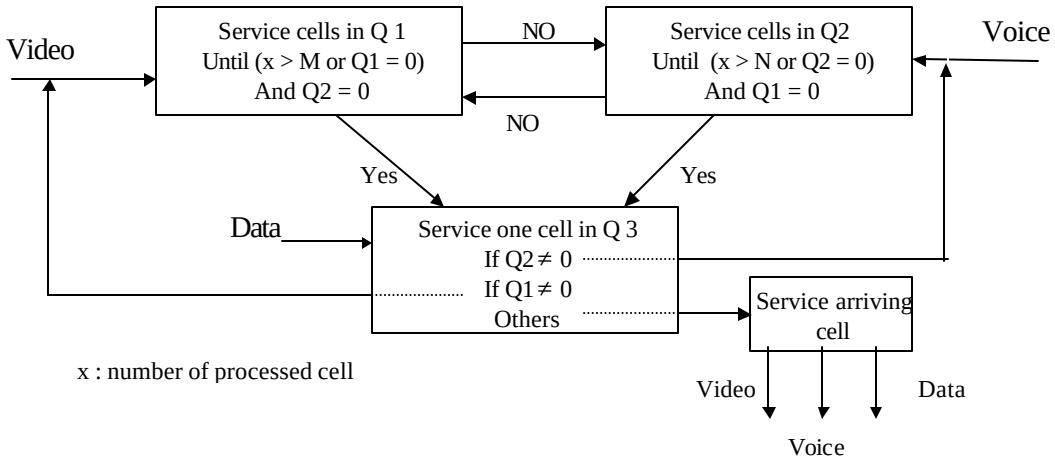

Figure 4-11 Processing Discipline Algorithm

4-4-3 The Proposed Control Method.

In the previous control methods [1], there are fixed ratio among traffics along the service time. That is caused some weak results when the data traffic offered load is dominant than the video and the voice traffics, resulting in unfairness among the traffic and the cells which were picked up from the queue corresponding to each traffic. The following algorithms proposed to overcome this problem:

** Let the number of cells to be picked up from Video, Voice and Data queues is M: N: D respectively.*

** To determine the ratios of all traffics, you should follow the next.*

1. Gets min = Minimum offered load of all applied traffics.

2. Set M = Video offered load / min.

3. Set N = Voice offered load / min.

4. Set D = Data offered load / min.

The proposed control mechanism method [47] provides the network to service fairly among all the applied traffics. However if the offered load of all

traffics is equal, then the ratio will be 1: 1: 1 for Video, Voice, and Data respectively. Figure 4-12, shows the processing algorithm of the proposed control mechanism method.

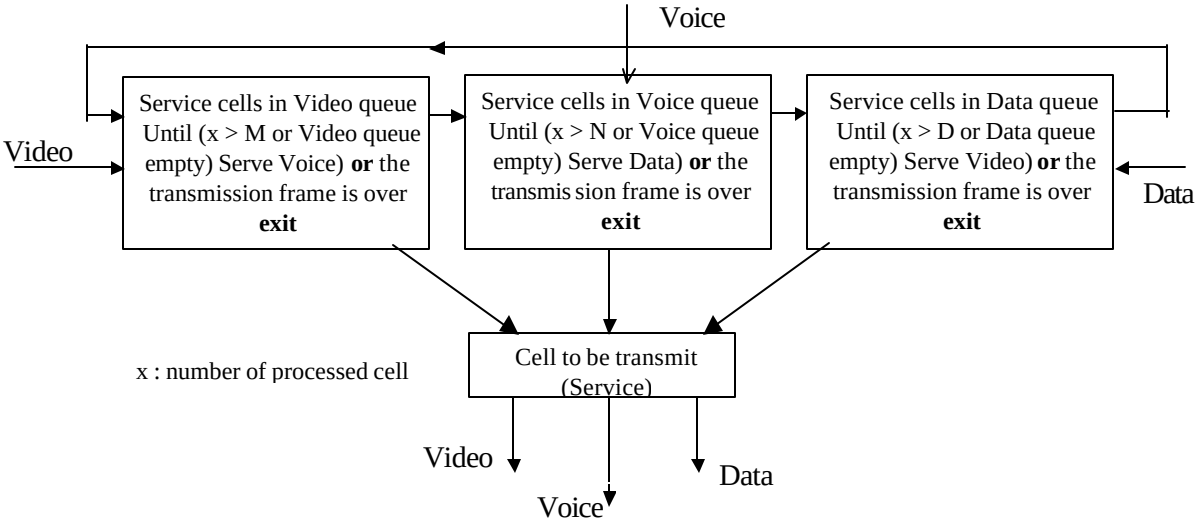

Figure 4-12 Processing Discipline Proposed Algorithm

If there are only two traffic such as video and data and their offered load are 0.25 and 0.10 respectively, then the ratio will be 2: 1 for video and data respectively. On the contrary, if the offered load of video and data are 0.10 and 0.25 respectively, then the ratio will be 1: 2 for video and data respectively. So we can say that the proposed control mechanism method has priority to the traffic within the node. However, with the proposed control mechanism method the node picks up cells from video queue, before picking up cells of voice and data queues. Also, the node picks up cells from voice queue, before picking up cells of data queue. Finally, we can say that the video traffic has higher priority than voice traffic and the voice traffic has higher priority than data traffic. It is to be mention here that is all the above depends upon the offered load of each traffic and the control mechanism method.

4-5 Proposed Fair Organizer for Calling

The VP concept is primarily used to nodal addressing for supporting different traffics routing. The VP used in the point-to-point VP add-drop multiplexing scheme carries VC connections between the same two ring nodes.

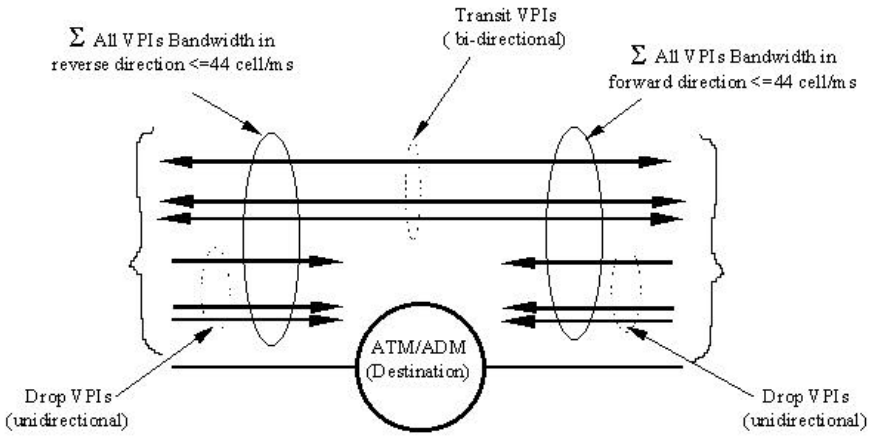

Figure 4-13 the VPIs of ATM/ADM

Figure 4-13 illustrates VPIs of ATM/ADM and the bandwidth in each direction. Each node has two types of VPI, transit VPIs that are in bidirectional and drop VPIs that has different VPI values. The sum of VPI bandwidths in physical link is not more than 44 cell/ms, each node, in the network of N nodes, has (N-1) drop VPI because the ATM ring network is point-to-point connection. The whole drop VPIs are not in the same direction but some in the forward direction and the other in the reverse direction. The number of drop VPIs in both directions depends on the number of nodes in the ATM ring network (i.e. if N is odd, the number of drop VPIs in both directions is the same. If N is even, the number of drops VPIs in forward direction is more than number of drops VPIs in reverse direction by one). In order to define the number of drop VPI in each direction and the number of transit cell in each direction, there are two functions for that.

We have proposed that the destination node define the bandwidths for each call dynamically depending on the QoS of each call, and satisfied the equation in which the sum of VPI bandwidths in physical link is fixed at 44 cell/ms.

4-6 Broadband Network Performance

Broadband networks based on ATM cell transfer must meet certain performance requirements in order to be accepted by potential users and network providers. In this section, a brief discussion will be given about ATM layer-specific network performance. However, the quality of service (QoS) as perceived by the user may be influenced not only by the ATM transport network performance but also by higher layer mechanisms. Cells belonging to specified virtual connection are delivered from one point in the network to another. For example, from A to B. A and B may indicated the very endpoints of a virtual connection, or may delimit a certain portion of the cell transport route (for example, A and B may indicate national network boundaries of an international ATM connection). Because there is some transfer delay, cells sent from A arrive at B within $\Delta t > 0$ (see Figure 4-13). Note that the cell exits event occurs when the first bit of the ATM cell has completed transmission across A, and the cell entry event occurs when the last bit of the ATM cell has completed transmission across B. A Discussion about measuring cell delay and cell delay variation or cell jitter is presented in [21].

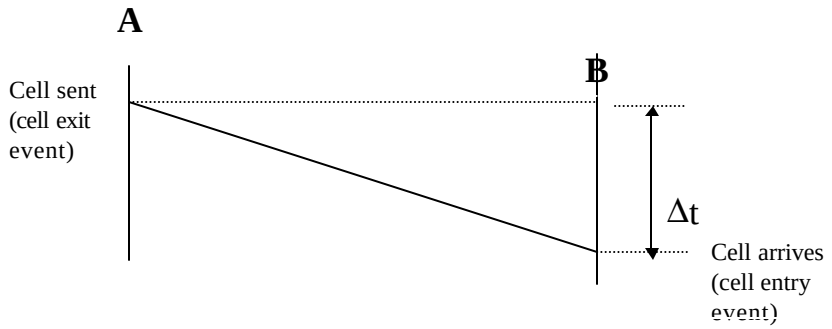

Figure 4-13 Cell Transfer (Schematic)

In order adequately to describe the quality of ATM cell transfer, ITU-T recommendation first defines the following outcome categories:

. Successfully transferred cell.

. Errored cell.

. Lost cell.

. Misinserted cell.

If Δt is less than a maximum allowed time T (the exact value is not yet specified) and the cell is not affected by bit errors, then the cell has been successfully transferred. If the cell arrives in due time but there are one or more bit errors in the received cell information field, the cell is errored. A lost cell outcome occurs if the cell arrives after time T (or never reaches B). Errors in the ATM cell header that can not be corrected or cell buffer overflows in the network (for example, in an ATM switch) lead to lost cells. If a cell that has not been sent from A on this virtual connection arrives at B, then this misdelivered cell produces a misinserted cell outcome. Header errors that are not detected or are erroneously corrected may produce misinserted cells. By making use of the above considerations, it is possible to define the performance parameters. The parameters and their definitions are listed in Table 4-1[21].

Parameters	Definition
Cell loss ratio.	Ratio of lost cells to transmitted cells.
Cell misinsertion rate.	Number of misinserted cells per second.
Cell error ratio.	Ratio of errored cells to the number of delivered (Successfully transferred + errored) cells.
Cell transfer delay	Δt.
Mean cell transfer delay	Arithmetic average of a specified number of cells transfer delays.
Cell delay variation.	Difference between a single observation of cell transfer delay and the mean cell transfer delay on the same connection.

Table 4-1 ATM Performance Parameters

There are other parameters such as Throughput (TP) and Offered load (OL). Throughput of a network is defined as the number of cells delivered to their destination station per unit of time. An analysis of throughput, cell loss and delay is discussed in [48]. Offered load (cells/sec) is defined as the number of cells transmitted by all subscribers. Here, the offered load is defined as the ratio of the transit ATM cells plus the added ATM cells to the maximum transmitted ATM cells through the link. So the maximum number of cells can be determined with keeping in mind that the SONET frame has approximately 44 cells. The transmission frame is transmitted in 0.125 ms, the transmitted rate equals to 44/0.125=352 cell/ms. Figure 4-14 depicts the offered load of the ADM/ATM Node.

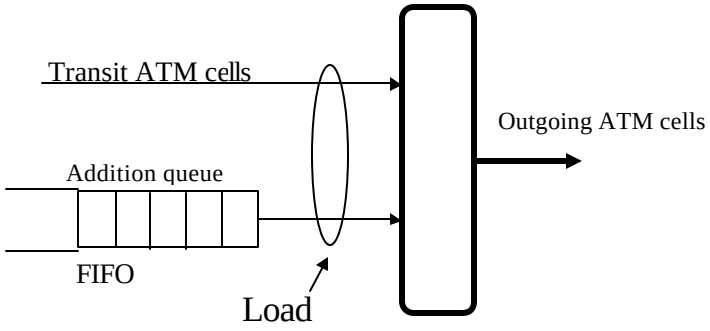

Outgoing ATM cells = transit ATM cells + added ATM cells.

Load = Outgoing ATM cell per unit of time

Offered load = Load (cells/ms) / 352 (cells/ms).

Figure 4-14 Offered load of ATM/ADM Node

The successful probability of a cell passing through the network is determined by equation (4-3). Thus, the TP is calculated by equation (4-4) by given the arrival rate of the OL.

P(cell success) = 1 – P(cell loss) ---------- **(4-3)**

TP = OL (1 – P(cell loss)) ---------- **(4-4)**

Dividing the throughput (TP) by the effective input load (OL), gives probability of the success cell which also represent the node utilization by the following equations (4-5), and (4-6).

U = P(cell success) = TP/ OL ---------- **(4-5)**

P(cell loss) = 1 - (TP/ OL) ---------- **(4-6)**

Usually most arriving cells wait in the queue for at least one time slot. However, under a light load of traffic, more cells can be delivered directly through the network upon their arrivals. An end-station queuing model is shown in figure 4-15. The total cell delay consists of three components: queuing time, access time and transmission time [49].

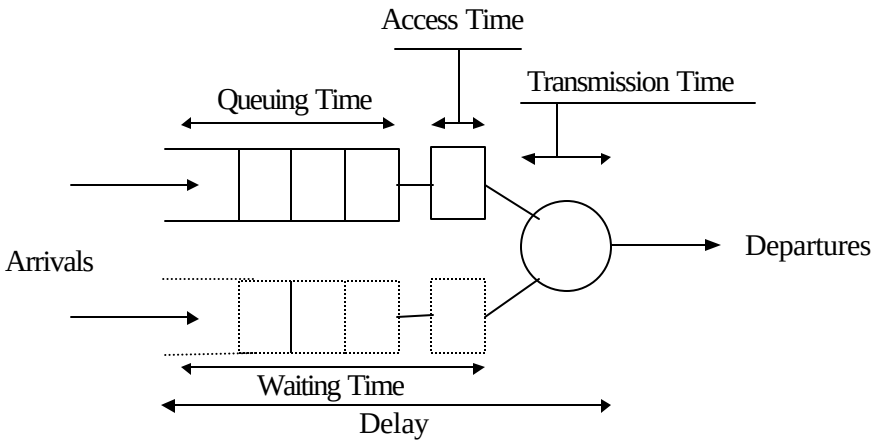

Figure 4-15 End-Station Delay Model

The queuing time is the time a cell spends in the queue, (i.e. from the time it arrives to the queue to the time it reaches to the head of the queue. The access time is the time elapsed from the moment a cell reaches the head of the queue to the time a transmission frame is captured for its transmission. The transmission time is the time needed to transmit a cell.

4- 7 Simulation Check Point

In this section a simulation checkpoint is presented. It is the classic example and the analytical techniques required rather elementary. Whereas these techniques do not carry over into more complex queuing system, the behavior of queue model is in many ways similar to that observed in the more complex cases.

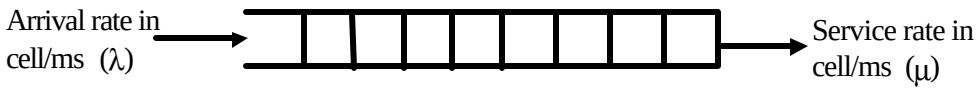

Figure 4-16 The Queue model

The queue model is defined by many parameters such as arrival rate (l), service rate (m), traffic intensity (r), Mean Waiting Time (MWT), and Average queue size (B_{siz}). Figure 4-16 describes the queue model, which can be represented by the following equations [50].

$$r = \frac{l}{m} \qquad \text{----------} \qquad \textbf{(4-6)}$$

$$\textbf{MWT} = \frac{1}{m}\left(\frac{1}{1-r}\right) \qquad \text{----------} \qquad \textbf{(4-7)}$$

$$\mathbf{B_{siz} = (MWT)}\ l \qquad \text{----------} \qquad \textbf{(4-8)}$$

A comparison between the results of the simulation and the analytical can be shown in Figure 4-17.

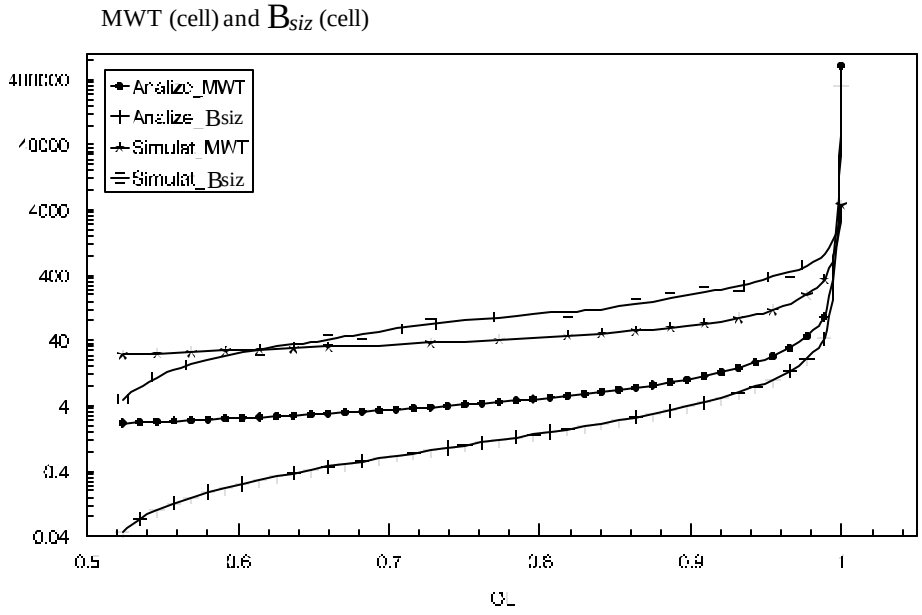

Figure 4-17 Comparison between Analytical and Simulation Results

Figure 4-17 illustrates the MWT and B_{siz} versus OL, it is very clear that the behavior of both analytical and simulation results is almost similar. However, as the OL increases, the MWT and B_{siz} slightly increasing up to saturation limit. Beyond the saturation limit, MWT and B_{siz} sharply increase, this is due to the huge number of cells which increases the MWT and MBS. Also cearly that at a certain OL, MWT and B_{siz} in the case of simulation results are more than MWT and B_{siz} in the case of analytical results. That is because the system serve the coming cells by rate of 352 cell/ms for time interval 0.0625 ms and wait with no serve the coming cells in next time interval of 0.0625 ms. To make the simulation model closed to the analytical model, we have to considered the service time as effective service time (0.0625 ms) as shown in the Figure 4-18.

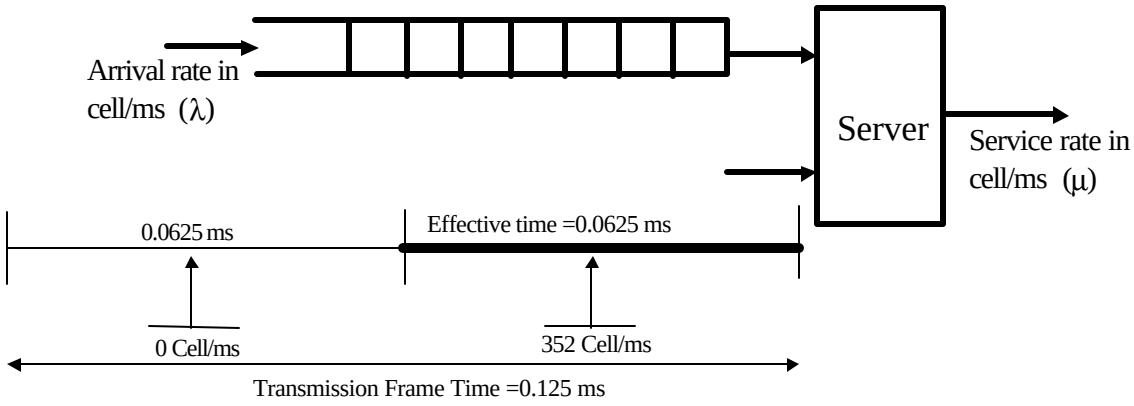

Figure 4-18 Simulation Queue Model

In the simulation model, the server picks up cells from the queue by rate equal to 352 cell/ms through the time interval of 0.0625 ms, then no service for the cell within the next interval of 0.0625 ms, and so on. Another results of the simulation and analytical have been compared using equation used in Figure 4-19. The simulation and analytical results have the same characteristic behavior as shown in Figure 4-19, the increasing of OL, increases MWT and B_{siz} up to saturation limit. Beyond the saturation limit, MWT and B_{siz} rapidly increase because the increasing of OL after the saturation limit increases the number of cells resulting in long queue and MWT. From the Figure, it is also obviously that at a certain OL, MWT of simulation and analytical models are closed to each other and B_{siz} of simulation and analytical models are closed to each other. By the way, the analytical results are approximation results and the purpose of the analytical model to confirm that the proposed simulation is working properly.

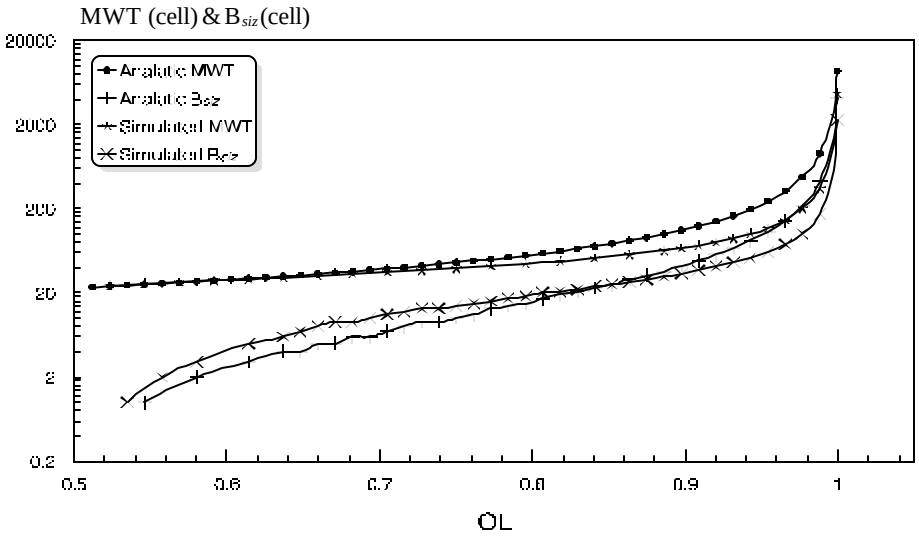

Figure 4-19 Comparison between Simulation and Analytical Results

Chapter 5

ATM VP-Based Ring Network Exclusive Video or Data Traffics

In this chapter, the performance characteristic of the proposed ATM VP-Based Ring Network exclusive video or data traffic is studied. The maximum capacity is also located for unidirectional and bi-directional nodes, however, the results indicate that the capacity is double in case of using unidirectional nodes. We have to mention here that some of performance results are closed to the results in [51], such as the relation between the offered loads versus end-station delays, inspite the difference in the proposed model and generation of traffic.

We have explained the relationship between number of video sources (N_{vi}) and many parameters such as Mean Waiting Time (MWT) which represents the time spent in the queue from the last bit arrived to the whole cell delivered, and Maximum Buffer Size (MBS) required for supporting the sources. The following represents the definition we have used such as the Utilization of the node as (U), the Throughput as (TP), the fixed video encoding rate as (R_{vi}), and the Offered video Load as (OL_{vi}). The frame transmission time (t_f) is 0.125 ms depending on SONET STS-3c, the frame size (F_s) is 44 cells depending on both cell size (53 octets) and payload size in transmission frame (2340 octets). However, the calculation of the transmission rate (R_T) is given by the following equation (5-1).

$$R_T = \frac{F_s(cells)}{t_f(ms)} = 352 \text{ cell/ms} \quad \text{..... (5-1)}$$

..

The transmission rate (R_T = 352 cell/ms) is used for the supported video sources and the transit cells (i.e. the cells coming from previous node to next node). The transit rate has the range from 0 cell/ms to 352 cell/ms, and the

average transit rate (GR_t) theoretically is calculated from the following equation (5-2).

$$GR_t = \frac{352(cell/ms) - 0(cell/ms)}{2} = 176 \text{ cell/ms} \quad \cdots\cdots\cdots\cdots\cdots\cdots \quad (5\text{-}2)$$

.

5-1 ATM Exclusive Video Traffic Only.

Video traffic is represented as video stream and generated from codec for various encoding rates such as MPEG (2 and 1.5 Mbps), H.261 (384 Kbps), and low quality (192 Kbps), as explained in chapter 3.

The main goal is to locate the maximum capacity of the video sources (N_{vi}), which depends on R_{vi}. However, the ideal maximum values of N_{vi} depends on R_{vi} (Kbps) and R_T =352 cell/ms, follows the SONET physical transmission as can seen in the following equations (5-3) and (5-4)

$$\text{max. } N_{vi} = \frac{352(cell/ms) - transit\_rate(cell/ms)}{GR_{vi}(cell/ms)}, \quad \cdots\cdots\cdots\cdots\cdots\cdots \quad (5\text{-}3)$$

.

$$\text{where, } GR_{vi} = \frac{Rvi(Kbps)}{47(octets)x8(bits)}(cell/ms) \quad \cdots\cdots\cdots\cdots\cdots\cdots \quad (5\text{-}4)$$

.

Using equations (5-3) and (5-4) helps to calculate GR_{vi}, for each video source and maximum N_{vi} for various values of R_{vi}. Table 5-1 summaries the ideal maximum N_{vi} for various values of R_{vi}.

From Table 5-1, obviously the increasing of R_{vi} decreases N_{vi}, this is because the increasing of R_{vi} increases GR_{vi} (from equation 5-4); resulting in increases number of video cells generated, which has significant effect on the number of video sources (N_{vi}) that can be served by the network.

In fact the measured N_{vi} definitely would be less or equal to that ideal calculated values.

R_{vi}	Ideal max. N_{vi}
192 Kbps	345
384 Kbps	173
1.5 Mbps	44
2.0 Mbps	34

Table 5-1 Ideal Maximum N_{vi}

The following values of R_{vi} we have used in our simulation studies: 192 Kbps, 384 Kbps, 1.5 Mbps, and 2 Mbps respectively. That is to study the video MWT, MBS, U_{vi}, and TP_{vi} versus N_{vi}, and video MWT and MBS versus offered load (OL_{vi}).

Figure 5-1 shows video MWT versus N_{vi} sources, for the values of R_{vi} have mentioned above. From Figure 5-1 obviously that the increasing of R_{vi}, increases number of cells resulting in decreases the number of video sources (N_{vi}). The video MWT slightly increases with the increasing of N_{vi} up to the saturation limits after that video MWT sharply increases due to the large number of cells and queuing delay. It is to be mentioning here that the saturation limit that corresponds to the maximum N_{vi} decreases with the increasing of R_{vi} according to the equations 5-3, and 5-4.

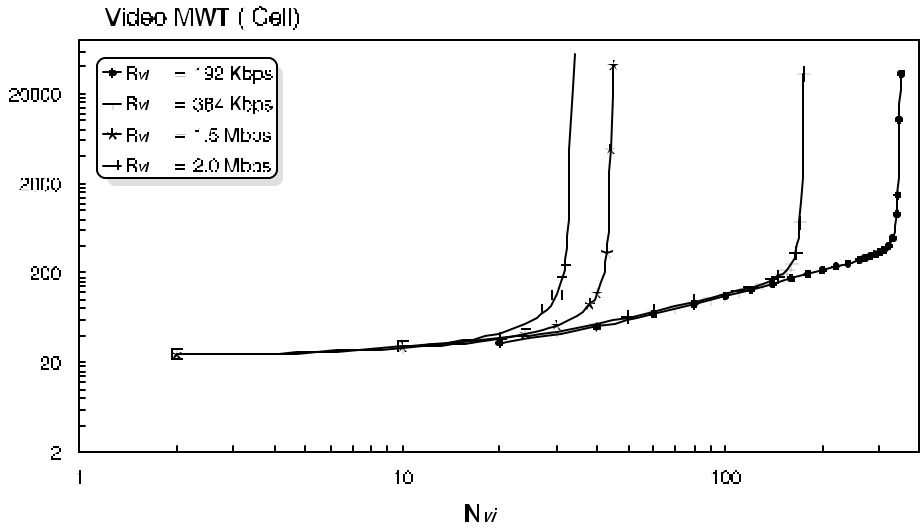

Figure 5-1 Video MWT versus N_{vi}.

Figure 5-2 depicts video MWT versus OL_{vi}. The video MWT slightly increases with the increasing of OL_{vi} up to the saturation limit then video MWT sharply increases due to the fact that the generated video cells are much more than the transmitted cells resulting in long video MWT. The video MWT decreases as R_{vi} increases because the transmission of cells increases with the high R_{vi} resulting in short video MWT.

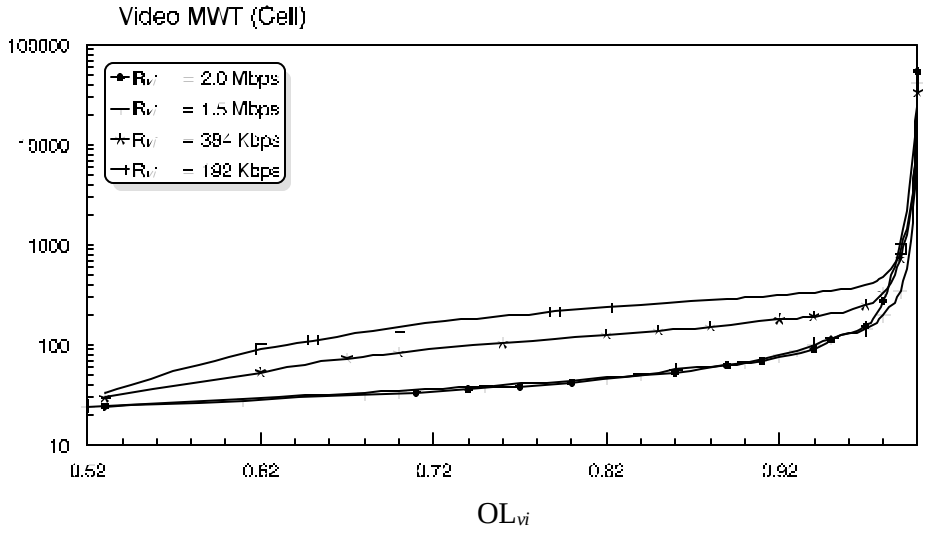

Figure 5-2 Video MWT versus OL_{vi} .

Figure 5-3 illustrates video MBS in cells versus N_{vi}, for the values of R_{vi} mentioned above. The video MBS is the maximum number of cells enters to input video queue at any time. It may be less than the maximum value, and not more. The behavior is similar to that of Figure 5-1. So, the video MBS slightly increases with the increasing of N_{vi} up to the saturation limit, after that the video MBS sharply increases, this is due to the large number of cells waiting in the queue for transmission. The video MBS and N_{vi} decrease as the R_{vi} increases for the same reasons mentioned with Figure 5-1.

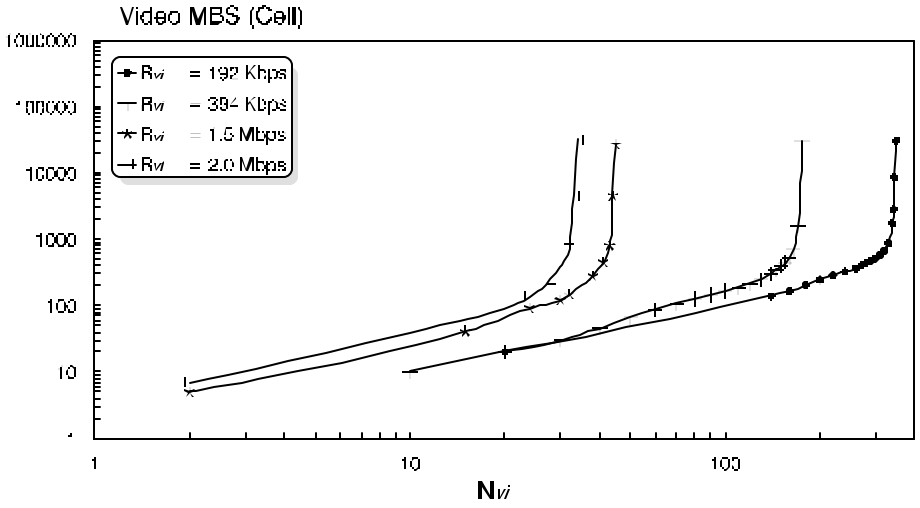

Figure 5-3 Video MBS versus N_{vi}.

Figure 5-4 depicts video MBS versus OL_{vi}. The video MBS slightly increases with the increasing of OL_{vi} up to the saturation limit then video MBS sharply increases due to the fact that the generated cells are much more than the transmitted cells resulting in large number of video cells waiting for transmission (i.e. large video MBS). The video MBS decreases as R_{vi} increases because the transmission of cells increases with the high R_{vi} resulting in small video MBS (similar to Figure 5-2).

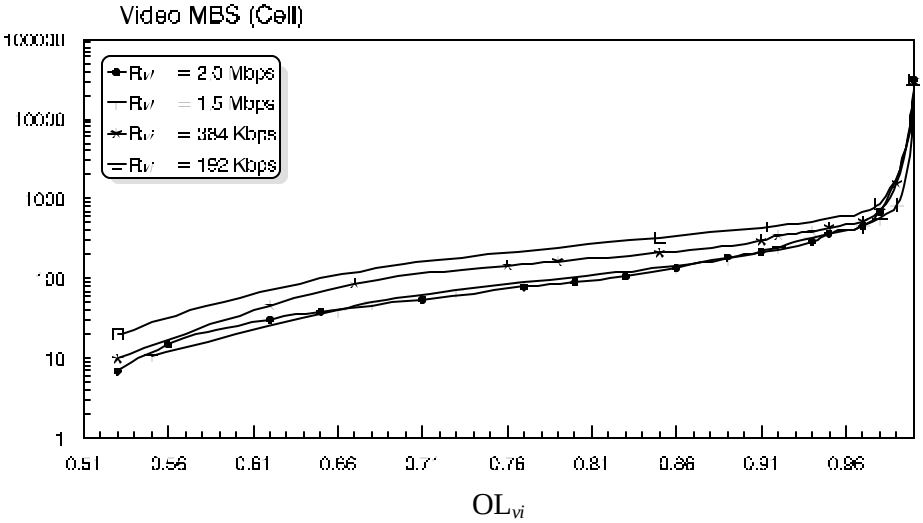

Figure 5-4 Video MBS versus OL_{vi}

Figure 5-5 shows U_{vi} versus N_{vi}. The U_{vi} remains constant with the increasing of N_{vi}, up to the saturation limit of N_{vi}, then U_{vi} slightly decreases, this is because after the saturation limit the node couldn't serve any video cells resulting in decreases of U_{vi}. It is to be mention here. That the saturation limit depends upon R_{vi} that is because the number of the generated cells is almost equal to the service duration of these generated number of cells, resulting in constant value of U_{vi}.

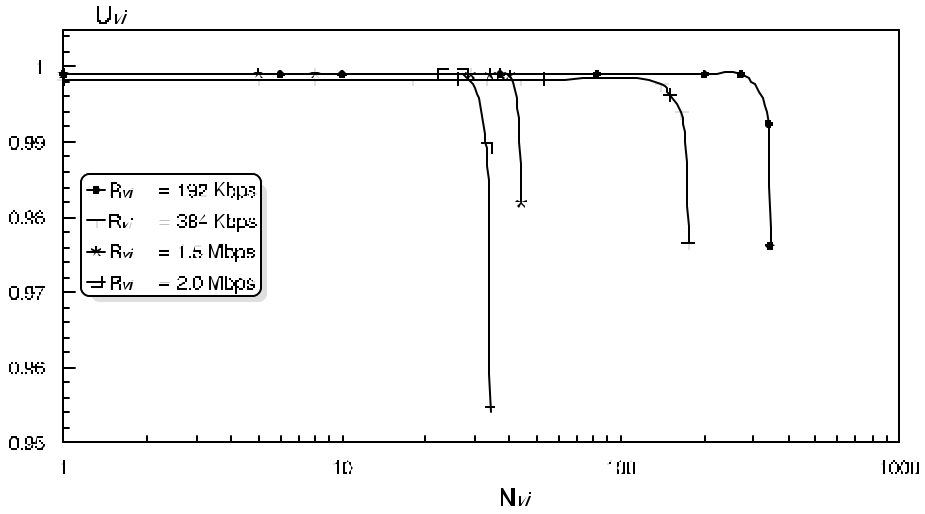

Figure 5-5 U_{vi} versus N_{vi}

Figure 5-6 illustrates TP_{vi} versus N_{vi}. From the Figure the increasing of N_{vi}, increases TP_{vi} up to saturation limits. Beyond the saturation limits, the TP_{vi} remains constant because the generated number of video cells is greater than the number of cells to be served. Also, it is clear that the increasing of $R_{vi,}$ reduces N_{vi} (i.e. reduces the saturation limits). Table 5-2 summaries the results of the proposed ATM/ADM exclusively video traffic only.

R_{vi}	N_{vi}	Video MWT (cell)	Video MBS (cell)	OL_{vi} (ratio)	U_{vi} (ratio)
192 Kbps	342	1490.7	2819	0.997	0.993
384 Kbps	170	732.14	1579	0.994	0.994
1.5 Mbps	43	346.96	827	0.988	0.999
2.0 Mbps	32	277.6	700	0.984	0.999

Table 5-2.

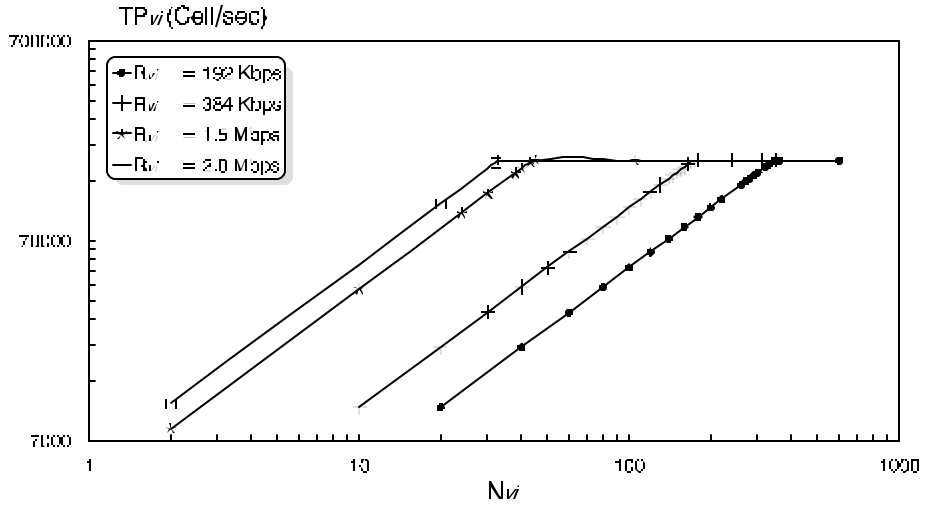

Figure 5-6 TP_{vi} versus N_{vi}.

5-2 ATM Exclusive Data traffic only

The data traffic consists of one message or several messages, its arrival process defined by two parameters; message size (M_{siz}) and interarrival time which is presented by an exponential distribution with mean values (μ) equal to 5 and 10 ms, as explained in chapter 3.

The ideal maximum message size (M_{siz}) which depends on μ can be calculated from the following equations (5-5) and (5-6).

$$\max. M_{siz} = \frac{352(cell/ms) - transit\_rate(cell/ms)}{(1/m)cell/ms]}, \quad \text{.....} \quad (5\text{-}5)$$

.

$$\text{where, } GR_{da} = \frac{M_{siz}(Cell)}{m}(cell/ms) \quad \text{.....} \quad (5\text{-}6)$$

.

By substituting in the above equations (5-5) and (5-6), we can get the ideal maximum M_{siz} for various values of μ, obviously from the equations the increasing of μ, increases M_{siz}. Table 5-3 summaries the ideal maximum M_{siz} will full load carried by the node (i.e. OL_{da} 100 %)

m	Ideal max. M_{siz}
5 ms	880
10 ms	1760

Table 5-3 the Ideal max. M_{siz} cells.

In our simulation studies, we have assumed that μ equals to 5 and 10 ms respectively, that is to study the different performance characteristics such as data MWT, MBS, U_{da}, and TP_{da} versus M_{siz}, data MWT and MBS versus OL_{da}.

Figure 5-7 depicts Data MWT versus M_{siz},. The data MWT smoothly increases with the increasing of M_{siz} up to certain M_{siz} (depending on the value of m). The data MWT increases more than started values of M_{siz}, this is because the increases of M_{siz} increase the service times, resulting in long queue and the data message suffers long MWT. Within the interval 5 ms, the node transmits $\frac{m(ms)}{t_f(ms)} = \frac{5ms}{0.125ms} = 40$ frames, each frame includes an average of 22 cells. The M_{siz} of 500 cells needs to (500cells/22cell/frame) 23 frames. Then, the needed frames are less than the transmitted frames within 5 ms.

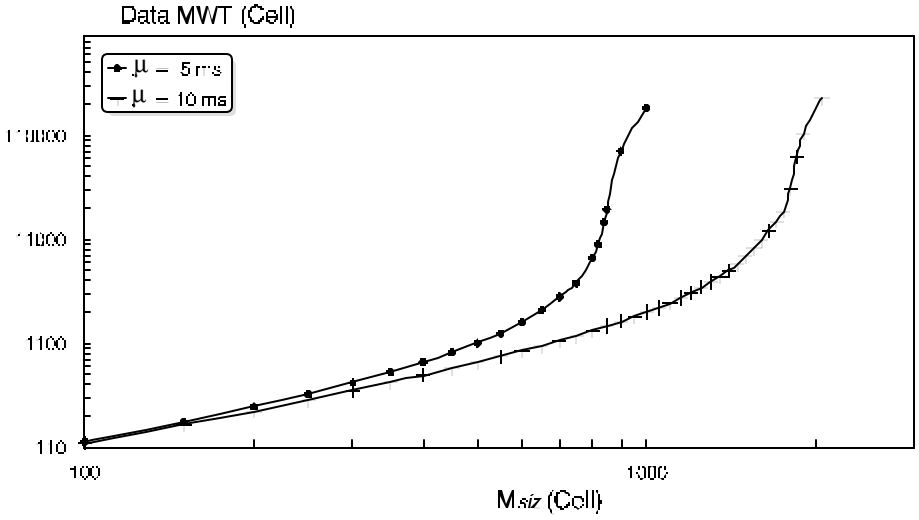

Figure 5-7 Data MWT versus M_{siz} .

Figure 5-8 shows data MWT versus OL_{da}. Clearly that the data MWT is slightly increases with the increasing of OL_{da} up to the saturation limit, then it sharply increases for the same reasons mentioned above. The absolute value of MWT depends upon the value of μ. Obviously, that the increasing of μ increases the MWT, this is because the increases of μ, increases the M_{siz} resulting in very long MWT.

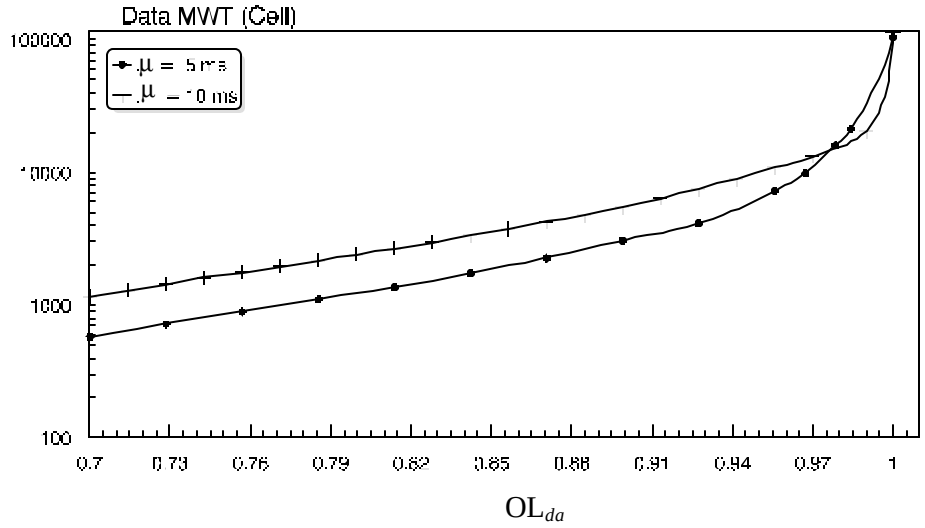

Figure 5-8 Data MWT versus OL_{da}.

Figure 5-9 illustrates data MBS versus M_{siz}. From the Figure, it is clear that the increasing of M_{siz} slightly increases data MBS up to saturation limits. Beyond the saturation limits, the data MBS is rapidly increase for the same reasons mentioned with Figures 5-7 and 5-8.

Figure 5-10 shows data MBS versus OL_{da}. The data MBS slightly increases with the increasing of OL_{da} up to the saturation limit, then data MBS sharply increases due to the same reasons mentioned above. It is to be mention here that the data MBS decreases as m decreases, because μ has a significant effect in M_{siz}, however, the decreasing of μ decreases M_{siz} resulting in short service time, which yields short queue and data MBS.

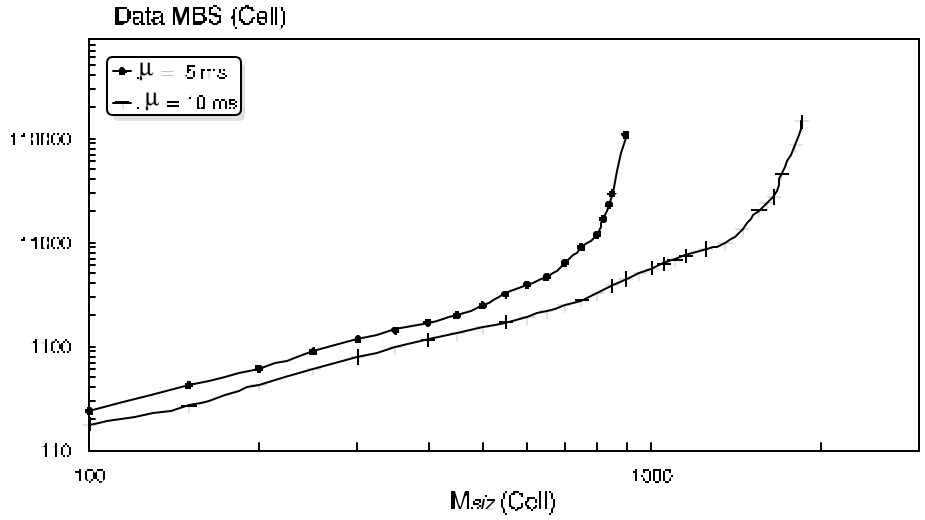

Figure 5-9 Data MBS versus M_{siz}.

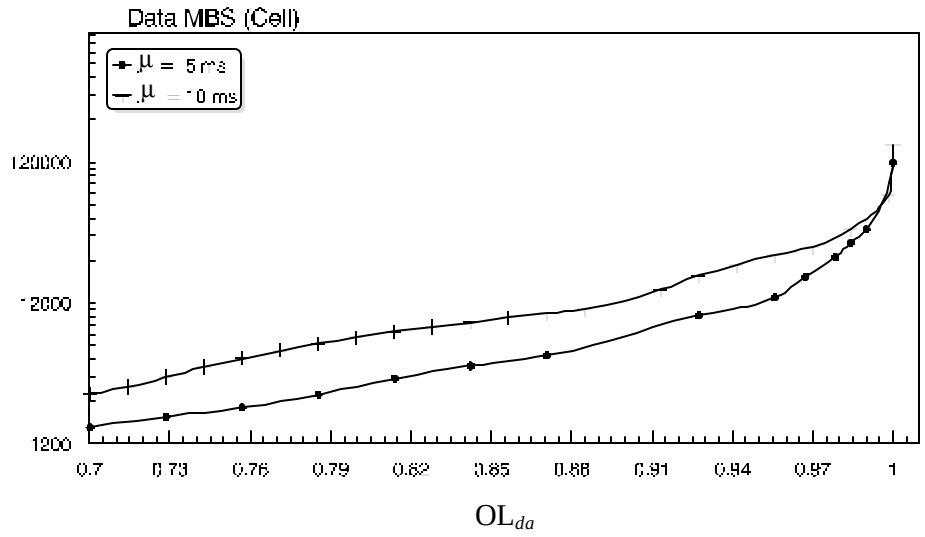

Figure 5-10 Data MBS versus OL_{da}

Figure 5-11 depicts U_{da} versus M_{siz} with μ equal to 5 and 10 ms respectively. The M_{siz} has no affect on U_{da}, therefore, U_{da} remains constant up to saturation limits which corresponding to the optimal M_{siz}, beyond U_{da} sharply decreases, because the increases of M_{siz} after optimal length decreases the

number of cells to be service resulting in decreases the U_{da}. Obviously, that with long μ the number of cells generated reduces, therefore, the saturation limit (optimal M_{siz}) is with longer M_{siz} as shown in Figure 5-11 (μ =10 ms). It is necessary to mention here that the optimal M_{siz} (saturation limit) depends upon μ, in which optimal M_{siz} increases with the increasing of μ.

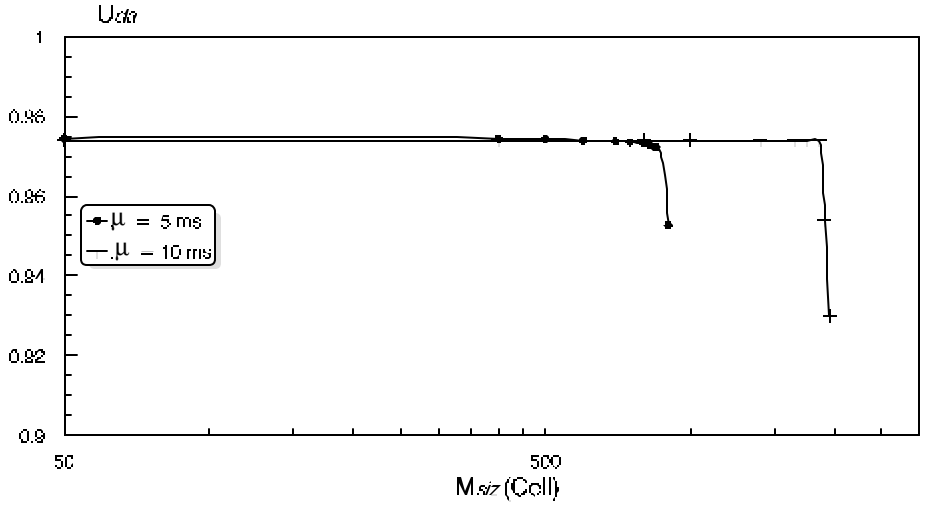

Figure 5-11 U_{da} versus M_{siz}

Figure 5-12 depicts TP_{da} versus M_{siz}. Obviously, that the increasing of M_{siz}, increases TP_{da} up to the saturation limits. Beyond the saturation limits, TP_{da} remains content because there is no chance for more service to cells. Again, recall that the saturation limit depends on μ. Table 5-4 summaries the results of the proposed ATM/ADM exclusively data traffic only.

m	M_{siz}	Data MWT (cell)	Data MBS (cell)	OL_{da} (ratio)	U_{da} (ratio)
5 ms	860	28133.9	32580	0.997	0.99
10 ms	1750	20422.0	32652	0.998	0.99

Table 5-6

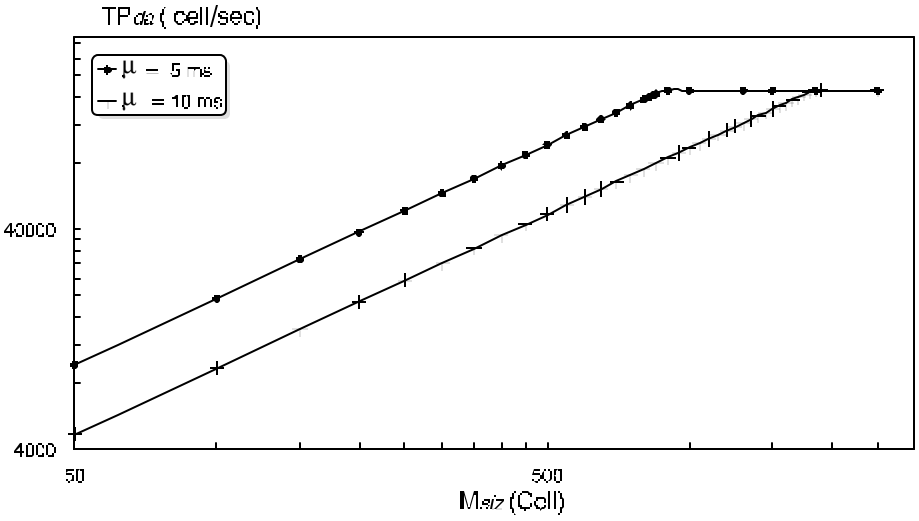

Figure 5-12 TP_{da} versus M_{siz}

Chapter 6

ATM VP-Based Ring Network Exclusive Two traffics

In this chapter, the performance characteristic of the ATM VP-Based Ring Network exclusive the integration of video/data traffics and video/voice traffics is considered.

The same characteristics we have studied in chapter 5, have been considered here to study the effects of the integration of two traffics on the networks performance.

A proposed method namely "Control Mechanism Method" [47] to determine the number of cells to be service from each queue traffic is presented. It provides fairness among the traffics as explained in chapter 4.

6-1 The Integration of Video/Data Traffics

In our study, we have defined the number of video sources as (N_{vi}), Video encoding rate as $R_{vi,}$ which equals to 1.5 Mbps as a fixed data rate, and the data traffic as message size (M_{siz}). The interarrival time is represented by an exponential distribution with mean value (^{m}) equals to 5 ms. The study of the integration of video and data traffics starts with M_{siz} having various fixed values. We have to mention here that the maximum N_{vi} depending on both GR_{vi} and GR_{da}. However, the calculation of the ideal values of N_{vi} from equation (6-1), depends on GR_{vi} in cell/ms, where R_T =352 cell/ms depends on SONET physical transmission, and transit rate in cell/ms.

$$\text{Max.}N_{vi} = \frac{[352(cell/ms) - transit\_rate(cell/ms)] - GR_{da}}{GR_{vi}} \quad \text{----------} \quad (6\text{-}1)$$

Using equation (6-1) helps to find out the maximum N_{vi} for various values of M_{siz} as shown in Table 6-1. It is to be noted here that the increasing of M_{siz}

decreases the maximum N_{vi}, this is because the long M_{siz} yields less number of messages to serve resulting in few sources get the networks service and vice versa.

M_{siz}	Ideal max. N_{vi}
100 cells	39
200 cells	34
400 cells	24

Table 6-1 Ideal Maximum N_{vi}.

Figure 6-1 illustrates video MWT and data MWT versus N_{vi} for R_{vi} equals to 1.5 Mbps, m =5 ms and M_{siz} equals to 100, 200 and 400 cells respectively. From the Figure it is clear that video and data MWT are slightly increasing with the increasing of N_{vi} up to the saturation limit, which depends upon the M_{siz} length. After that those sharply increase due to the fact that the increasing of N_{vi} increases the number of cells resulting in long queue and MWT. Obviously, MWT increases with the increasing of M_{siz}, this is because the increasing of M_{siz} yields long messages, which require long service time therefore, the queue and MWT increase. The data MWT is longer than video MWT, this is because the highest priority for service is given first to video cells, then followed by data cells.

Figure 6-2 illustrates video MWT and data MWT versus OL, with the same values of R_{vi}, m and M_{siz} used above in Figure 6-1. Clearly that, the video and data MWT behave the same behavior in Figure 6-1. That is video and data MWT slightly increase with the increasing of OL up to the saturation limit, beyond MWT sharply increases, this is due the same reasons we have mentioned above. Also, the increase of data MWT is more than the video MWT, for the same reasons mentioned with Figure 6-1.

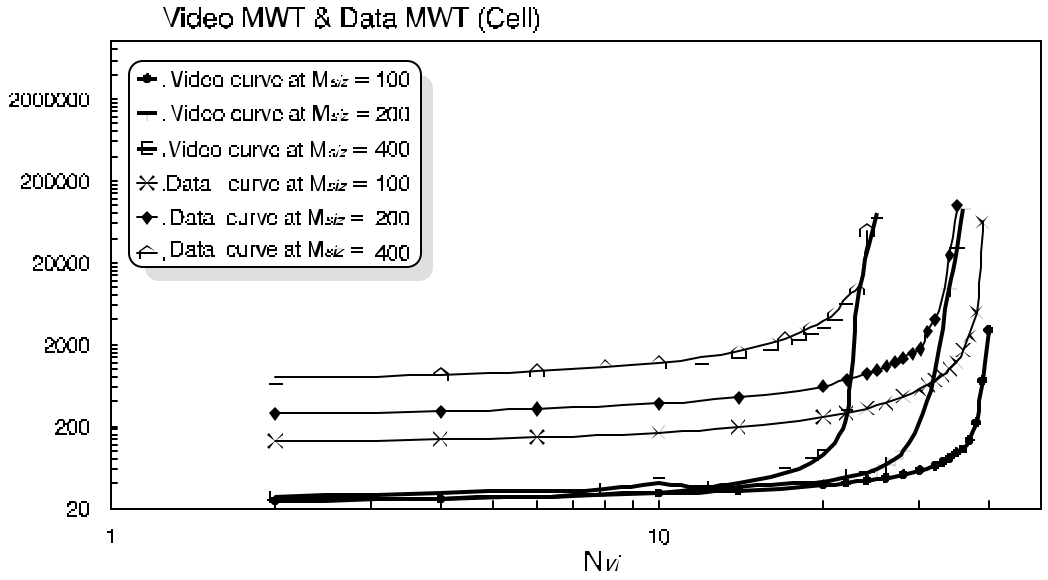

Figure 6-1 Video MWT & Data MWT versus N_{vi}

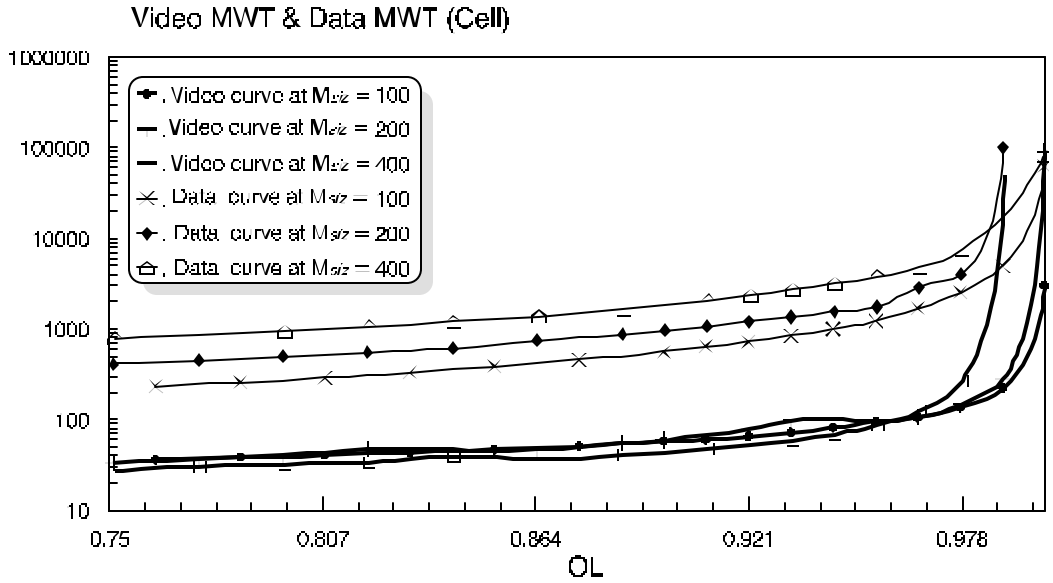

Figure 6-2 Video MWT & Data MWT versus OL

Table 6-2 summaries the simulation results which represents the maximum N_{vi} which can be supported by the network, and the corresponding video and data MWT for various values of M_{siz}.

M_{siz}	N_{vi}	Video MWT (cell)	Data MWT (cell)	OL
100	37	135.81	2556.15	0.98
200	32	148.29	4005.80	0.98
400	22	269.40	7526.24	0.98

Table 6-2 Simulation Results of Figure 6-1 and 6-2.

Figure 6-3 shows video MWT and data MWT versus M_{siz}, for R_{vi} equals to 1.5 Mbps, μ = 5 ms and N_{vi} equals to 10 and 20 respectively. From the Figure, it is clear that video MWT almost remains constant with the increasing of M_{siz}, meanwhile the data MWT slightly increases with increasing of M_{siz} up to the saturation limit, which depends upon the N_{vi}. After that, the data MWT monotonically increases due to the fact that the increasing of M_{siz} increases the number of cells resulting in long queue and MWT. Obviously, MWT increases with the increasing of N_{vi}, this is because the increasing of N_{vi} yields large number of cells which requires long service time therefore the queue and MWT increase. The data MWT is longer than video MWT, this is because the highest priority for service is given first to video cells, then followed by data cells.

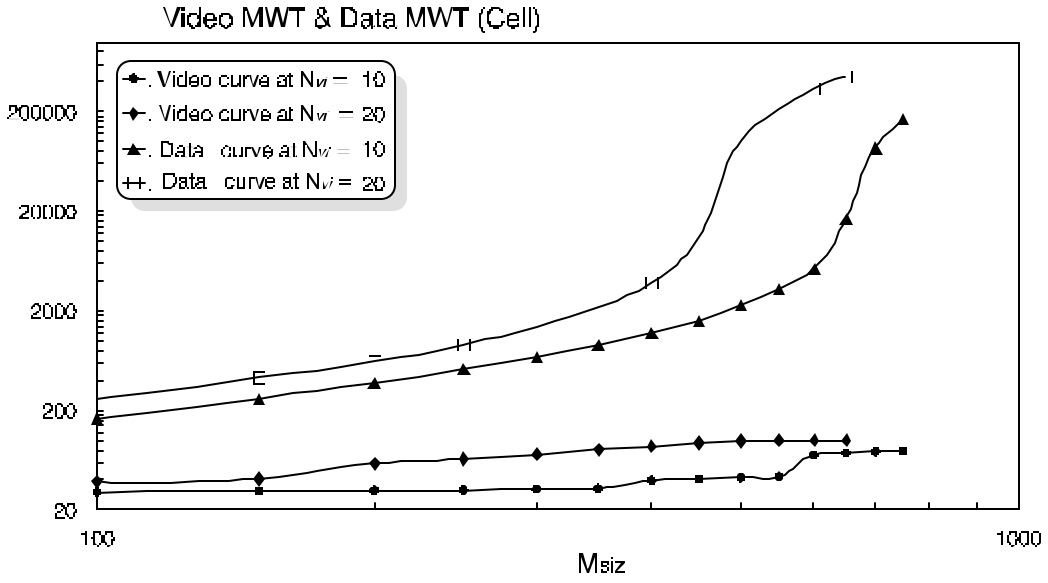

Figure 6-3 Video MWT & Data MWT versus M_{siz}

Figure 6-4 illustrates video MWT and data MWT versus OL, with the same values of R_{vi}, μ, and N_{vi} used above in Figure 6-3. Clearly that the video and

data MWT behave the same behavior in Figure 6-3. That is the video MWT almost remains constant, meanwhile, the data slightly increases with the increasing of OL up to the saturation limit, beyond data MWT sharply increases, this is due to the same reasons we have mentioned above.

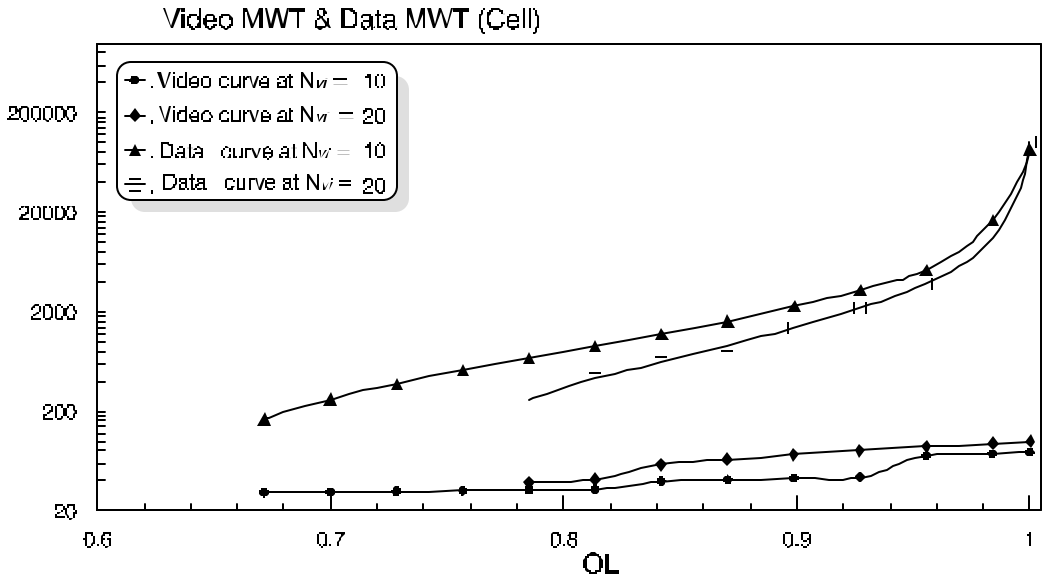

Figure 6-4 Video MWT & Data MWT versus OL

Figure 6-5 and Figure 6-6 indicate the video and data MBS versus N_{vi} and OL (total Offered Load for video and data traffics) respectively. For the same values of R_{vi}, m, and M_{siz} used with Figure 6-1 and 6-2. The characteristics of both Figures are more or less very closed to that of Figure 6-1 and Figure 6-2, for the same reasons.

Table 6-3 summaries the simulation values as that of Table 6-2.

M_{siz} (cell)	N_{vi}	Video MBS (cell)	Data MBS (cell)	OL
100	37	412	1004	0.98
200	32	370	2563	0.98
400	22	380	7201	0.98

Table 6-3 Simulation Results of Figure 6-5 and 6-6.

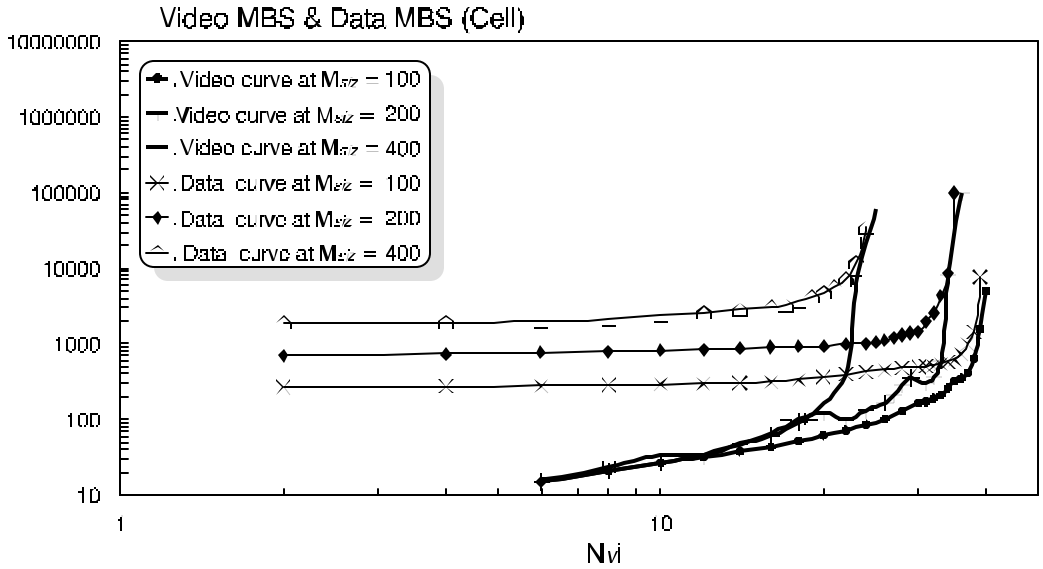

Figure 6-5 Video MBS & Data MBS versus N_{vi}

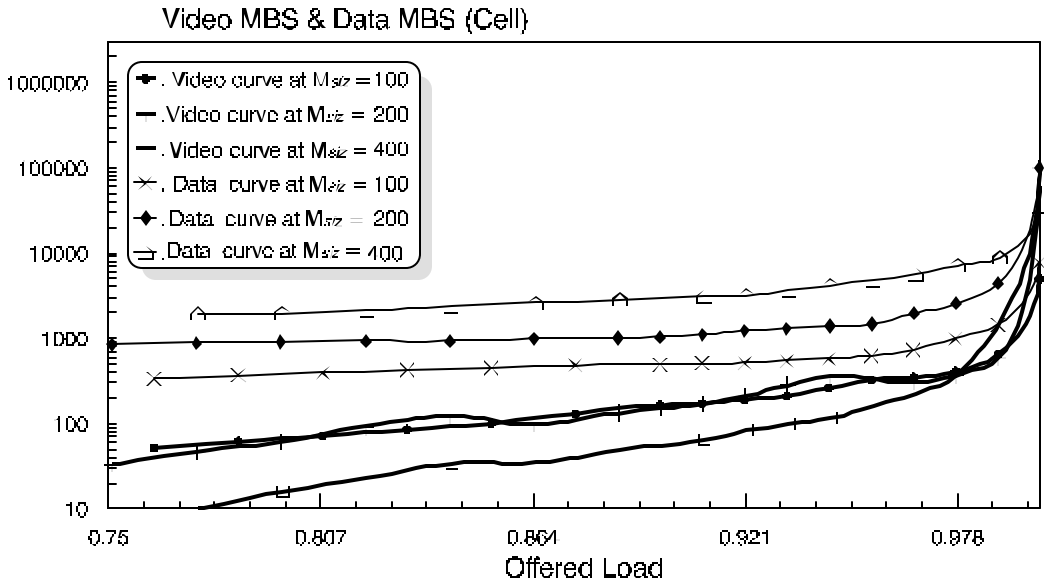

Figure 6-6 Video MBS & Data MBS versus OL

Figure 6-7 and Figure 6-8 illustrate the video and data MBS versus M_{siz} and OL respectively, for the same values of R_{vi}, and μ used above, and N_{vi} equals to 10 and 20. The characteristics of both Figures are more or less very closed to that of Figures 6-3 and 6-4, for the same reasons.

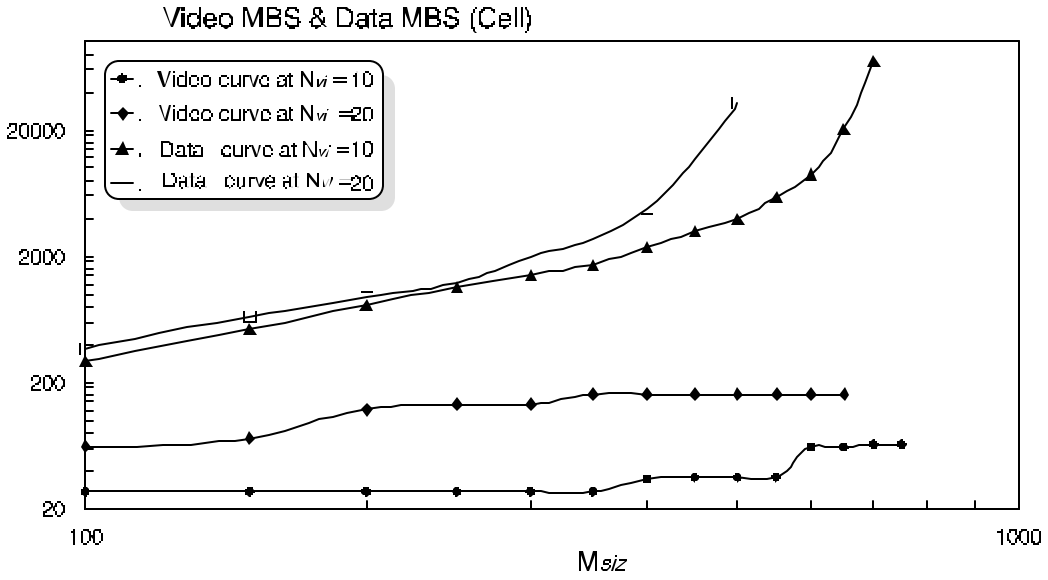

Figure 6-7 Video MBS & Data MBS versus M_{siz}

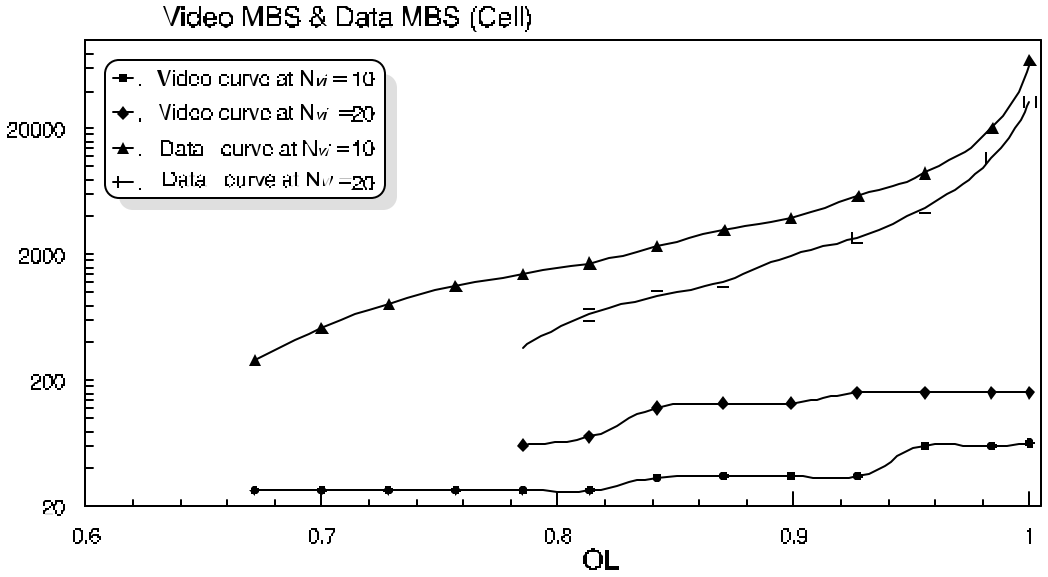

Figure 6-8 Video MBS & Data MBS versus OL

Figure 6-9 shows N_{vi} versus M_{siz}, for the same values of R_{vi}, and ^{m}. In the ideal case, the relationship between the N_{vi} and M_{siz} is linear that is clear from the following equations (6-2).

$$GR_{vi} + GR_{da} + GR_{t} = R_{T} = 352 \text{ cell/ms} \quad \text{----------} \quad (6\text{-}2)$$
$$\text{or } OL_{vi} + OL_{da} + OL_{tr} = 1$$

By substituting in equation (6-2), we can note that the increasing of M_{siz},

decreasing the N_{vi} due to the fixed transmission rate (R_T) belongs to the fixed link data rate. In the normal case, the relation is represented by the following inequality equation (6-3).

$$GR_{vi} + GR_{da} + GR_t < R_T = 352 \text{ cell/ms} \quad \text{or} \quad OL_{vi} + OL_{da} + OL_{tr} < 1 \qquad \text{----------} \quad (6\text{-}3)$$

From Figure 6-9, we can observe that the actual curve is closed to the ideal curve. Equation (6-3) is considered in the actual case because at heavy load, the generated cells are accumulated into the queue that is increase video MBS and data MBS due to the long video MWT and long data MWT.

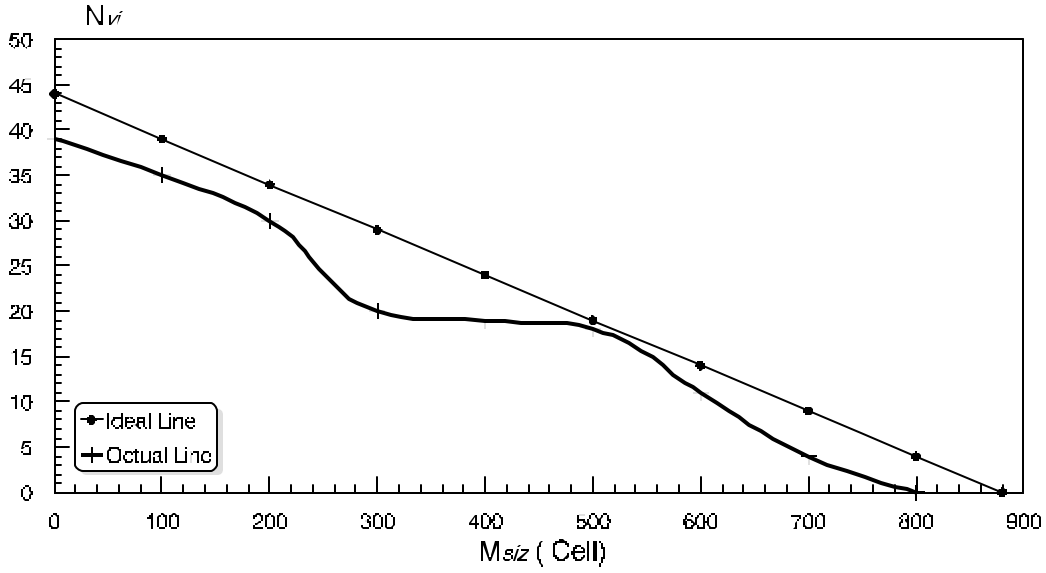

Figure 6-9 N_{vi} versus M_{siz}

Figure 6-10 illustrates TP_{vi} and TP_{da} versus N_{vi}, for R_{vi}=1.5 Mbps, ^{m}=5 ms and M_{siz}=100 cells. The Figurer shows that the increasing of N_{vi}, increases TP_{vi} but TP_{da} remains constant almost at 19.5 cells/ms. That is because, the increasing of N_{vi} increases the number of generated video cells. The M_{siz} and ^{m} are constant at 100 cells and 5 ms respectively, therefore GR_{da} remains constant. Beyond the saturation limit, TP_{vi} is also increase with the increasing of N_{vi}, and TP_{da} decreases with the increasing of N_{vi}. That is because the increasing of N_{vi}

increases the number of generated video cells, which increases the TP_{vi}. Meanwhile, beyond the saturation limit of TP_{da}, the chance of serve data cells decreases because the video cells are dominant and have also highest priority of service than data cells, resulting in decrease of TP_{da}.

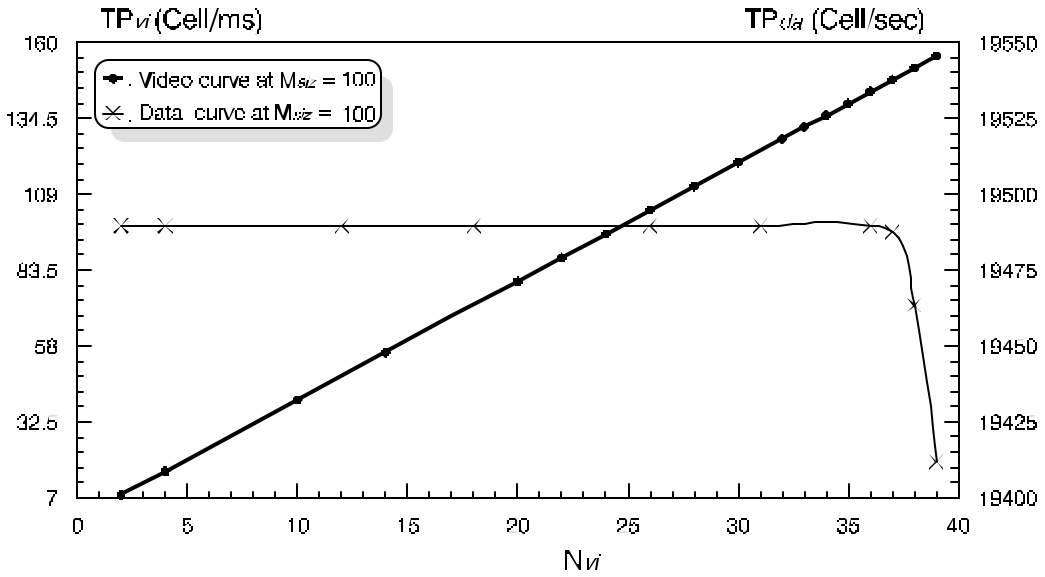

Figure 6-10 TP_{vi} & TP_{da} versus N_{vi}

Figure 6-11 shows the same study of Figure 6-10, for M_{siz} equals to 200 cells. Clearly the behavior is similar to that in Figure 6-10, except that the saturation limit is changed here. So we can recall the reason of that the saturation limit is depends upon the length of M_{siz}, in which as the length of M_{siz} increases the saturation limit decreases, as shown in Figure 6-10 and Figure 6-11.

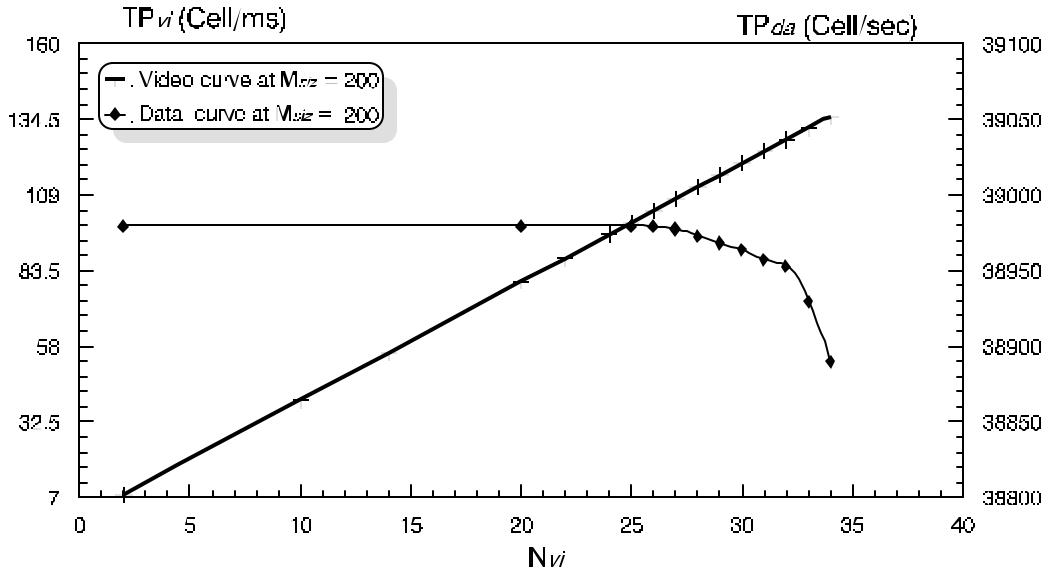

Figure 6-11 TP_{vi} & TP_{da} versus N_{vi}

Figure 6-12 and Figure 6-13 studies the TP_{vi} and TP_{da} versus M_{siz}, for various values of N_{vi}. Obviously, that M_{siz} has no effect on the TP_{vi}. The increasing of M_{siz} increases TP_{da} almost linearly up to the optimal M_{siz}, which represents the saturation limit, after that the TP_{da} remains constant. This is because the service will be saturated with the optimal M_{siz}. Meanwhile TP_{vi} remains constant for all values of M_{siz}. It is to be mention here that the increasing of N_{vi} decreases the saturation limit (optimal M_{siz}), because the chance of serve of data traffic becomes less for the same reasons mentioned above in Figure 6-10 and Figure 6-11.

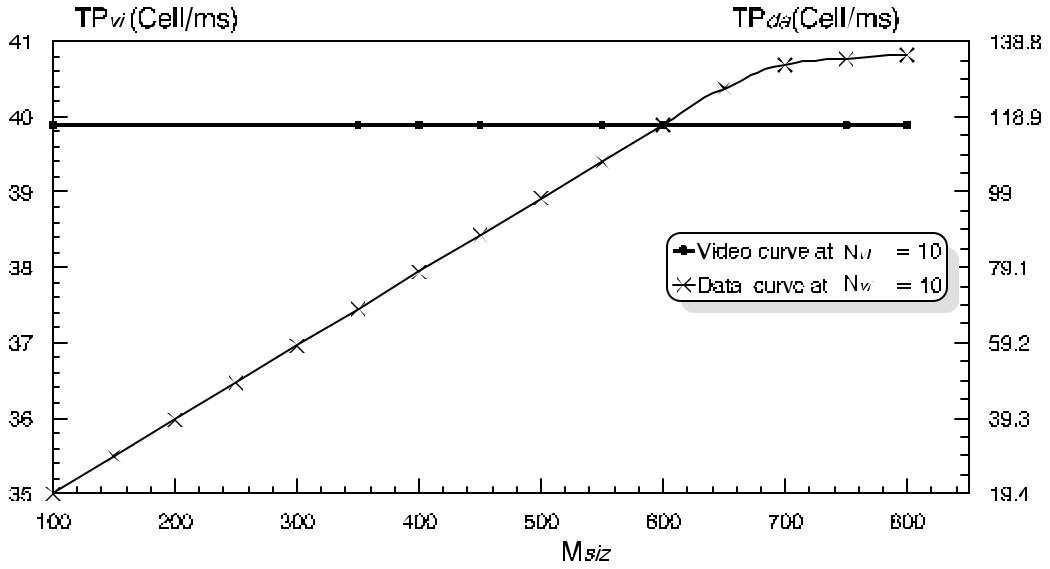

Figure 6-12 TP_{vi} & TP_{da} versus M_{siz}

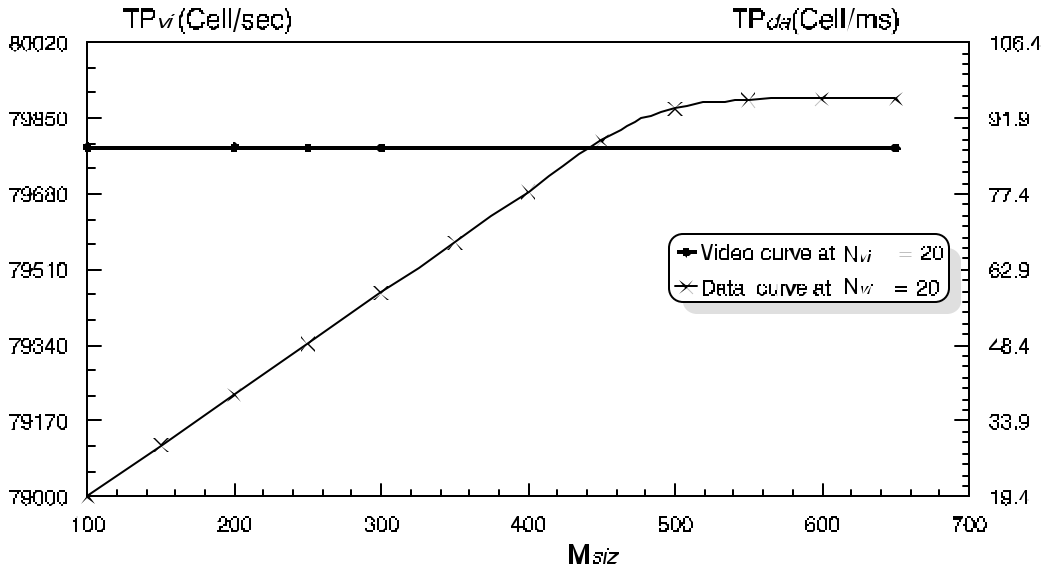

Figure 6-13 TP_{vi} & TP_{da} versus M_{siz}

Figure 6-14 illustrates the video MWT versus N_{vi}, for the same values of R_{vi}, and μ used above and M_{siz} equals to 0, 100, and 200 cells. This Figure summaries the effect of data traffic on the video traffic. Obviously that, the increasing of N_{vi}, slightly increases the video MWT up to the saturation limit, which depends upon the M_{siz}. Beyond the saturation limit, the video MWT

sharply increases due to the large number of cells and queuing delays. The increasing of M_{siz}, has slightly effect on the video MWT and the saturation limit.

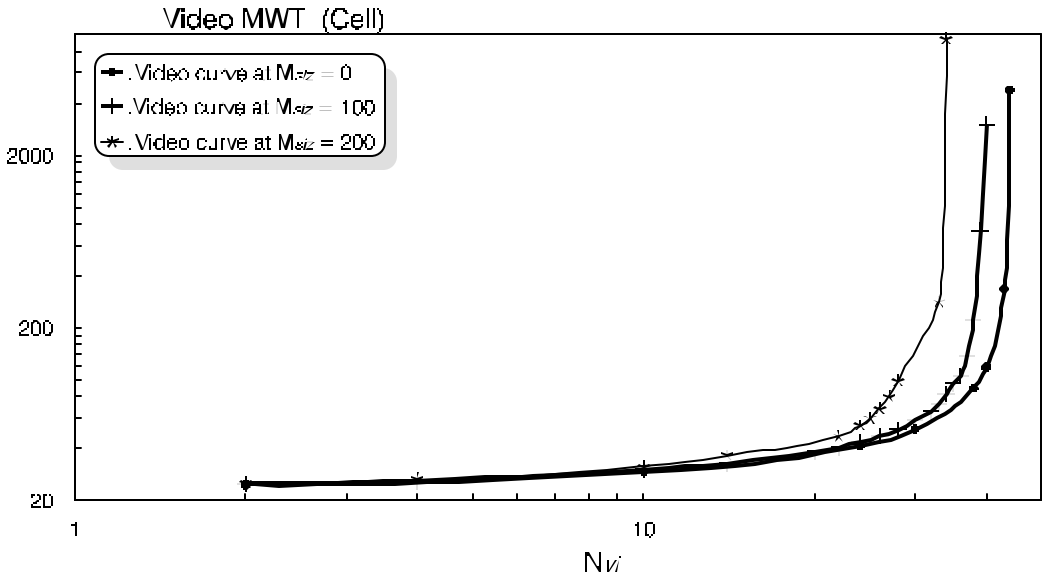

Figure 6-14 Video MWT versus N_{vi}

Figure 6-15 illustrates the data MWT versus M_{siz}, for the same values of R_{vi}, and μ used above and N_{vi} equals to 0, 10, and 20. This Figure summaries the effect of video traffic on the data traffic. It is clear that, the increasing of M_{siz}, slightly increase the data MWT up to the saturation limit, which depends upon the N_{vi}. Beyond the saturation limit, the data MWT monotonically increases due to the large number of cells and queuing delays. The increasing of N_{vi}, slightly increases the data MWT and slightly decreases the saturation limit for M_{siz}.

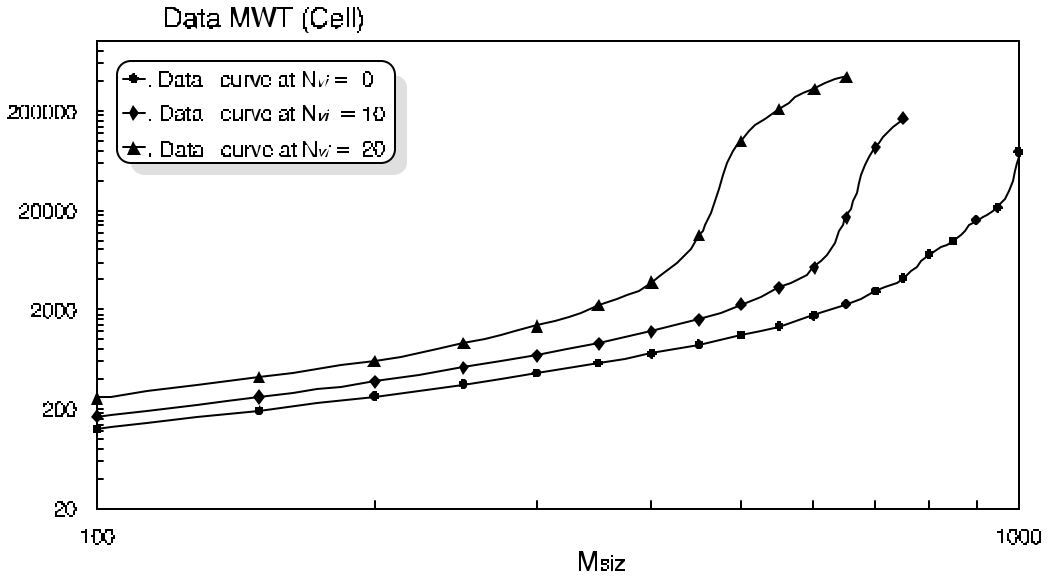

Figure 6-15 Data MWT versus M_{siz}

Table 6-4 summaries the simulation values at two cases: traffic alone and integration video/data. It is clear that the data traffic has slightly effect on video traffic but the video traffic has high effect on data traffic.

At R_{vi} = 1.5 Mbps and μ = 5 ms			
At N_{vi} = 20 sources		At M_{siz} = 350 cells	
M_{siz} (cell)	Video MWT (cell)	N_{vi} Sources	Data MWT (cell)
0 100 200	37 38 58	0 10 20	579 912 2197

Table 6-4 Simulation Results of Figure 6-14 and 6-15

6-2 The Integration of Video/Voice Traffics.

In our study of the performance characteristics of the integration of video/voice traffics, we have defined the following: the number of voice sources as N_{vo}, voice-encoding rate as R_{vo}, and the definition of video sources and its encoding rate is the same as we have used earlier (N_{vi} and R_{vi} = 1.5 Mbps).

It is well known that the voice source is represented by the two periods, which defined as talkspurt and silent periods. In our study, we have represented both by using an exponential distribution with mean value equals to 352 ms for talkspurt period and 650 ms for silent period. It is to be mentioning here that all the voice sources have the same mean values of talkspurt and silent periods.

The video and voice MWT versus N_{vi} for various values of N_{vo}, video and voice MBS versus offered load (OL) for various values of N_{vo}, and the maximum N_{vi} have been discussed.

The GR_{vi} and GR_{vo} have serious effect on the maximum N_{vi} for clarification we can calculate the ideal values of N_{vi}, using equation (6-4), which very depend upon GR_{vi} in cell/ms, and R_T =352 cell/ms which depends on SONET physical transmission, and transit rate in cell/ms.

$$\text{Max.}N_{vi} = \frac{[352(cell/ms) - transit\_rate(cell/ms)] - GR_{vo}}{GR_{vi}} \quad \text{----------} \quad (6\text{-}4)$$

Using equation (6-4) helps to calculate the maximum N_{vi} for various values of N_{vo} as shown in Table (6-5).

N_{vo}	Ideal maximum N_{vi}
50	37
200	18
250	12

Table 6-5 Ideal Maximum N_{vi}.

Obviously, from Table 6-5 the increasing of N_{vo} corresponding decreases of N_{vi} that is because the network can only support maximum number of sources which is distributed between the different traffics.

Figure 6-16 shows video MWT and voice MWT versus N_{vi} for R_{vi} equals to 1.5 Mbps, R_{vo} =192 Kbps, and N_{vo} equals to various values such as 50, 200 and 250. From the Figure it is very clear that the effect of N_{vo} on the MWT particularly on the voice MWT because the increasing of N_{vo} increases the number of generated voice cells, which increases the queue and MWT. The video MWT is slightly effect with the increases of N_{vo}, because the priority of serve is given to the video cells, then followed by voice cells.

Also, the increasing of N_{vi} has slightly effect on the increasing of video and voice MWT up to the saturation limit. Beyond the saturation limit the video and voice MWT sharply increase due to the large number of cells which yields long queues and delays. Obviously, the saturation limit varied according to the values of N_{vo}, however with the increasing of the value of N_{vo}, resulting in decreases the value of N_{vi} caused the saturation limit which corresponding the maximum N_{vi} very early as shown from Figure 6-16.

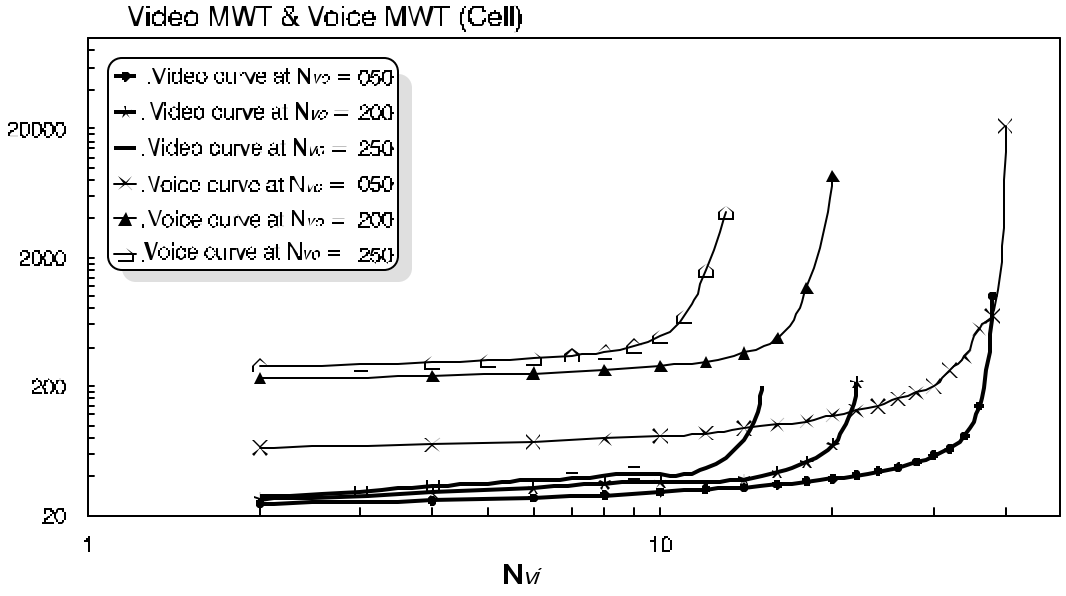

Figure 6-16 Video MWT & Voice MWT versus N_{vi}

Figure 6-17 illustrates video and voice MWT versus OL, for the same values of R_{vi}, R_{vo}, and N_{vo} used above. The behavior is similar to that in Figure 6-16 for the same reasons. Table 6-6 summaries the simulation results of Figure 6-16 and 6-17.

N_{vo}	N_{vi}	Video MWT (cell)	Voice MWT (cell)	OL
50	34	82.23	339.77	0.96
200	16	42.97	471.45	0.97
250	11	41.43	695.06	0.98

Table 6-6 Simulation Results of Figure 6-16 and 6-17.

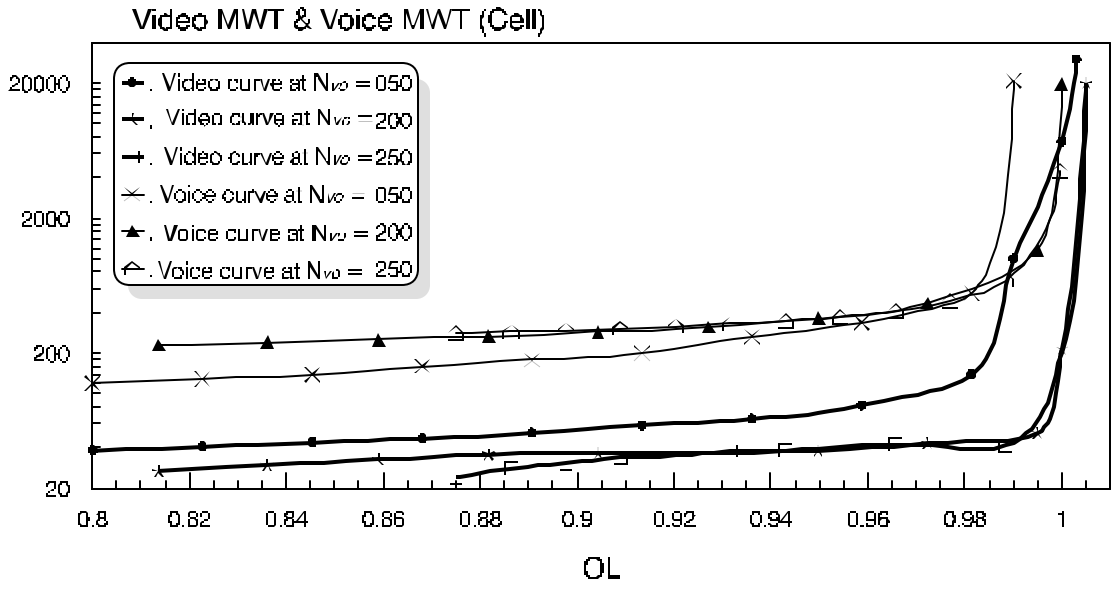

Figure 6-17 Video MWT & Voice MWT versus OL

Figure 6-18 shows the video MWT and voice MWT versus N_{vo} for R_{vi} equals to 1.5 Mbps, R_{vo} equals to 192 Kbps, and N_{vi} equals to 10, and 20 respectively. From the Figure, the effect of N_{vi} on the MWT of video and voice is clear.

The increasing of N_{vo} has slightly effect on the increasing of video and voice MWT up to the saturation limit. Beyond the saturation limit the video and voice MWT sharply increase due to the large number of cells, which yields long queues and delays. Obviously, the saturation limit depends on the value of $N_{vi,}$ however the increasing of N_{vi} resulting in decreases the value of N_{vo} as shown from Figure 6-18.

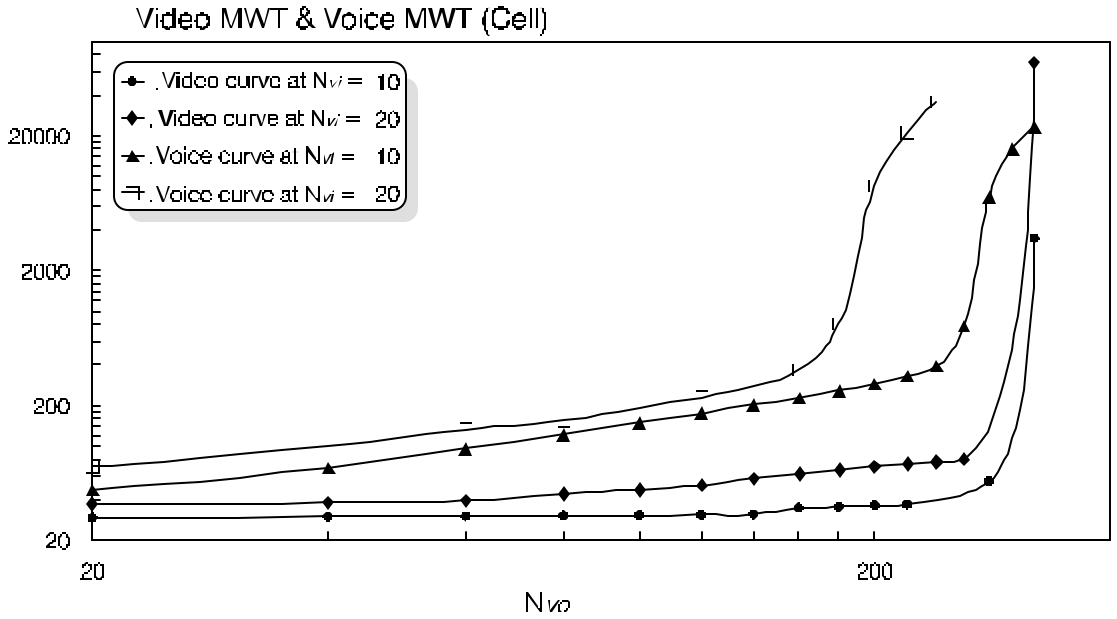

Figure 6-18 Video MWT & Voice MWT versus N_{vo}

Figure 6-19 illustrates video and voice MWT versus OL (for both traffics), for the same values of R_{vi}, R_{vo}, and N_{vi} used above. The behavior is similar to that in Figure 6-18 for the voice MWT, for the same reasons. However, the video MWT slightly increases with the increasing of OL, because the video cells have higher priority than voice cells.

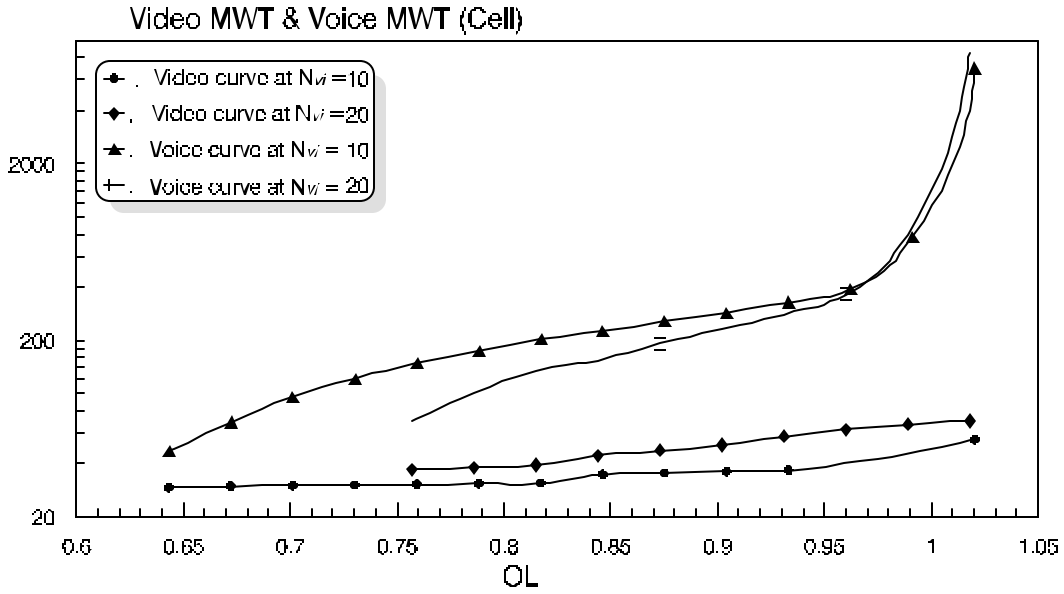

Figure 6-19 Video MWT & Voice MWT versus OL

Figure 6-20 and 6-21 show video and voice MBS versus N_{vi} and OL respectively, for the same values of R_{vi}, $R_{vo,}$ and N_{vo} used in Figure 6-16 and Figure 6-17. The behavior of both carves is similar to the previous carves for the same reasons. Table 6-7 summaries the simulation results of both Figure 6-18 and 6-19.

N_{vo}	N_{vi}	Video MBS (cell)	Voice MBS (cell)	OL
50	34	297	131	0.96
200	16	61	571	0.97
250	11	41	1032	0.98

Table 6-7 Simulation Results of Figures 6-18 and 6-19.

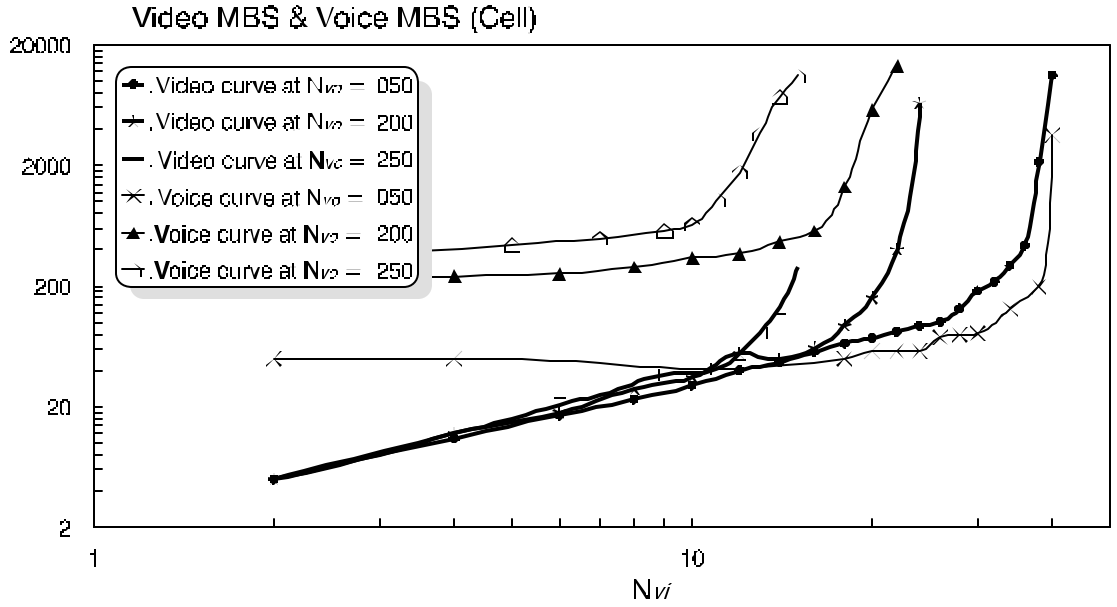

Figure 6-20 Video MBS & Voice MBS versus N_{vi}

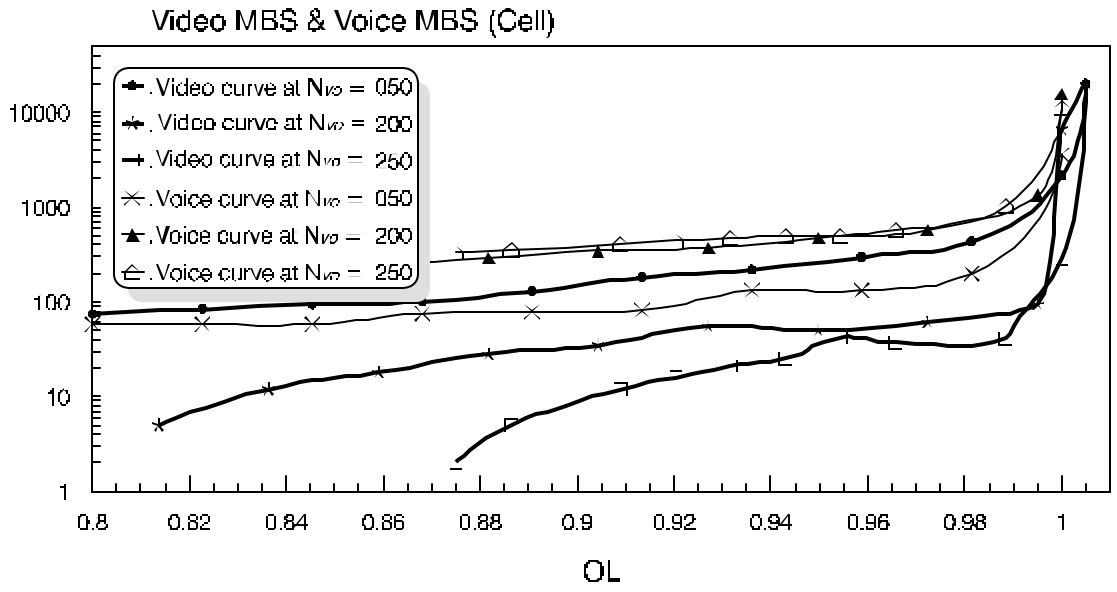

Figure 6-21 Video MWT & Voice MWT versus OL

Figure 6-22, and Figure 6-23 illustrates video and voice MBS versus N_{vo} and OL respectively, for the same values of R_{vo}, R_{vo} and N_{vi} used with Figure 6-18 and 6-19. The characteristics of both Figures are more or less very closed to that of Figures 6-18 and 6-19, for the same reasons.

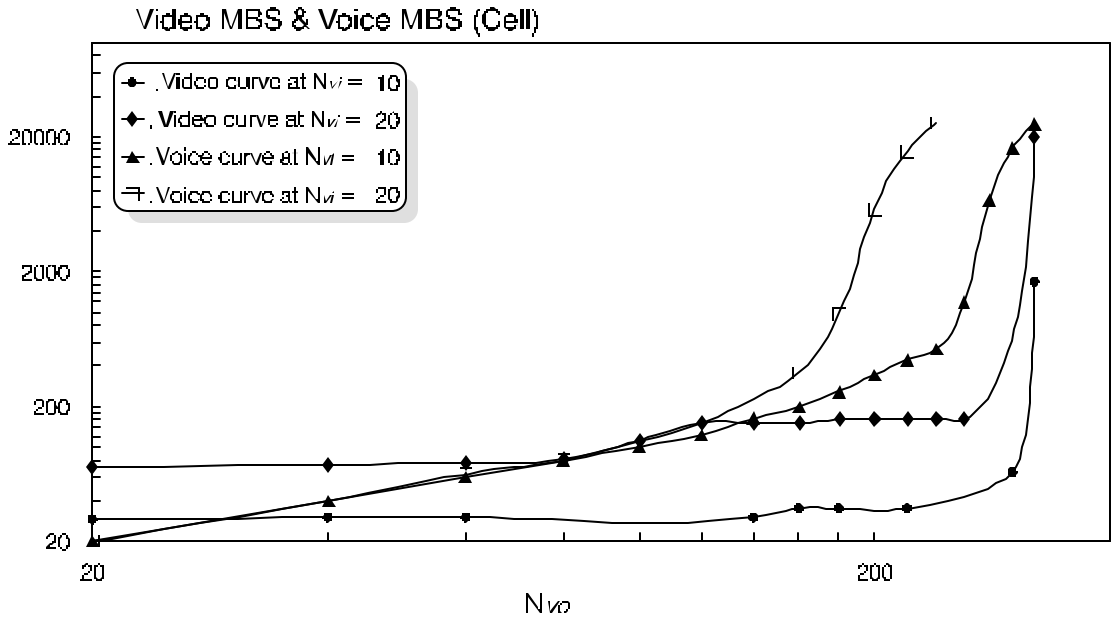

Figure 6-22 Video MBS & Voice MBS versus N_{vo}

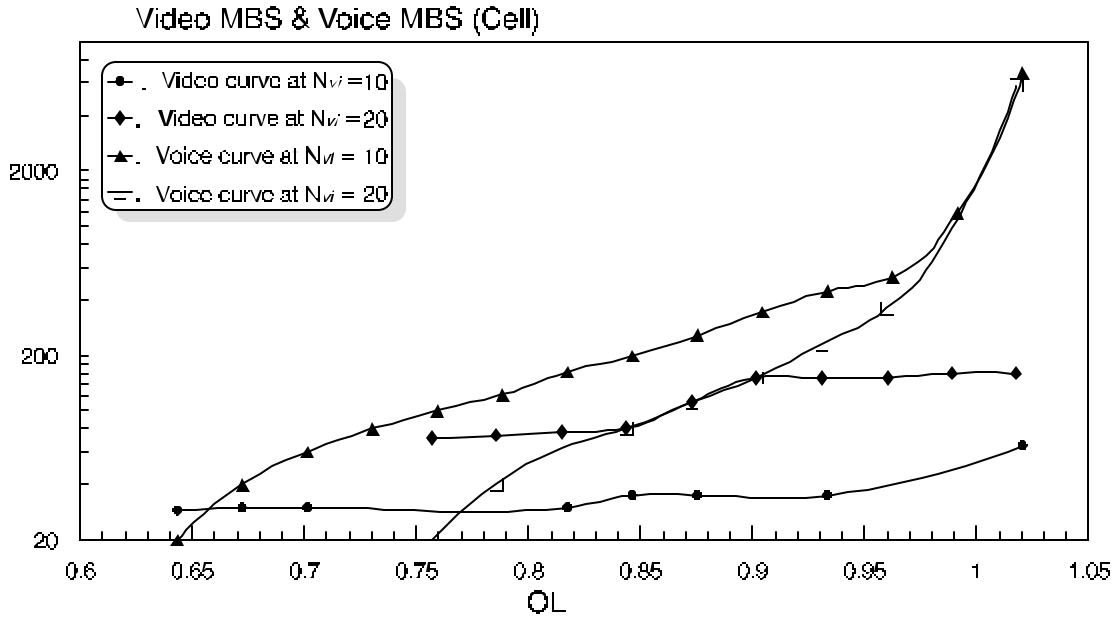

Figure 6-23 Video MBS & Voice MBS versus OL

Figure 6-24 illustrates N_{vi} versus N_{vo} for the same values used earlier. Using equation (6-5) which represents ideal case and the equation (6-6) which represents normal case, confirm that the increasing of N_{vo} corresponding decreasing of N_{vi}, for the same reason we have mentioned earlier, in which that the network can support maximum number of sources, that can distributed between all traffics. It is to be mention here that the equation which represents normal case is considered, because at heavy load the number of generated cells are accumulated in queues resulting in increases of video and voice MBS due to the large number of cells, long queues and delays. For the ideal case the relation is linear, and is represented by equation (6-5) and the normal case can be represented by equation (6-6).

$$GR_{vi} + GR_{vo} + GR_t = R_T = 352 \text{ cell/ms} \quad \text{or} \quad OL_{vi} + OL_{vo} + OL_{tr} = 1 \qquad (6\text{-}5)$$

$$GR_{vi} + GR_{vo} + GR_t < R_T = 352 \text{ cell/ms} \quad \text{or} \quad OL_{vi} + OL_{vo} + OL_{tr} < 1 \qquad (6\text{-}6)$$

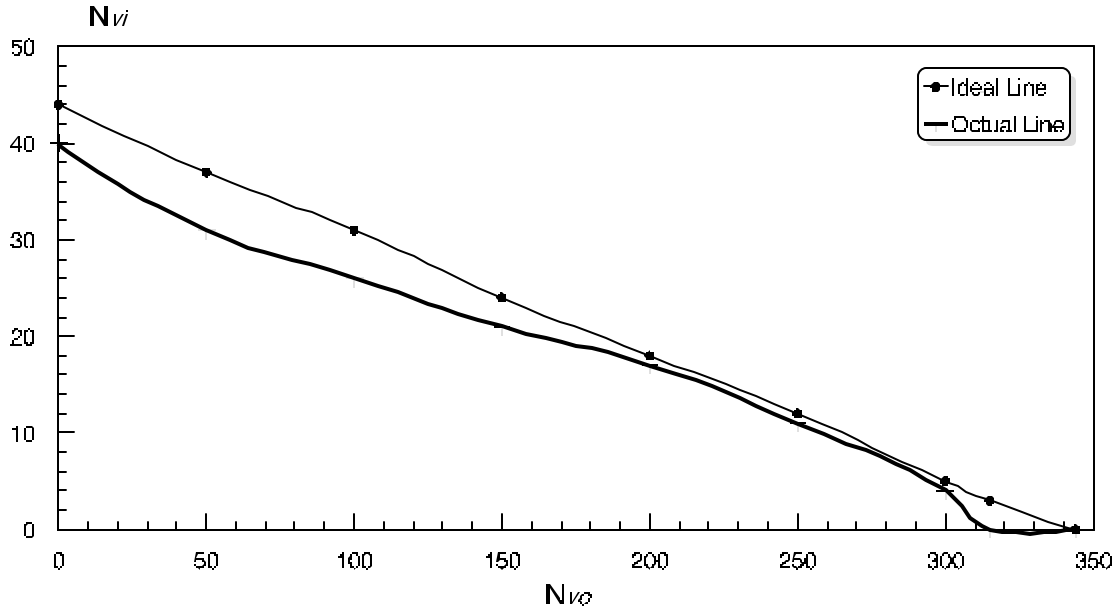

Figure 6-24 N_{vi} versus N_{vo}

Figure 6-25 illustrates TP_{vi} and TP_{vo} versus N_{vi}, for R_{vi} =1.5 Mbps, R_{vo} =192 Kbps and N_{vo} =50. From the Figure clearly the increasing of N_{vi}, increases TP_{vi} linearly but TP_{vo} remains constant at 12.9 cells/ms. That is because, the increasing of N_{vi} increases the number of generated video cells but voice cells are with the same number. Since the N_{vo} and R_{vo} are constant at 50 and 192 Kbps respectively therefore, GR_{vo} remains constant. Beyond the saturation limit, the TP_{vi} continually increases with the increasing of N_{vi}, and TP_{vo} decreases with the increasing of N_{vi}. That is because the increasing of N_{vi} increases the number of generated video cells, which increases the TP_{vi}. Meanwhile, beyond the saturation limit of TP_{vo}, the chance of serve voice cells decreases because the video cells are dominant and have also highest priority of service than voice cells, resulting in decrease of TP_{vo}.

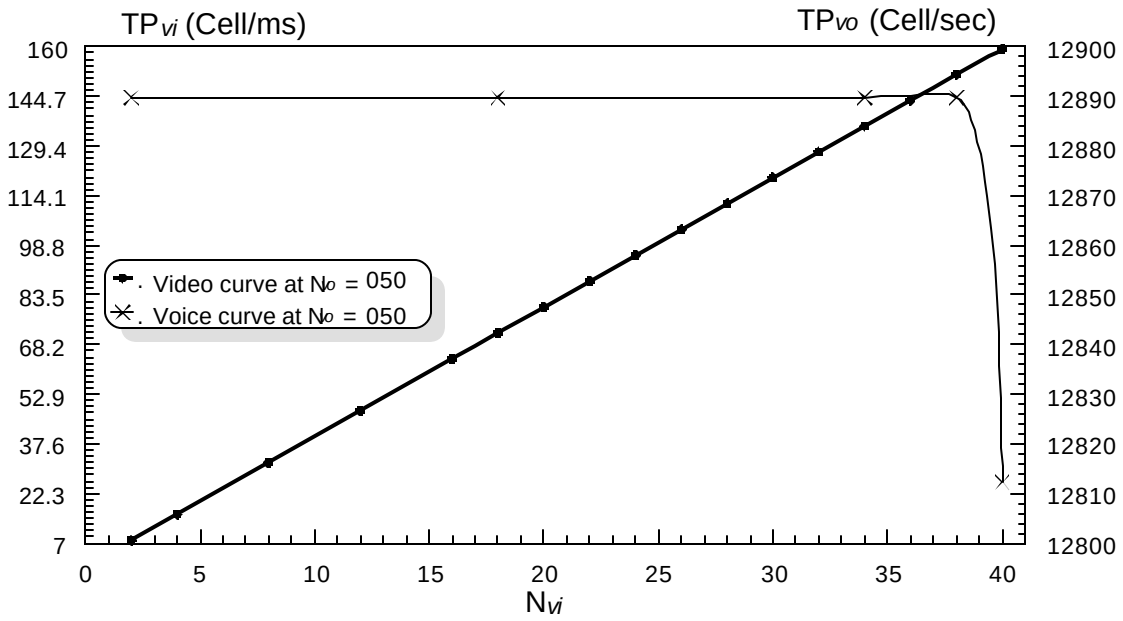

Figure 6-25 TP_{vi} & TP_{vo} versus N_{vi}

Figure 6-26 shows the same study of Figure 6-25, for N_{vo} equals to 250. Clearly the behavior is similar to that in Figure 6-25, as excepted that the saturation limit should change. So we have to recall the reasons of that the saturation limit depends upon the N_{vo}, in which as the N_{vo} increases the saturation limit decreases, as shown in Figure 6-25 and Figure 6-26.

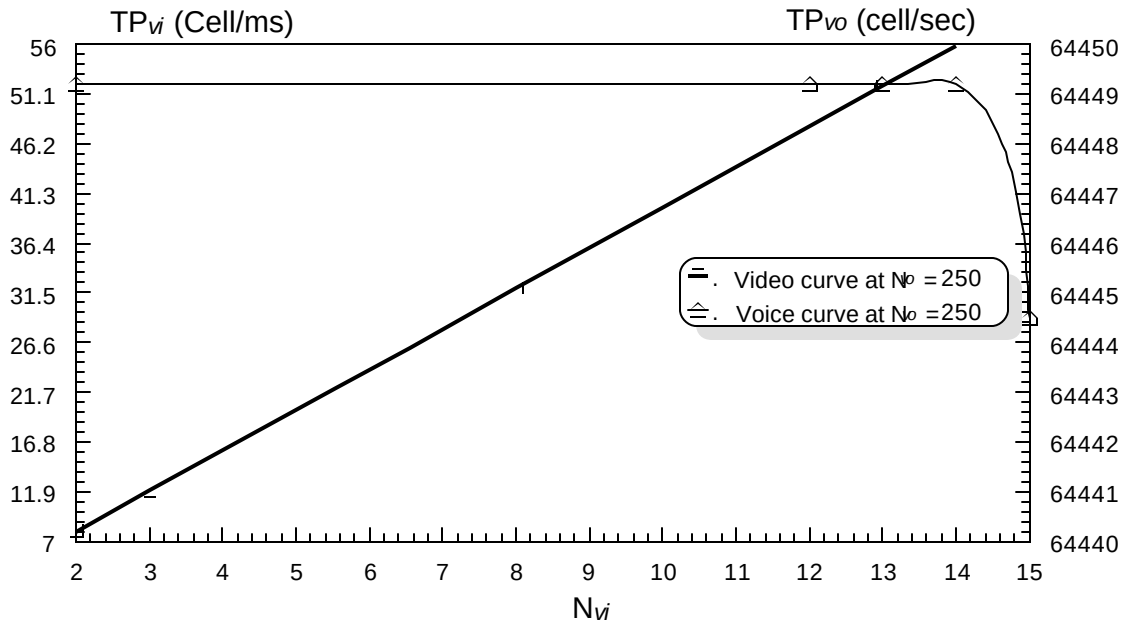

Figure 6-26 TP_{vi} & TP_{vo} versus N_{vi}

Figure 6-27 and Figure 6-28 studies the TP_{vi} and TP_{vo} versus N_{vo}, for various values of N_{vi}. Obviously, that N_{vo} has no effect on the TP_{vi}. The increasing of N_{vo} increases TP_{vo} almost linearly up to the allowed number of N_{vo} to be served, which represents the saturation limit, after that the TP_{vo} remains constant. Meanwhile TP_{vi} remains constant for all values of N_{vo}, because the increasing of N_{vo} has no effects on the number of video cells. It is to be mention here that the increasing of N_{vi} decreases the saturation limit (allowed number of N_{vo}), because the chance of serve of voice cells becomes less for the same reasons mentioned above to Figures 6-24 and 6-25.

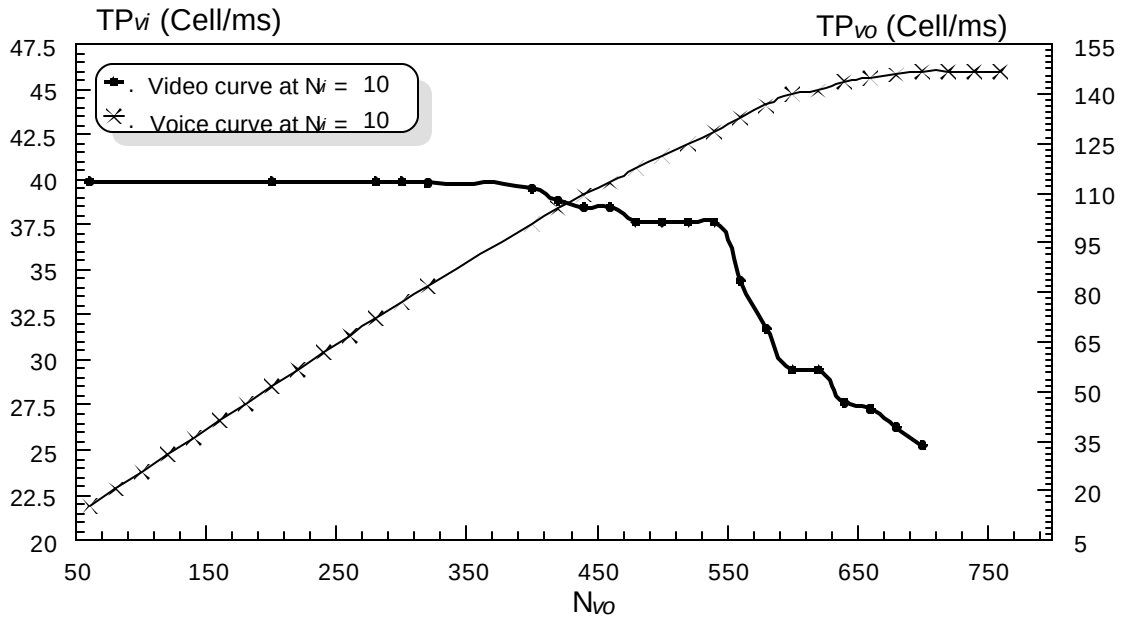

Figure 6-27 TP_{vi} & TP_{vo} versus N_{vo}

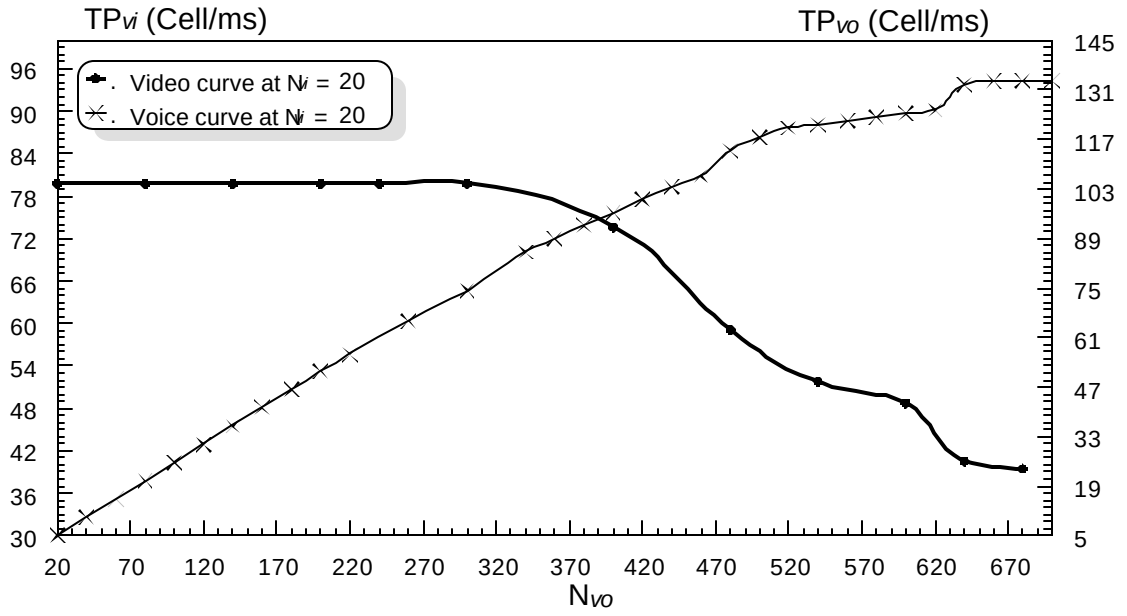

Figure 6-28 TP_{vi} & TP_{vo} versus N_{vo}

Figure 6-29 illustrates the video MWT versus N_{vi}, for the same values of R_{vi} and R_{vo} used above and N_{vo} equals to 0, 50, and 250. The Figure summaries the effect of voice traffic on the video traffic. Obviously that, the increasing of N_{vi}

slightly increases the video MWT up to the saturation limit, which depends up on the number of N_{vo}. Beyond the saturation limit, the video MWT sharply increases due to the large number of cells and queuing delays. The increasing of N_{vo}, slightly increases the video MWT and decreases the saturation limit, which corresponding to the maximum allowed number of N_{vi} to be served by the network.

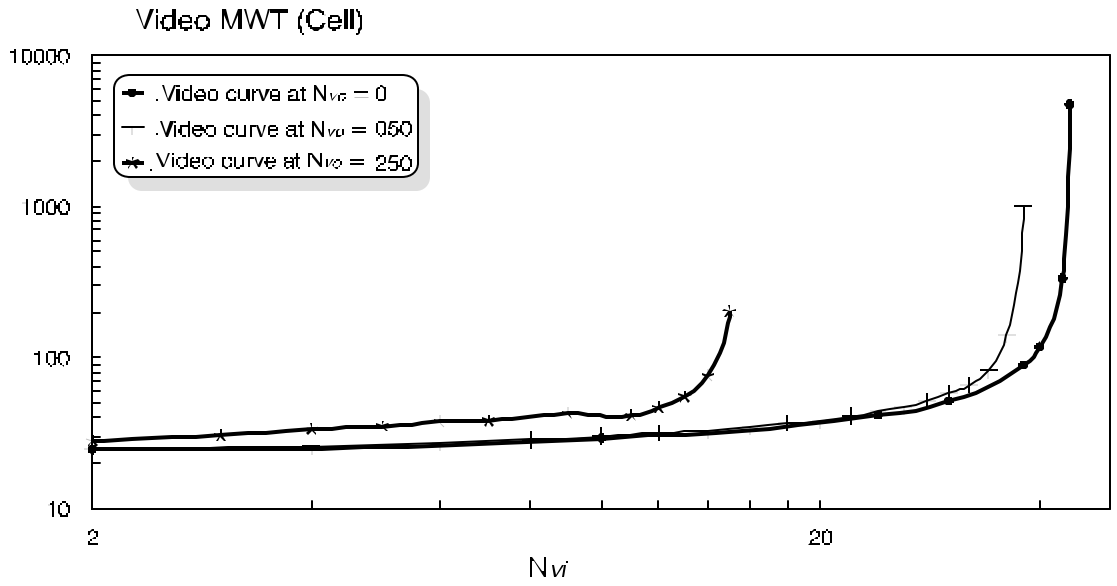

Figure 6-29 Video MWT versus N_{vi}

Figure 6-30 illustrates the voice MWT versus N_{vo}, for the same values of R_{vi}, and R_{vo} used above and N_{vi} equals to 0, 10, and 20. The Figure summaries the effect of video traffic on the voice traffic. It is clear that, the increasing of N_{vo} slightly increase the voice MWT up to saturation limit, which depends upon the N_{vi}. Beyond the saturation limit, the voice MWT sharply increases due to the large number of cells and queuing delays. The increasing of N_{vi}, increases the voice MWT and decreases the saturation limit for N_{vo}, for the same reasons mentioned earlier.

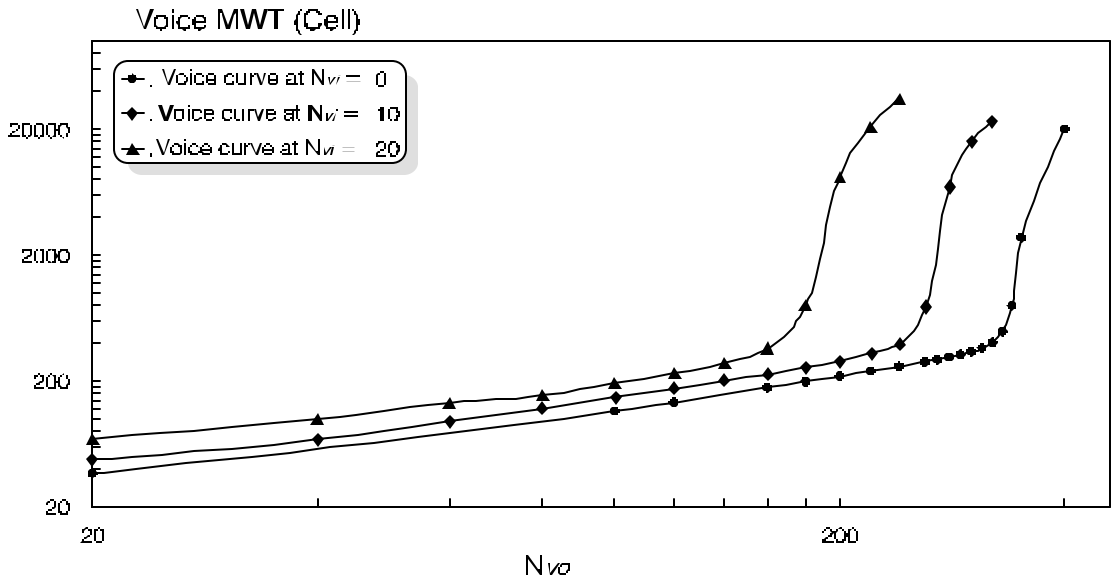

Figure 6-30 Voice MWT versus N_{vo}

Table 6-8 summaries the simulation values at two cases: traffic alone and integration video/voice. It is clear that the voice traffic has slightly effect on video traffic but the video traffic has high effect on voice traffic.

At R_{vi} = 1.5 Mbps and R_{vo} = 192 Kbps			
At N_{vi} = 12 Sources		At N_{vo} = 140 Sources	
N_{vo} (Sources)	Video MWT (cell)	N_{vi} (Sources)	Voice MWT (cell)
0 50 250	30 31 46	0 10 20	156 202 278

Table 6-8 Simulation Results of Figure 6-29 and 6-30

Chapter 7

Multimedia Traffic Over ATM VP-Based Ring Network

The performance characteristics of the multimedia traffic over the proposed network are studied in this chapter. The effect of including voice and data to the integration of video/data and video/voice respectively is considered. In order to achieve and guarantee fairness among traffics, the proposed control mechanism method is applied. The results confirm that the proposed network along with the control method is promising enough.

7-1 The Integration of Voice/Video/Data traffics

The performance measurements of including voice traffic with the integrated of video/data traffics, which has been studied in the previous chapter is considered in this section [52, 53, 54].

The same definitions of all parameters we have defined earlier are also used here, such as N_{vo}, N_{vi}, R_{vo} equals to 192 Kbps, R_{vi} equals to 1.5 Mbps, talkspurt period equals to 352 ms, silent period equals to 650 ms, and M_{siz} with interarrival time represents by an exponential distribution with mean value (μ) equals to 5 ms.

We have to mention that the maximum N_{vo} depends upon GR_{vi} and GR_{da}, however the calculation of the ideal maximum values of N_{vo} depends on GR_{vo} (cell/ms), R_T = 352 cell/ms, and transit rate (cell/ms) as shown in following equation (7-1).

$$\text{Max. } N_{vo} = \frac{[352(cell/ms) - transit\_rate(cell/ms)] - (GR_{vi} + GR_{da})}{GR_{vo}} \quad \text{---------} \quad (7\text{-}1)$$

Also, the generation of video and data ($GR_{vi} + GR_{da}$) depends upon GR_{vi}, GR_{da} and N_{vi} as shown from the following equation (7-2).

$$(GR_{vi} + GR_{da}) = GR_{da} + N_{vi}\, GR_{vi} \quad \text{----------} \quad (7\text{-}2)$$

Using equations (7-1) and (7-2) helps to determine the ideal maximum N_{vo}, for various values of N_{vi} and M_{siz}. Table 7-1 summaries the ideal maximum N_{vo}. However, the measured values could be less than or equal to those values of N_{vo}. The values of the parameters have mentioned above are used here.

N_{vi}	M_{siz} (cell)	$(GR_{vi} + GR_{da})$ (cell/ms)	N_{vo}
10	100	60	227
10	300	100	149
20	100	100	149

Table 7-1 Ideal Maximum N_{vo}.

Figure 7-1 shows video and data MWT versus N_{vo} for various values of N_{vi} such as 10 and 20, and M_{siz} equals to 100 and 300 cells. From the Figure, it is clear the effect of M_{siz} and N_{vi} on the video and data MWT. The increasing of either M_{siz} or N_{vi} yields increases of video and data MWT. The absolute value of data MWT is higher than that of video MWT, this is because the highest priority given to serve the video cells first followed by the data cells. The increasing of N_{vo} corresponding slightly increase of video and data MWT up to the saturation limit (which corresponding the maximum number of N_{vo} that can be supported by the network, and it changes according to the value of M_{siz} and N_{vi}). Beyond the saturation limit the video and data MWT smoothly increase with the increasing of N_{vo}, because the increasing of N_{vo}, increases the number of generated voice cells which yields long queue and delays however the data MWT increases because the scheduling algorithm which gives the voice cells highest priority. It is to be mentioning here that the effect of the proposed control mechanism method is very clear. So, inspire

the heavy load carried by the network and the highest priority given to the real-time traffic (video and voice), the non-real-time served properly, and all traffics served with acceptable delays as shown in Figure 7-1.

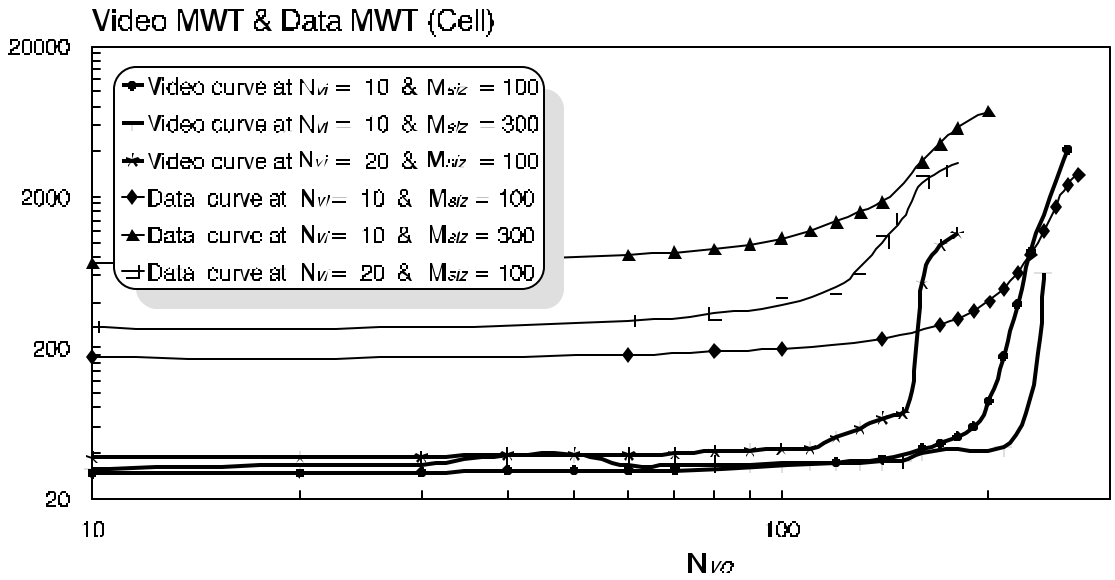

Figure 7-1 Video MWT & Data MWT versus N_{vo}

Table 7-2 summaries the simulation results which represent the fixed generated rates of video/data integration, and corresponding N_{vo}, video MWT, and data MWT.

N_{vi}	M_{siz} (cell)	(GR_{vi} +GR_{da}) (cell/ms)	N_{vo}	Video MWT (cell)	Data MWT (cell)
10	100	60	210	175.58	491.49
10	300	100	140	35.29	1869.61
20	100	100	140	68.45	1003.73

Table 7-2 Simulation Results of Figure 7-1.

Figure 7-2 shows video and data MBS versus N_{vo} with the same values of N_{vi} and M_{siz} used above. From the Figure obviously, the effect of M_{siz} and N_{vi} on the video and data MBS. The increasing of either M_{siz} or N_{vi} yields increases of video and data MBS. The absolute value of data MBS is higher than that of video MBS, this is because the highest priority given to serve video cells first followed by data

cells. The increasing of N_{vo} slightly increase of video and data MBS up to the saturation limit. Beyond the saturation limit the video and data MBS smoothly increase with the increasing of N_{vo}, due to the increasing of N_{vo}, increases the number of generated voice cells, which yields long queue and delays meanwhile the data cells serve next after video cells served. It is to be mentioning here that the effect of the proposed control mechanism method is very clear. So, inspire the heavy load carried by the network and the highest priority given to the real-time traffic (video and voice), the non-real-time served properly, and all traffics served with acceptable delays as shown in Figure 7-2. Table 7-3 summaries the simulation results which represents the fixed generated rates of video/data integration, and corresponding N_{vo}, video MBS, and data MBS.

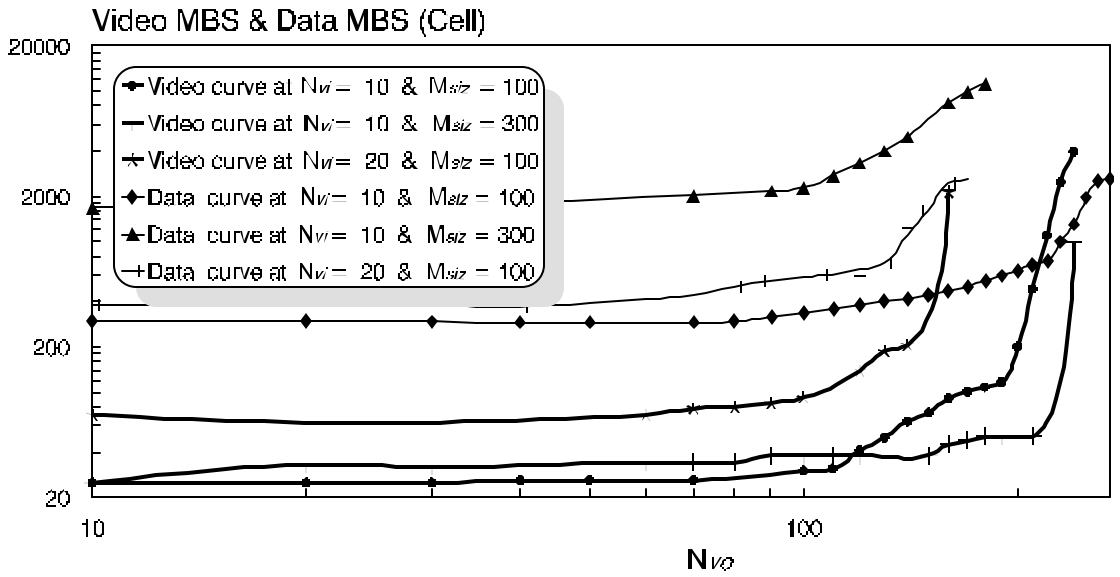

Figure 7-2 Video MBS & Data MBS versus N_{vo}

N_{vi}	M_{siz} (cell)	(GR_{vi} +GR_{da}) (cell/ms)	N_{vo}	Video MBS (cell)	Data MBS (cell)
10	100	60	210	485	708
10	300	100	140	38	4997
20	100	100	140	206	1125

Table 7-3 Simulation Results of Figure 7-2.

Figure 7-3 illustrates TP_{vi} and TP_{da} versus N_{vo}, for R_{vi} =1.5 Mbps, N_{vi} =10, m =5 ms and M_{siz}=100 cells. The Figure shows that TP_{vi} and TP_{da} remain constant at 39.89 cell/ms and 19.98 cells/ms respectively with the increasing of N_{vo} up to the saturation limit after that TP_{vi} and TP_{da} decrease with the increases of N_{vo}. In contrast TP_{vo} increases linearly with the increasing of N_{vo}, that is because, the increasing of N_{vo} increases the number of generated voice cells. It is to be mentioning here that the reasons that make both GR_{da} and GR_{vi} are constant, the M_{siz} and m are constant at 100 cells and 5 ms respectively, therefore GR_{da} remains constant, the N_{vi} and R_{vi} are constant at 10 and 1.5 Mbps respectively therefore GR_{vi} remains constant.

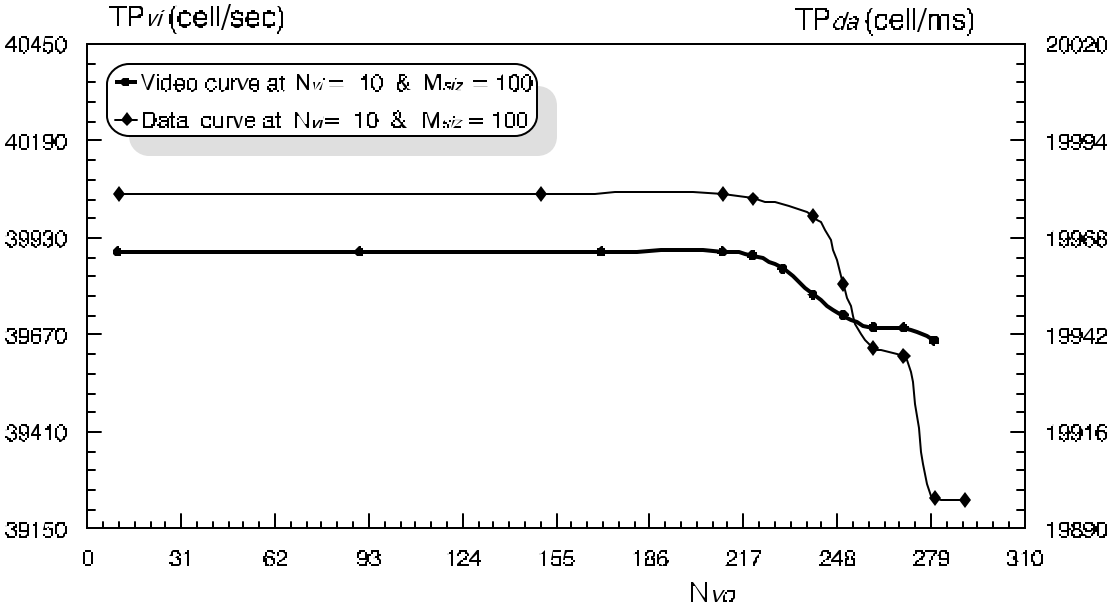

Figure 7-3 TP_{vi} and TP_{da} versus N_{vo}

Figure 7-4 shows the same study of Figure 7-3, except the value of M_{siz} equals to 300 cells. Clearly the behavior is similar to that in Figure 7-3, except that the saturation limit is changed here. So we have to recall the reason of that the saturation limit is depends upon the length of M_{siz}, in which as the length of M_{siz} increases the saturation limit decreases, as shown in Figure 7-3 and 7-4.

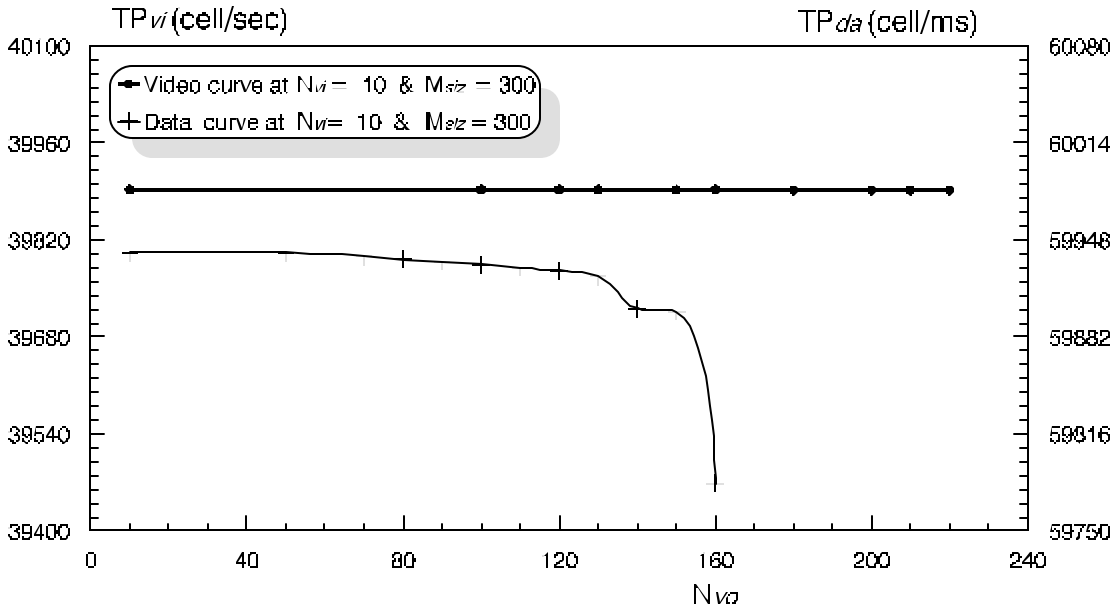

Figure 7-4 TP_{vi} and TP_{da} versus N_{vo}

Figure 7-5 shows the same study of Figure 7-3, except the value of N_{vi} equals to 20 cells. Clearly the behavior is similar to that in Figure 7-3, except that the saturation limit is changed here. So we have to recall reason of that saturation limit is depends upon the N_{vi}, in which as the value of N_{vi} increases the saturation limit decreases, as shown in Figure 7-3 and Figure 7-5.

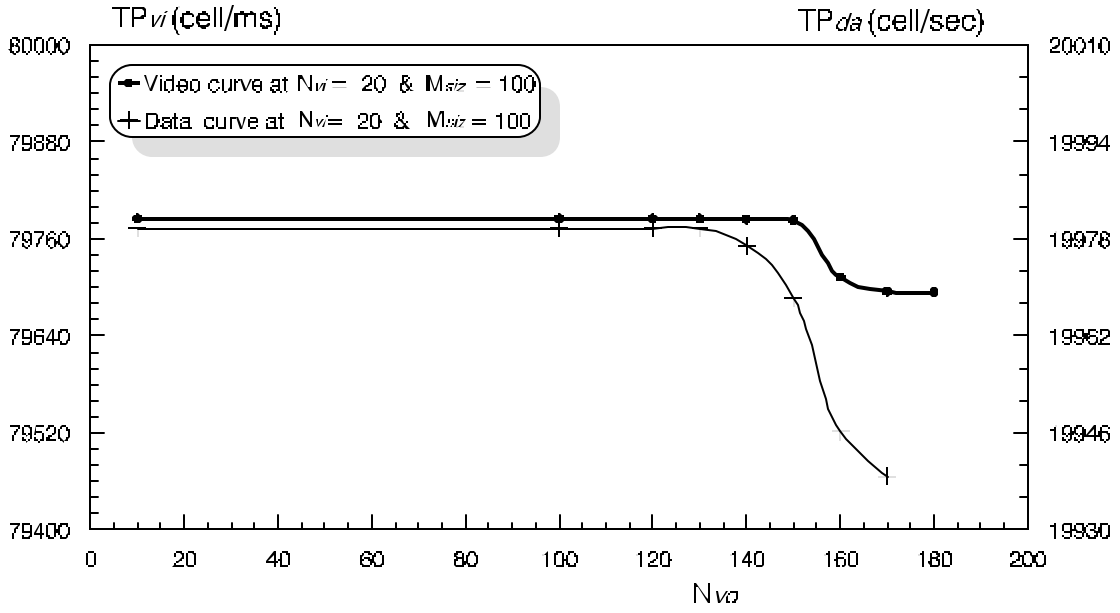

Figure 7-5 TP_{vi} and TP_{da} versus N_{vo}

Figure 7-6 illustrates the video and data MWT versus N_{vi}, for the same values of R_{vi}, R_{vo}, and μ used above, the M_{siz} equals to 100 cells, and the N_{vo} equals to 0, 50, and 200. The Figure summaries the effect of voice traffic on the video/data traffics. Obviously that, the increasing of N_{vi} slightly increase the video and data MWT up to the saturation limit, which depends up on the N_{vo}. Beyond the saturation limit, the video and data MWT sharply increase due to the large number of video cells and queuing delays. The increasing of N_{vo}, slightly increase the video and data MWT and decreases the saturation limit, which corresponding to the maximum number of N_{vi} can be supported by the network.

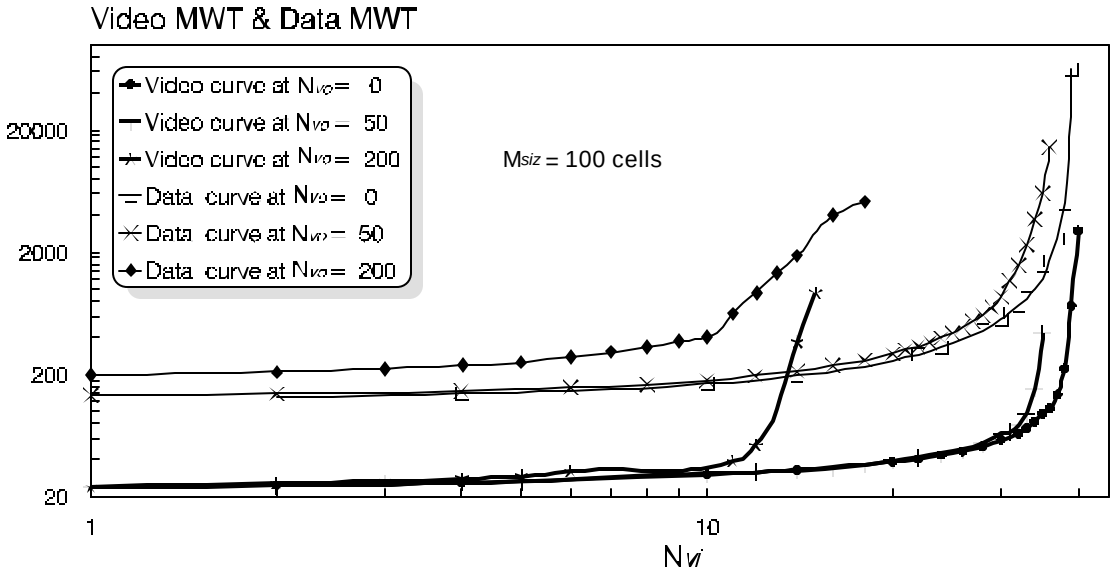

Figure 7-6 Video MWT & Data MWT versus N_{vi}

Figure 7-7 illustrates the video and data MWT versus M_{siz}, for the same values of R_{vi}, R_{vo}, and μ used above, the N_{vi} equals to 10, and the N_{vo} equals to 0, 50, and 100. The Figure summaries the effect of voice traffic on the video/data traffics. Obviously that, the increasing of M_{siz} slightly increase the video and data MWT up to the saturation limit, which depends up on the N_{vo}. Beyond the saturation limit, the data MWT smoothly increases but the video MWT very slightly increases, due

to the large number of voice cells, queuing delays, and the scheduling algorithm which gives the video cells the highest priority followed by voice cells and then data cells. That is clear from the absolute values of video MWT and data MWT shown in Figure 7-7.

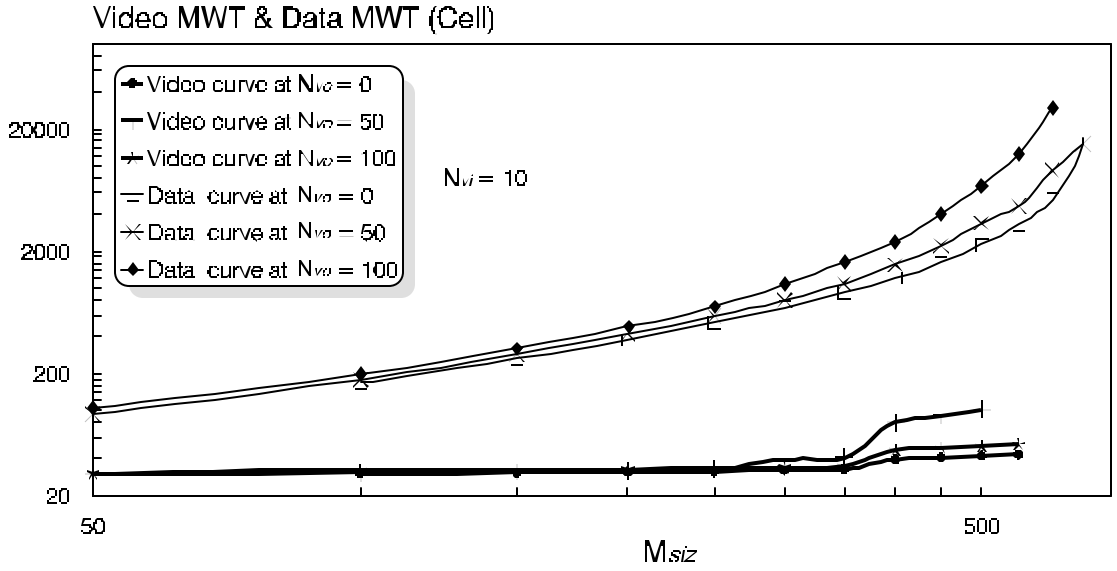

Figure 7-7 Video MWT & Data MWT versus M_{siz}

Table 7-4 summaries the simulation values at two cases: integration video/data and integration voice/video/data. It is clear that the voice traffic has very slightly effect on video traffic but the voice traffic has high effect on data traffic.

At R_{vi} = 1.5 Mbps, R_{vo} = 192 Kbps, μ = 5 ms, and N_{vi} = 10 Sources					
At M_{siz} = 100 cells			At M_{siz} = 200 cells		
N_{vo}	Video MWT (cell)	Data MWT (cell)	N_{vo}	Video MWT (cell)	Data MWT (cell)
0	30	167	0	31	378
50	30	177	50	31	421
200	88	403	100	32	482

Table 7-4 Simulation Results of Figure 7-6 and 7-7

7-2 Adding Data Traffic to Video/Voice Integration

The performance measurements of including data traffic with the integrated of video/voice traffics, which has been studied in the previous chapter is considered in this section. The same definitions of all parameters, we have defined earlier which are also used here, such as N_{vo}, N_{vi}, R_{vo} equals to 192 Kbps, R_{vi} equals to 1.5 Mbps, talkspurt period equals to 352 ms, silent period equals to 650 ms, and M_{siz} with interarrival time represented by an exponential distribution with mean value (μ) equals to 5 ms. Again, we have to mention that the maximum M_{siz} depends upon GR_{vi} and GR_{vo}, however the calculation of the ideal maximum values of M_{siz} depends on μ (ms), R_T = 352 cell/ms, and transit rate (cell/ms) as shown from the following equation (7-3).

$$\text{Max. } M_{siz} = [[352(cell/ms) - transit\_rate(cell/ms)] - (GR_{vi} + GR_{vo})]xm \qquad (7\text{-}3)$$

The generation of video and voice (GR_{vi} + GR_{vo}) depends upon GR_{vi}, GR_{vo}, N_{vi}, and N_{vo} as shown from the following equation (7-4).

$$(GR_{vi} + GR_{vo}) = (N_{vi}\ x\ GR_{vi} + N_{vo}\ x\ GR_{vo}) \qquad \text{----------} \qquad (7\text{-}4)$$

Using equation (7-3) and (7-4) helps to determine the ideal maximum M_{siz} for various values of N_{vi} and N_{vo}. Table 7-5 summaries the ideal maximum M_{siz}. However, the measured values could be less than or equal to those values of M_{siz}. The values of the parameters have mentioned above are used here.

N_{vi}	N_{vo}	(GR_{vi} + GR_{vo}) (cell/ms)	M_{siz} (cell)
10	50	65	555
10	100	91	425
20	50	105	355

Table7-5 Ideal Maximum M_{siz} (cell).

Figure 7-8 illustrates video and voice MWT versus M_{siz} for the values of N_{vi} equals to 10 and 20, and N_{vo} equals to 50 and 100. The Figure shows the effect of N_{vo} and N_{vi} on the video and voice MWT. The increasing of either N_{vo} or N_{vi} yields increase of video and voice MWT. The absolute value of voice MWT is higher than that of video MWT, this is because the highest priority given to serve video cells first followed by voice cells. The increasing of M_{siz} corresponding slightly increase of video and voice MWT up to the saturation limit (which corresponding the optimal length of M_{siz} and it changes according to the value of N_{vo} and N_{vi}). Beyond the saturation limit the video and voice MWT smoothly increase with the increasing of M_{siz}, because the increasing of M_{siz}, increases the transmission (service) time used for data cells. We have to recall that the effect of the proposed control mechanism method is very clear. So, inspire the heavy load carried by the network and the highest priority given to the real-time traffic (video and voice), the non-real-time served properly, and all traffics served with acceptable delays as shown in Figure 7-8.

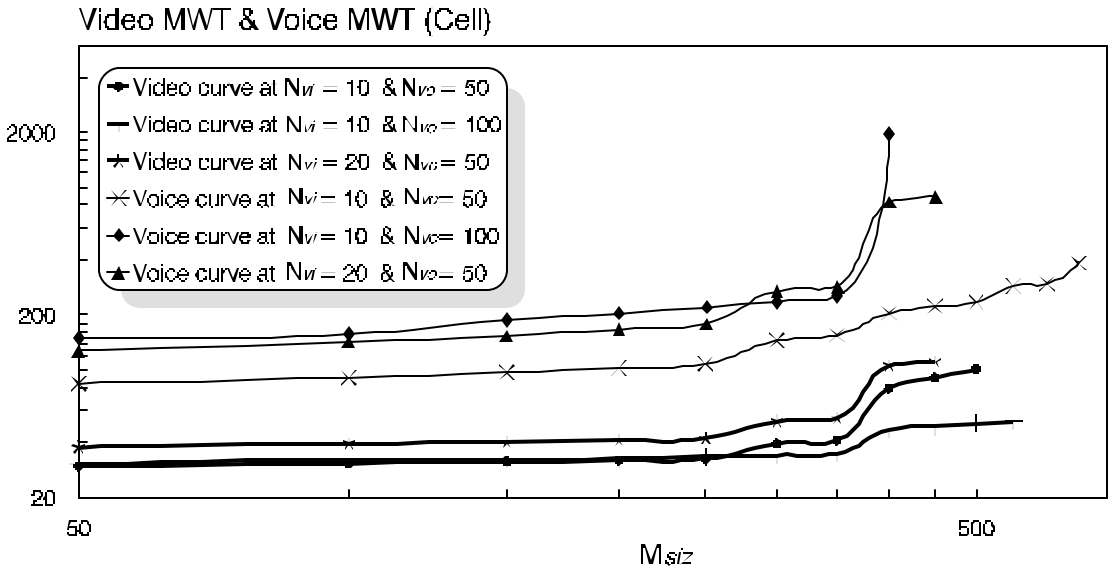

Figure 7-8 Video MWT & Voice MWT versus M_{siz}

Table 7-6 summaries the simulation results which represents the fixed generation rates of video/voice integration, and corresponding M_{siz}, video MWT, and voice MWT.

N_{vi}	N_{vo}	(GR_{vi} + GR_{vo}) (cell/ms)	M_{siz} (cell)	Video MWT (cell)	Voice MWT (cell)
10	50	65	500	100.84	234.76
10	100	91	400	47.08	1951.47
20	50	105	350	54.44	285.94

Table 7-6 Simulation Results of Figure 7-8.

Figure 7-9 illustrates video and voice MBS versus M_{siz} with the same values of N_{vi}, and N_{vo} used above in Figure 7-8. From the Figure, obviously that the characteristics behavior are similar to that in Figure 7-8 and for the same resons mentioned. Table 7-7 summaries the simulation results of Figure 7-9.

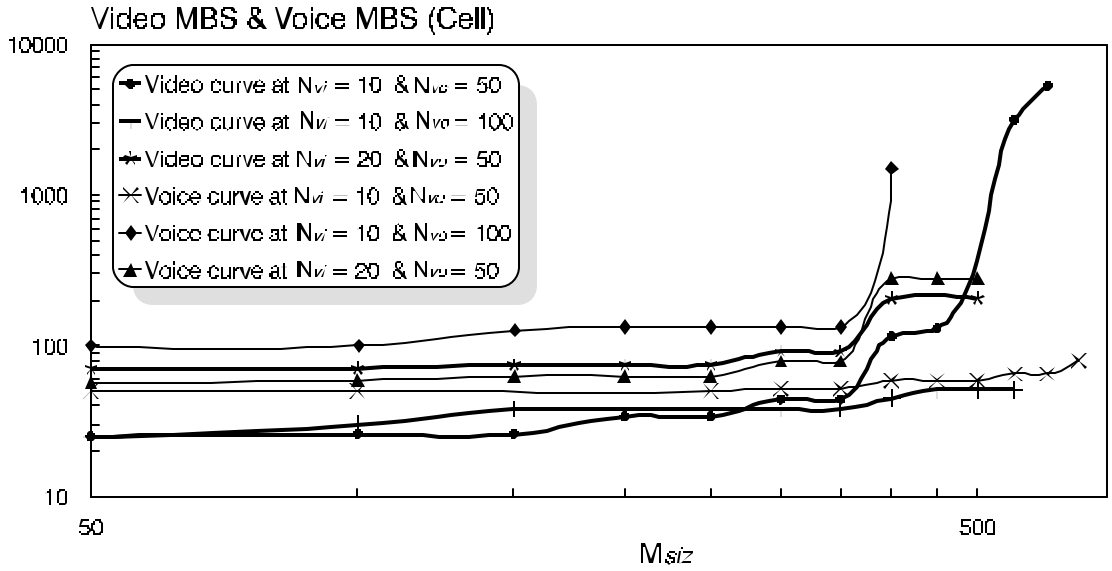

Figure 7-9 Video MBS & Voice MBS versus M_{siz}

N_{vi}	N_{vo}	(GR_{vi} + GR_{vo}) (cell/ms)	M_{siz} (cell)	Video MBS (cell)	Voice MBS (cell)
10	50	65	500	130	59
10	100	91	400	45	1509
20	50	105	350	92	79

Table 7-7 Simulation Results of Figure 7-9.

Figure 7-10 illustrates TP_{vi} and TP_{vo} versus M_{siz}, for R_{vi} = 1.5 Mbps, R_{vo} = 192 Kbps, N_{vi} = 10, N_{vo} = 50, and ^{m} = 5 ms. Obviously that the TP_{vi} and TP_{vo} remain constant at 39.89 cell/ms and 5.83 cell/ms respectively with the increasing of M_{siz} up to the saturation limit after that TP_{vi} and TP_{vo} decrease with the increases of M_{siz}. In contrast TP_{da} increases linearly with the increasing of M_{siz}, that is because, the increasing of M_{siz} increases the number of generated data cells. It is to be mentioning here that the reasons that make both GR_{vi} and GR_{vo} are constant, the N_{vi} and R_{vi} are constant at 10 and 1.5 Mbps respectively therefore GR_{vi} remains constant, the N_{vo} and R_{vo} are constant at 50 and 192 Kbps respectively therefore GR_{vo} remains constant.

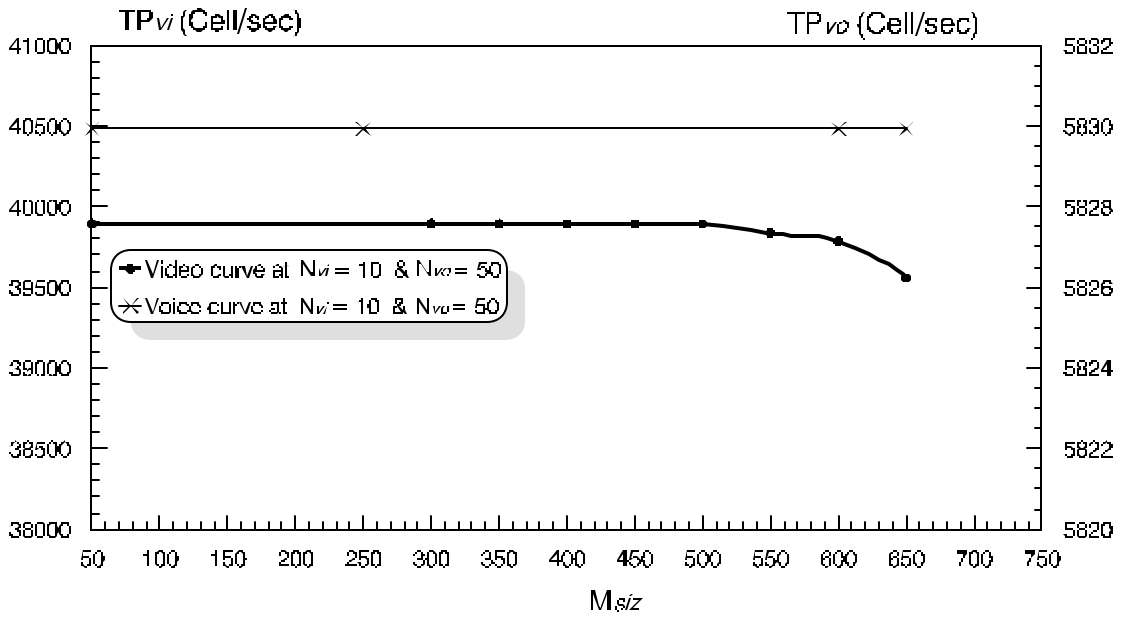

Figure 7-10 TP_{vi} and TP_{vo} versus M_{siz}

Figure 7-11 shows the same study of Figure 7-10, except the value of N_{vo} equals to 100. Clearly the behavior is similar to that in Figure 7-10, except that the saturation limit is changed here. So, we have to recall reason of that saturation limit is depends upon the values of N_{vo} in which as the value of N_{vo} increases the saturation limit decreases, as shown in Figure 7-10 and Figure 7-11.

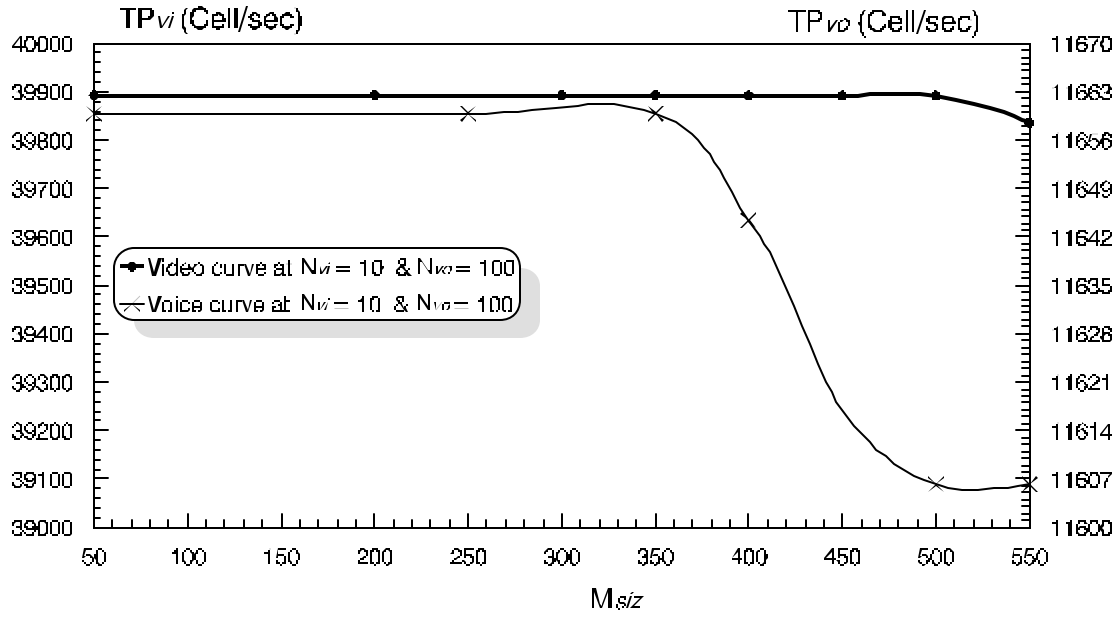

Figure 7-11 TP_{vi} and TP_{vo} versus M_{siz}

Figure 7-12 shows the same studies of Figure 7-10, except the value of N_{vi} equals to 20. Clearly the behavior is similar to that in Figure 7-10, except that the saturation limit is changed here. So, we have to recall the reason of that saturation limit is depends upon the N_{vi} in which as the value of N_{vi} increases the saturation limit decreases, as shown in Figure 7-10 and Figure 7-12.

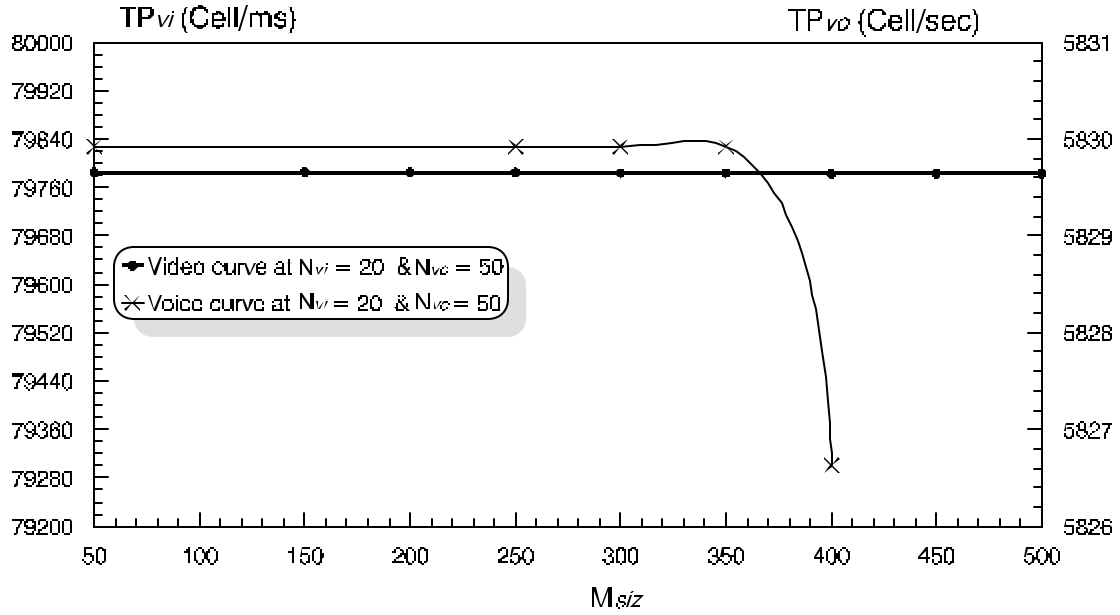

Figure 7-12 TP_{vi} and TP_{vo} versus M_{siz}

Figure 7-13 illustrates the video and voice MWT versus N_{vo}, for the same values of R_{vi}, R_{vo}, and μ used above, the N_{vi} equals to 10, and the M_{siz} equals to 0, 100, and 300. The Figure summaries the effect of data traffic on the video/voice traffics. Obviously that, the increasing of N_{vo} slightly increases the video and voice MWT up to the saturation limit, which depends up on the M_{siz}. Beyond the saturation limit, the video and voice MWT sharply increase due to the large number of voice cells and queuing delays. The increasing of M_{siz}, slightly increase the video and voice MWT and decreases the saturation limit for N_{vo}.

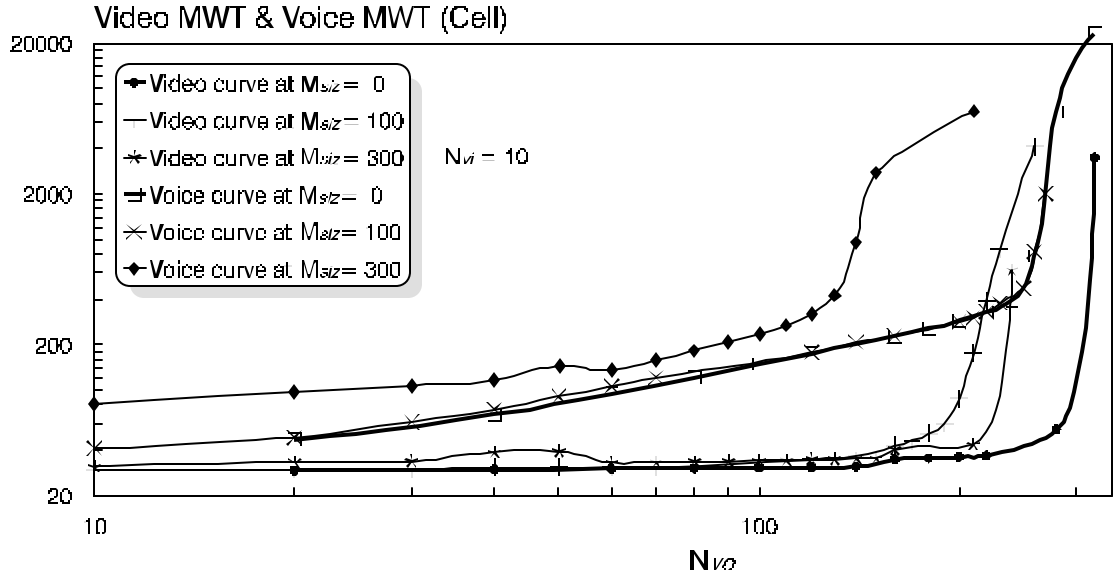

Figure 7-13 Video MWT and Voice MWT versus M_{siz}

Figure 7-14 illustrates the video and voice MWT versus N_{vi}, for the same values of R_{vi}, R_{vo}, and μ used above, the N_{vo} equals to 50, and the M_{siz} equals to 0, 100, and 300. The Figure summaries the effect of data traffic on the video/voice traffics. Obviously that, the increasing of N_{vi} slightly increases the video and voice MWT up to the saturation limit, which depends up on the M_{siz}. Beyond the saturation limit, the video and data MWT sharply increase due to the large number of video cells and

queuing delays. The increasing of M_{siz}, slightly increase the video and voice MWT and decrease the saturation limit for N_{vi}.

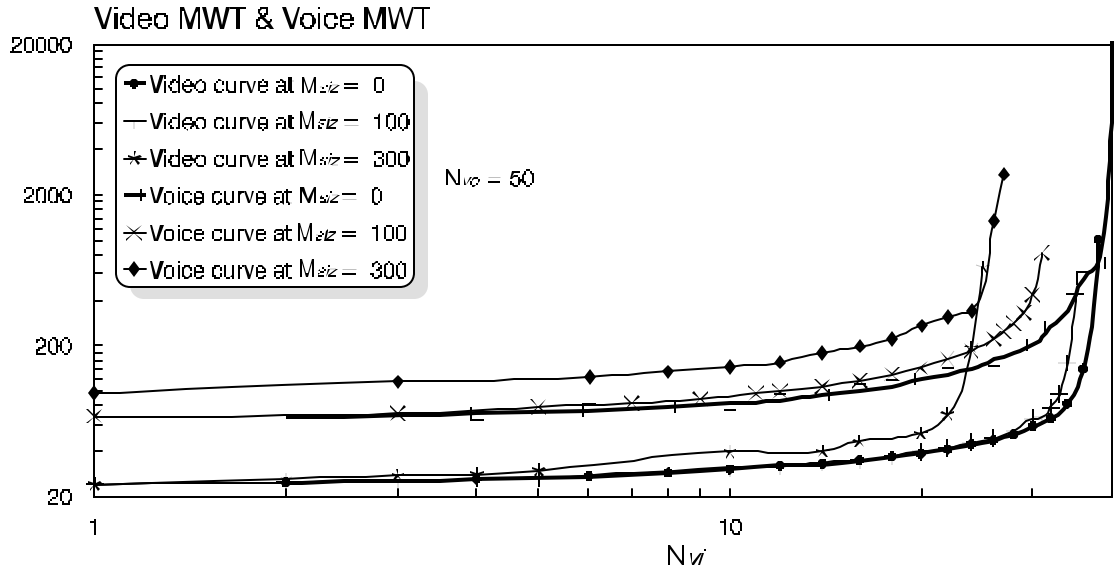

Figure 7-14 Video MWT and Voice MWT versus N_{vi}

Table 7-8 summaries the simulation values at two cases: integration video/voice and integration data/video/voice. It is clear that the data traffic has very slightly effect on video traffic but the data traffic has a small effect on voice traffic.

At R_{vi} = 1.5 Mbps, R_{vo} = 192 Kbps, μ = 5 ms					
At N_{vo}=100Sources & N_{vi}=10 Sources			At N_{vo}=50 Sources & N_{vi}=10 Sources		
M_{siz} (cell)	Video MWT (cell)	Voice MWT (cell)	M_{siz} (cell)	Video MWT (cell)	Voice MWT (cell)
0 100 300	30 32 34	148 156 236	0 100 300	30 30 39	82 90 144

Table 7-8 Simulation Results of Figure 7-13 and 7-14

Chapter 8

Conclusion

In this thesis, extensive simulations were developed to examine the effectiveness of the VP-Based ATM Network for supporting multimedia applications. We have adopted discrete event driven simulation methodology to evaluate the performance of integrated video, voice, and data traffics on the VP-Based ATM Ring Network. The study confirms that, the system parameters (e.g., number of video/voice sources, and data message size) have sensitive effects on the performance characteristics of the network. These parameters can be adapted to enable the ATM ring networks to support multimedia applications with acceptable performance. Using the data obtained through simulations, the following issues were examined:

I) The Mean Waiting Time (MWT) for video, voice, and data cells;

II) The Maximum Buffer Size (MBS) (queue length) for video, voice, and data cells;

III) The maximum number of video/voice sources can be supported with the network while satisfying the real-time constraints of both video and voice; and

IV) The achievable throughput and utilization of each traffic.

The simulation results confirm that, the VP-Based ATM ring networks can effectively handle video, voice, and data traffic in real-world network environments.

In this thesis, we have also proposed a control mechanism method to provide the fairness among the traffics to maximize the guaranteed throughput for asynchronous traffic. Though the video and voice traffics remain having higher priority than data traffic. In the proposed control mechanism method, the

numbers of cells to be picked up from each queue depending upon its offered load for completing the transmission frame.

The simulation results have proved that, the proposed method, which we have called as *Control Mechanism Method*, can derive optimal control method renders the highest guaranteed throughput for asynchronous cells.

Our future work will focus on the generalization of the model to include different types of time constrained cells (e.g., cells with different delay requirements) and applications to real-life problems.

References

[1] Shinya Nogami, "**Quality Control at the Cell Level and Its Characteristics in the ATM Network,**" *Electronics and Communication in Japan, Part 1, vol.74, no.7, pp.10-21, 1991.*

[2] Nail Kavak, "**Data Communication in ATM Networks,**" *IEEE Network, pp.28-37, Jan./Feb. 1996.*

[3] Lars Staalhagen, " **A Comparison Between the OSI Reference Model and the B-ISDN Protocol Reference Model,**" *IEEE Network, pp.24-33, Jan./Feb. 1996.*

[4] Tsong Ho. Wu, Dennis T. Kong, and Richard C. Lau," **An Economic Feasibility Study for a Broadband Virtual Path SONET/ATM Self-Healing Ring Architecture,**" *IEEE Journal on selected Areas in Communications, vol. 10, no. 9, pp. 1459-1473,Dec.1992.*

[5] David Clark, "**Are ATM, Gigabit Ethernet Ready for Prime Time**," *IEEE Computer magazine, vol. 31, no. 5, pp.11-13, May 1998.*

[6] Norman Finn, Cisco systems, Inc. Tony Mason, "**ATM LAN Emulation,**" *IEEE Communications magazine, pp.96-100, June 1996.*

[7] Allyn Romanow, and Sally Floyd," **Dynamics of TCP Traffic Over ATM Networks**," *IEEE Journal on selected Areas in Communications, vol. 13, no. 4, pp.633-641, Dec. 1995.*

[8] Flavio Bonomi and Kerry W. Fendick, "**The Rate-Based Flow Control Framework for the Available Bit Rate ATM Service,**" *IEEE Network, pp.25-39, March/April 1995.*

[9] **ATM Forum Traffic Management Specification**, *Working Document atm95-0013, Jan. 1995.*

[10] H. T. Kung and Robert Morris, "**Credit-Based flow control for ATM networks,**" *IEEE Network, pp.40-48, March/April 1995.*

[11] H. T. Kung, T. Blackwell, and A. Chapman, " **Credit-Based Flow Control for ATM Networks: Credit Update Protocol, Adaptive Credit Allocation, and Statistical Multiplexing**," *proc. of SIGCOMM'94, London, Sep. 1994.*

[12] K. K. Ramakrishnan and Peter Newman, " **Integration of Rate and Credit Schemes for ATM Flow Control,**" *IEEE network, pp.49-56, March/April 1995.*

[13] Yoshio Kajiyama, Nobuyuki Tokura, and Katsuaki Kikuchi, " **An ATM VP-Based Self-Healing Ring,**" *IEEE Journal on Selected Areas in Communications, vol. 12, no. 1, pp.171-178, January 1994.*

[14] Ryutaro Kawamura ,Ken-ichi Sata and Ikuo Tokizawa, " **Self-Healing ATM Networks Based on Virtual Path Concept,**" *IEEE Journal on Selected Areas in Communications, vol. 12, no. 1, pp.120-127, January 1994*

[15] Thierry van landgem, Patrick van kwikelberge, and Hany vanders traeten , "**A self-healing ATM Network Based on Multilink Principles**," *IEEE Journal on Selected Areas in Communications, vol. 12, no. 1, Dec.1994.*

[16] Lishenghong and Liu Zemin, "**A More General Traffic Model On ATM Networks,**" *Proc. Of IEEE APCC/CCCS'98, Singapore, vol. 1, pp.103-106, Nov.1998.*

[17] D.S. Eom, M. Sugano, Murata, and H. Miyahara, " **Call Admission Control For QoS Provisioning in Multimedia Wireless ATM Networks,**" *Proc. Of IEEE APCC/CCCS'98, Singapore, vol.1, pp.14-18, Nov.1998.*

[18] S. S. Petrovic ,"**A Stochastic Traffic Management Scheme for ABR Service in ATM Local Area Networks,**" *Proc of IEEE APCC/CCCS'98, Singapore, vol.1, pp.83-87, Nov. 1998.*

[19] D. Gan, and S. Mckenzie ,"**Traffic Policing in ATM Networks with Multimedia Traffic:The Super Leaky Bucket**," *Computer Communications, vol. 22, Issue 5, pp.439-450, April 1999.*

[20] E. Yaprak, A. T. Chronopoulos, K. Psarris, and YiXiao, " **Dynamic Buffer Allocation in an ATM Switch,**" *Computer Communications, vol. 31, Issue 18, pp.1927-1933, August 1999.*

[21] R. Handel, M. N. Huber, S. Schroder, "**ATM Networks: Concepts, Protocols, Applications,**" *2nd edition Addison wesly 1994.*

[22] J. B. Kim, T. Suda, and M. Yoshimura, "**International Standardization of B-ISDN**," *Computer Networks and ISDN Systems, vol. 27, 1994.*

[23] **CCITT Recommendation I-Series.**

[24] W. Stallings, "**Networking Standards: A guide to OSI, ISDN, LAN, and MAN Standards**," *Addison wesly 1993.*

[25] George C. Sackett and Christopher Y. Metz, **" ATM and Multiprotocol Networking**," *McGraw-Hill Companies, 1997.*

[26] Art Edmonds, Jr, "**ATM Network Planning and Implementation**," *International Thomson Computer Press, 1997.*

[27] **CCITT Recommendation G-Series.**

[28] W. Stallings, "**ISDN and Broadband ISDN with Frame Relay and ATM,**" *Prentice-Hall International, Inc., 1995.*

[29] F. Fluckiger, "**Understanding Networked Multimedia Applications and Technology**," *Prentice Hall, First Edition, 1995.*

[30] David M. Drury, " **ATM traffic management and the impact of ATM switch design**," *Computer Networks and ISDN systems 28, pp.471-479, (1996).*

[31] Tim Kwok, "**Avision for Residential Broadband Services: ATM-to-The-Home,**" *IEEE Network, pp.14-28, Sept./Oct.1995.*

[32] G. Wallaco, "**The JPEG Still Picture Compression Standard**," *Commun. of the ACM, vol. 34, no. 4, pp.30-44, April 1991.*

[33] Jan Crowcroft, Zheng Wang, Avril Smith, and John Adams, " **A Rough Comparison of the IETF and ATM Service Models,**" *IEEE Network, pp.12-16, Nov./Dec. 1995.*

[34] Mark W. Garrett, " **A Service Architecture for ATM: From Application to Scheduling,**" *IEEE Network, pp.6-14, May/June 1996.*

[35] Sudhir Dixit and Paul Skelly, " **MPEG-2 over ATM for Video Dial Tone Networks: Issues and strategies**," *IEEE Network, pp.30-40, Sept./Oct.1995.*

[36] P. V. Rangan, S. Kumar, and S. Rajan, " **Continuity and Synchronization in MPEG**," *IEEE J. on Selected Area in Comm., Vol. 14, No. 1, pp.52-60, Jan 1996.*

[37] P. Wong, and T. Peter, "**An Integrated Services Token Controlled Ring Network,**" *IEEE J. Select. Areas Commun., Vol. 7, No. 5, pp. 670-679, June 1989.*

[38] Mostafa H. Ammar, Victor O.K. Li, Mehmet Ulema, " **Broadband ISDN: Standards, Switches, and Traffic Management,**" *Computer Networks and ISDN system 27(1994), pp.1411-1427 (1-3).*

[39] William Stallings, "**Data and Computer Communications**," *2nd edition Macmillan Publishing Company, 1989.*

[40] ITU/CCITT, "**H.261: Video CODEC for Audio visual service at P X 64 Kbps**," *Geneva, 1990.*

[41] Ismail Dalgic, and Fouad A. Tobagi "**Constant Quality Video Encoding** *", IEEE Proceeding ICC'95, Seattle, Washington, pp.1-7, June 1995.*

[42] International Organization for Standardization (ISO),"**MPEG: Coding of moving Pictures and Associated Audio for Digital storage Media At up to About 1.5 Mbps,**" *Nov. 1991.*

[43] I. Dalgic, W. Chien, and F. Tobagi, "**Evaluation of 10Base-T and 100Base-T Ethernets Carrying Video, Audio and Data Traffic,**" *IEEE INFOCOM 94 Proceeding, Tronto, Canada, pp.1-9, June 1994.*

[44] Ciro A. Noronha Jr, and Fouad A. Tobagi, "**Evaluation of multicast routing algorithms for multimedia streams,**" *IEEE ITS 94 Proceeding, Rio de Janeiro, Brazil, pp.1-8, August 1994.*

45] T.H. Wu, **Fiber Network Service Survivability: Architectures, Technologies, and Design**. *Artech, May 1992.*

[46] T. H. Wu and R. C. Lau, "**A class of Self-Healing Ring Architectures for SONET Network Applications,**" *in Proc. IEEE GLOBECOM'90, San Diego, CA, pp. 403.2.1- 403.2.8, Dec. 1990.*

[47] E. Khalil, A. El-Sayed, N. Ismail, I. Z. Morsi, "**Control Mechanism for Fairness Among Traffics on ATM Network,**" *Accepted for Publication in 18th IASTED Intal. Conf. AI2000, Austria, Feb. 14-17,2000.*

[48] Xinyi Liu, and H. T. Mouftah, " **Queuing Performance of Copy Network with Dynamic Cell Splitting for Multicast ATM Switching,**" *IEEE Transactions on Communication, vol. 45, no. 4, pp.464-472, April 1997.*

[49] Chatschik Bisdikian, Baiju V. Patel, Frank Schaffa, and Marc Willebeek-LeMair, "**The Use of Priorities on Token-Ring Networks for Multimedia Traffic,**" *IEEE Network, pp.28-37, Nov./Dec.1995.*

[50] Leonard Kleinrock, "**Queuing Systems**," *volume II: Computer Applications, John Wiley & Sons, Inc., 1976.*

[51] Baij V. Patel and Chatschik C. Bisdikian," **End-Station Performance under Leaky Bucket Traffic Shaping,**" *IEEE Network, pp.40-47, Sep./Oct. 1996.*

[52] E. Khalil, A. El-Sayed, N. Ismail, and I. Z. Morsi, "**Multimedia Traffic Over VP-Based ATM Ring Network,**" *published in the 34th Annual Conference on Statistics Computer Sciences and Operations Research, Institute of statistical Studies and Research, Cairo University, Dec. 4-6, 1999.*

[53] E. Khalil, A. El-Sayed, N. Ismail, and I. Z. Morsi, "**Multimedia Traffic Over VP-Based ATM Ring Network,**" *published in the Electronic Engineering Bulletin, Faculty of Electronic Engineering, Menoufia University, No. 19, January 2000.*

[54] E. Khalil, A. El-Sayed, N. Ismail, and I. Z. Morsi, "**Multimedia Traffic Over VP-Based ATM Ring Network,**" *Accepted for publication in the 19th IEEE/IPCCC-2000, Arizona, USA, Feb 20-22, 2000.*